FRI 13/1973

M. Savage

F.R.I. 47

VERSLAG NR. _____ REPORT NO. 13

VAN _____ OF 1973

J1/G1312

BRANDSTOFNAVORSINGSINSTITUUT
VAN SUID-AFRIKA

FUEL RESEARCH INSTITUTE
OF SOUTH AFRICA

ONDERWERP: PARTICLE EQUILIBRIUM CONDITIONS AT THE BOUNDARY OF
SUBJECT: A STREAM AND ORIGINATING TRANSPORT PHENOMENA

AFDELING:
DIVISION:

A.C. BONAPACE

NAAM VAN AMPTENAAR:
NAME OF OFFICER:

Cosmi 9228 - B4

FUEL RESEARCH INSTITUTE OF SOUTH AFRICA

REPORT NO. 13 OF 1973

PARTICLE EQUILIBRIUM CONDITIONS AT THE BOUNDARY OF A STREAM AND ORIGINATING TRANSPORT PHENOMENA

SCOPE OF THE INVESTIGATION

Numerous phenomena, related to solid/liquid (or solid/gaseous) suspensions of particles, depend on the hydraulic forces which act on these particles as a result of the flow.

This can be said of natural streams like rivers transporting silt, of industrial processes where solids are purposely conveyed as slurries, or where solids must be separated from the liquid phase, etc.

A study of hydraulic forces and related phenomena is of fundamental importance in order to understand these phenomena from a general point of view and to make them exploitable.

In the separation of particles from a liquid, it is preferable to use the action of the gravitational field (e.g. in decanting), but also the action of electrical or magnetic fields of force, particularly in the technology of mineral dressing.

In other cases it is desired to prevent particles from being brought into suspension in the fluid, e.g. for safety or health reasons.

In respect of safety, the case of explosion propagation in the underground tunnels of fiery collieries may be mentioned.

/As .....

As is well known, the flame front can travel a long distance from the point of the initial explosion because of the coal dust lifted by the wind of the explosion, which continuously feeds the flame with new combustible matter.

The present work covers ,in appendix I, a typical example of the calculation of safe air velocity in a tunnel, and describes means to prevent the formation of a coal particle suspension. Moreover, it presents the premises for a study of particle separation in electric or magnetic fields.

In other words, the analysis, based on the action of the gravitational field, is extendible to other fields of forces of the electrical or magnetic type, as used in the technology of ore dressing.

SUMMARY

Following upon an experimental approach, the equilibrium conditions of a particle at the boundary were found to be equivalent both in relation to the phenomenon of particle lift followed by transport in saltation and in full suspension.

Using the description of the velocity profile in a pipe, particle equilibrium could also be determined from the properties of the undisturbed stream, i.e. in a section before the particle.

An expression of the lift force in the undisturbed fluid led to the definition of the potential function of the stream.

From a discussion of the potential function, critical conditions governing the phenomena of particle deposition, saltation, and the formation of dunes could be established.

Critical conditions of particle lift could also be extended from the turbulent region to the transition and smooth-wall regions of the flow.

/Index .....

INDEX

/1. .....

1. INTRODUCTION

1.1. Physical premises

The behaviour of a spherical particle in a stream is investigated here in relation to conditions providing particle movement in suspension, in saltation or particle deposition, mainly under the influence of the force due to gravity.

The theory can be extended to the action of other fields of force like electrical and magnetic ones, and useful interpretations of the phenomena of particle separation obtained.

The analysis is based on energy considerations related to certain initial conditions typical of particle equilibrium at the boundary.

By this method, much of the knowledge can be acquired which would otherwise require a more advanced and involved mathematical approach, for instance by means of the differential equation of the particle trajectory.

Well-known phenomena and laws of fluid mechanics are recapitulated in the following as a basis for this analysis.

1.2. The energy dissipative function

It is well known that a mixture of liquid and particles, when transported in full suspension, approximately dissipates the same total energy as a volumetrically equivalent mass of pure liquid*.

/When .....

---

*For this a sufficiently high transport velocity is required.

When particles move forward in saltation, a considerable amount of energy is dissipated in excess of the above amount because of the impact of the particle against the wall. The author has found (cf. ref. 1) that this excess energy is proportional to the frequency of the impacts and to the kinetic energy typical of the naturally falling particle in the liquid.

From the foregoing observations, it may be deduced that along a particle trajectory, either in saltation or in suspension, very little energy is dissipated except at the point of impact. This statement is equivalent to the following: The energy dissipated at the particle contour because of its motion relative to the liquid is about equivalent to the energy which would otherwise have been dissipated in turbulent mixing by the volume of liquid displaced by the particle.

Concluding

The particles-liquid system can be looked at as a whole as an ideal system in which liquid and particles exchange energy without dissipation, i.e. reversibly. This system will be denoted here as the "ideal suspension".

1.3. The lift force on a particle

The lift force on a particle can be expressed in two different ways.

In experimental hydrodynamics the lift force F_ℓ is usually written as follows:

$$F_\ell = C_\ell \frac{\pi d^2}{4} \frac{v_c^2 \rho}{2} \qquad (1.3.1)$$

where d is the particle diameter, v_c the local fluid velocity, (i.e. the velocity which would have existed at the position occupied by the particle centre in its absence), ρ the density of the liquid, and C_ℓ the

/coefficient .....

coefficient of lift (a parameter of experimental nature).

In theoretical hydrodynamics and for a two-dimensional motion the lift force is:

$$F_\ell = \rho\, v_c\, \Gamma \qquad (1.3.2)$$

i.e. it is given by the product of the velocity v_c, the density ρ of the fluid and the circulation Γ around the particle.

As is well known, the circulation Γ is the integral of the velocity calculated along a closed line which encircles the particle.

If r is the radius of the circumference and v_t the tangential velocity, the strength c of the vortex is defined by

$$v_t = \frac{c}{r} \qquad (1.3.3)$$

and the circulation Γ is

$$\Gamma = \oint v_t r\, d\varphi = \oint c\, d\varphi = 2\pi c \qquad (1.3.4)$$

(cf. figure 1-A)* as defined on the diagram.

Considering in Figure 1-B a stationary particle at a radial distance z_c from the wall, with local fluid velocity v_{zc} and velocity gradient $tg\,\gamma = \left(\frac{dv}{dz}\right)_{z=z_c}$ the tangential component of the velocity will be:

$$v_t = \left(\frac{dv}{dz}\right)_{z=z_c} \frac{d}{2} \qquad (1.3.5)$$

/The .....

*The letter d shall be used in the context to represent both differentiation and particle diameter.

The lift force $F_{\lambda zc}$ is directed, upward i.e. perpendicularly to the direction of the flow.

If the particle is free, it will move upwards, i.e. in the direction z, with a vertical velocity v'_z, as shown in Figure 1-C.

The combined effect of the circulation c and of the vertical velocity v'_z induces a force F'_{dz_c} opposite to the direction of the flow.

This force tends to retard the particle by causing a slip in velocity s in respect of the surrounding portion of the fluid.

Forces $F_{\lambda zc}$ and F'_{dzc} are applied at points S and S' of the particle, as shown in Figure 3-C.

The arrows relative to the circulation and v_{zc}, to the circulation and v'_z, oppose each other at S and S' respectively, i.e. create a positive pressure at these two points.

1.4. The velocity distribution profile in a pipe

Definition of particle equilibrium at the boundary requires an accurate description of the velocity at the boundary.

It is well known that the velocity profile in a pipe is logarithmic in the region of turbulent diffusion, and linearly decreasing to zero in the boundary layer near the wall.

The cases of smooth pipes (I) and rough pipes (II) are discussed separately hereunder.

/I .....

I. Smooth pipes. (cf. Figure 2)

(a) In the turbulent region the velocity profile is represented by the relationship (cf. ref. 2):

$$v_z = v_* \left(5{,}50+5{,}75 \lg \frac{z v_*}{\nu}\right) \qquad (1.4.1)(I.a)$$

where v_z is the local velocity measured at a radial distance z from the wall, ν is the kinematic viscosity of the liquid, and v_* the "friction velocity", defined later.

The velocity profile as a whole is shown in Figure 2-A and on a magnified scale near the wall in Figure 2-B.

(b) In the region near the wall (i.e. between the distances δ and δ_o) eqn (1.4.1) (Ia) represents the actual δ profile (i.e. the rectilinear part of the diagram) approximately only.

In the immediate vicinity of the wall (distance less than δ_o) the representation by means of a logarithmic function fails altogether, because of its divergence to $-\infty$. Consequently, the use of eqn (1.4.1) (Ia) will be limited up to a distance

$$z = \delta = \frac{\nu}{v_*} \qquad (1.4.2)$$

for $z = \delta = \frac{\nu}{v_*}$ eqn (1.4.1) (Ia) yields

$$v_\delta = v_{z=\delta} = 5{,}50\, v_* \qquad (1.4.3)(I)$$

(c) The linear part of the velocity profile can thus be expressed with eqns (1.4.2) and (1.4.3) (I) as follows:

$$v_z = v_\delta \frac{z}{\delta} = 5{,}50 \frac{v_*^2}{\nu} z \quad (\text{for } z < \delta) \qquad (1.4.1)(Ib)$$

/Let .....

Let the force per unit area (shear stress) exerted by the stream on the wall be τ_*.

Then τ_* is proportional to the slope of the velocity profile at the wall and to the dynamic viscosity μ of the fluid i.e.

$$\tau_* = \frac{v\delta}{\delta} \qquad (1.4.4)$$

τ_* can also be expressed by means of the hydraulic gradient i of the stream.

According to the well known Darcy-Weissbach equation, the hydraulic gradient of the stream is

$$i = f \frac{V^2}{2gD} \qquad (1.4.5)$$

where V is the mean velocity of the stream, D the pipe diameter, f the friction factor of the pipe, and g the acceleration due to gravity.

The loss of head ΔH (measured in meters of liquid column) for a unit length of pipe is

$$\Delta H = i \times 1$$

and the resultant thrust on the portion of liquid cylinder of unitary length is

$$i \rho g \frac{\pi D^2}{4}$$

This thrust is in equilibrium with the shear force exerted on the pipe wall which has the value $\tau * \pi D \times 1$.

/Then .....

Then the condition of equilibrium between the two forces yields:

$$l \times i \rho g \frac{\pi D^2}{4} = \tau_* \pi D l$$

By making use of eqns (1.4.4) and (1.4.5), one gets

$$\frac{f V^2}{8} = \frac{\tau_*}{\rho} \qquad (1.4.6)$$

Putting conventionally

$$\frac{\tau_*}{\rho} = v_*^2$$

One can express the friction velocity v_* as:

$$v_* = \left(\frac{f}{8}\right)^{\frac{1}{2}} V \qquad (1.4.7)$$

which is a well-known formula.

II. Rough pipes

Only the case of artificial roughness will be considered here since it is the only one which can be well defined experimentally.

The friction factor f of pipes artificially roughened with sand particles of diameter k were investigated by Nikuradse.

Well-known experiments have proved that the friction factor of the pipe depends only (for a sufficiently large pipe Reynolds number) on the coefficient of relative roughness $\frac{k}{D}$, and is a constant parameter otherwise.

/The .....

The equation representing the velocity profile in the turbulent region (a) as given by Nikuradse (cf. ref. 2) is:

$$v_z = v_* (8{,}50 + 5{,}75 \lg \frac{z}{k}) \qquad (1.4.1)(IIa)$$
(for $z \geq k$)

Comparison with eqn (1.4.1) (Ia) shows that the distance $\delta = \frac{\nu}{v_*}$ has now been replaced by k,(*) while the integration constant is 8,50 instead of 5,50.

(b) The expression of the velocity distribution inside the boundary layer for rough pipes is derived from (1.4.1) (IIa) as follows:

for $z = k$

$$v_k = 8{,}50\ v_* \qquad (1.4.3)(II)$$

for $z < k$

$$v_z = 8{,}50\ v_* \frac{z}{k} = 8{,}50\ \frac{v_*^2}{\nu}\ z \qquad (1.4.1)(IIb)$$

Eqn (1.4.1)(IIb) is the equivalent of (1.4.1) (Ib) It expresses the velocity distribution for rough pipes in the region $z < k$ (cf. later development).

Although this equation is an oversimplification of a very complex phenomenon, it has a physical meaning when referring to a section of the pipe corresponding to a pocket between two irregularity humps (e.g. section S'-S of Figure 3-C). It simply states that the velocity distribution decreases linearly with the distance from the solid contour.

/Concluding .....

(*) The statement is compatible with the following ones:

$$\delta = \frac{\nu}{v_{*I}} = k; \quad v_{*I} = v_{*II} \text{ and eqn (1.4.7).}$$

Concluding:

Velocity distribution functions have been defined for smooth and rough pipes inside as well as outside the boundary layer of the stream.

1.5. Definition of flow boundary conditions and related phenomena

The distinction between smooth (I) and rough pipes (II) is a way of distinguishing between basic phenomena to be discussed later.

Considerable attention will be given to the phenomenon of lift of a particle from the boundary.

In this respect a parallel analysis will be advantageous. One can study the hydraulic conditions in the turbulent region of the stream in an undisturbed state (e.g. as in section α of Figure 3-A), such that the stream would be able to lift the particle if it should be placed in its way.

This approach depends entirely on the properties of the undisturbed stream (in section α of Figure 3-A) and is therefore subject to theoretical analysis.

Alternatively, hydraulic conditions in the particle section can be studied, i.e. in the condition of a disturbed stream (e.g. as in section β) with the particle forming part of the boundary.

This approach is particularly useful in the interpretation of the experimental results. In the case of smooth pipes (I) one can simply consider the various positions of a particle of diameter d in relation to the thickness δ of the boundary layer. The boundary-layer

/thickness, ...

thickness, as given by equation (1.4.2), is inversely proportional to the friction velocity v_*, expressed in turn by eqn (1.4.7).

From the aforementioned expressions, a particle which at the beginning is fully inside the boundary layer, pierces it later if the stream velocity is sufficiently increased.

The case of rough pipes (II) is more complicated because the additional parameter of relative roughness $\frac{k}{D}$ has to be considered.

The relationship between $\frac{k}{D}$ and f is now well known and reported in technical literature in the form of the diagram reproduced in Figure 21 of Appendix III.

Of this diagram only the portion inside the fully turbulent region will be considered at first, in which the loci $\frac{k}{D}$ = constant are horizontal lines.

As is well known, in this region various resistance diagrams corresponding to various conditions of wall roughness (of the Nikuradse, Colebrook-White types, etc.) are practically coincident and can be expressed as a function of the parameter $\frac{k}{D}$ only.

The lifting of a particle from the boundary will be studied later in relation to particle size d, pipe diameter D, and absolute roughness k. If d is large compared to k, as in Figure 3-B-1°), the lifting of a particle will not depend much on the conditions at the boundary, but mainly on the ratio $\frac{d}{D}$.

/Consequently, ...

Consequently, $\frac{d}{D}$ can be used as a correlating parameter of the conditions providing particle lift.

Experimental results will also prove later that the lift of a particle, when this is part of an array of other similar particles (Figure 3-B-2), takes place in conditions very similar to those of Figure 3-B-1 .

Such equivalence can be justified simply by the fact that in both cases the particle contour is the actual (artificial) boundary of the stream.

The physical situation is different when the particle is smaller than the dimension k of the absolute roughness.

In Figure 3-C-1, $d = k_1$ consequently, from Figure 20 for $\frac{d}{D} = \frac{k}{D}$ the corresponding friction factor f_1 can be derived.

A friction velocity v_{*1}, related to f_1 can be determined (see later development) at which the particle is lifted from the boundary.

By considerably increasing the pipe roughness to k_o, while keeping D and d constant, the particle will end well below the crests of the irregularities (as in Figure 3-C-2).

Consequently, the frictional v_* velocity must be increased in the ratio $\frac{k_o}{d}$ in order that the particle can be lifted from its pocket by a velocity at the particle of value v_{*1}.

/Concluding: .....

Concluding:

Particle lift from the boundary will be studied later: theoretically under the conditions of an undisturbed stream (as in section α of Figure 3-A); experimentally in a situation as illustrated, in section β of Figure 3-A.

For particle diameters larger than or of the same order as the pipe wall irregularities ($\frac{d}{k} < 1$), the phenomenon of lift will be studied in relation to a solitary particle, or to a particle belonging to a bed of other similar particles.

When a particle dimension is smaller than the absolute roughness dimension of the pipe ($\frac{d}{k} < 1$), the frictional velocity providing particle lift must be increased in the ratio of these linear dimensions (i.e. by $\frac{k}{d}$).

2. THE EXPERIMENTAL DETERMINATION OF THE LIFT COEFFICIENT OF A PARTICLE

2.1. Introductory remarks

Experiments on the hydraulic transport of particles in pipes, reported in the technical literature, have provided the author with the basic material for this analysis.

These experiments are presented and discussed briefly in Appendix II and are described in detail in ref. 1. 3. 4. 5, 6. They have been grouped into normal cases (five sets of diagrams), and anomalous cases (two sets of diagrams).

The introduction of this classification is due only to the fact that normal cases are most frequently encountered in the technology of solid transport in pipes.

/Typical .....

Typical parameters used in the course of the analysis, and derived from these diagrams, have been listed in Table 1.

The phenomenon of the lifting and transportation of particles will be considered here only in relation to a negligibly small concentration of material transported, for a particle moving away either from the bare wall or from a bed of similar other particles, and for a trajectory which carries the particle away (in suspension), or which ultimately brings it back to the boundary (saltation).

2.2. The experimental coefficient of lift

Assume that water flows through a pipe with particles resting on its inner wall, as shown in Figure 3-B-2.

Assume further that by slowly increasing the fluid velocity, one can gradually carry away all the particles except one.

The fluid velocity at which this happens discriminates between conditions of flow where the pipe is completely clear and conditions of flow with particle deposits.

As no particle transport is ultimately assumed to exist under steady conditions, clear liquid only is collected at the end of the pipe-line.

For instance, referring to Figure 10-b of the appendix, this velocity has a value $v_o = v_{10} = 4{,}92\ (\frac{m}{s})$.

It corresponds to the vertex of a parabola $x = o$, representing the excess loss due to stationary material deposits in the pipe.

/Particle .....

Particle lift will only be possible whenever the lift force F_ℓ (a superficial force) is equal to or greater than the force due to gravity Fg (a body force), i.e.

for $\frac{F_\ell}{Fg} \geq 1$ (2.2.1)

Because the particle shapes the boundary streamlines with its contour, let us express the lift force by means of the frictional velocity v_* of eqn (1.4.7).

Then eqn (2.2.1) with (1.3.1) expresses the condition of equilibrium between the force due to gravity and the lift force, as follows:

$$\frac{\pi d^3}{6} (\rho_m - \rho) g = C_\ell \frac{\pi d^2}{4} \frac{v_*^2 \rho}{2} \qquad (2.2.2)$$

valid for a particle at the boundary.

In eqn (2.2.2) let us group the quantities as follows:

$$\frac{v_*^2}{dg} = Fr_* \qquad (2.2.3)$$

$$\frac{v_* d}{\nu} = Re_* \qquad (2.2.4)$$

where Fr_* and Re_* are the well known Froude and Reynolds numbers referring to the frictional velocity v_*.

Then eqn (2.2.2) can be written as:

$$\frac{3}{4} C_\ell \frac{\rho}{\rho_m - \rho} \frac{v_*^2}{gd} = 1$$

Division of both members by Re_*^2 yields:

$$\frac{3}{4} C_\ell \frac{\rho}{\rho_m - \rho} \frac{Fr_*}{Re_*^2} = \frac{1}{Re_*^2} \qquad (2.2.5)$$

/By .....

By introducing the Grashof number

$$\frac{\rho_m-\rho}{\rho} \quad \frac{Re_*}{Fr_*} = \frac{\rho_m-\rho}{\rho} \quad \frac{gd^3}{\nu^2} = Gr \qquad (2.2.6)$$

into (2.2.5), one gets:

$$C_\lambda = \frac{4}{3} \quad \frac{Gr}{Re_*^2} = \frac{4}{3} \quad \frac{\rho_m-\rho}{\rho} \quad \frac{gd}{V_*^2} \qquad (2.2.7)$$

which expresses the lift coefficient of a particle at the boundary as a function of easily accessible parameters typical of the particle and of the stream.

Eqn (2.2.7) can be compared with the expression of the drag coefficient of a particle settling in a liquid with velocity v_{se} as done hereunder.

Equilibrium between the force due to gravity and the hydraulic drag force yields:

$$(\rho_m - \rho)\, g\, \frac{\pi d^3}{6} = C_d \quad \frac{\pi d^2}{4} \quad \rho \frac{v_{se}^2}{2} \qquad (2.2.8)$$

Then an analogous reasoning leads to the following:

$$C_d = \frac{4}{3} \quad \frac{Gr}{Re^2} = \frac{4}{3} \quad \frac{\rho_m-\rho}{\rho} \quad \frac{gd}{v_{se}^2} \qquad (2.2.9)$$

where $Re = \frac{v_{se}\, d}{\nu}$ is the Reynolds number of the particle (cf. ref. 7) when settling at its terminal velocity.

When comparing particles of different densities, the condition of having the same Grashof number fixes a relationship between density and particle diameter.

/Taking .....

Taking as a reference density that of sand (suffix sa) ($\rho_{sa} = 2650 \ \frac{Kg}{m^3}$), and that of an unspecified material (suffix m), the density ρ_m and particle diameter d_m are related to ρ_{sa} and d_{sa}, as follows:

$$\frac{d_{sa}}{d_m} = \left(\frac{\rho_m - \rho}{\rho_{sa} - \rho}\right)^{\frac{1}{3}} \quad \text{(for Grsa = Grm)} \qquad (2.2.10)$$

Equality between the viscous forces, i.e. between the Reynolds numbers, also requires:

$$d_m \ V^*_m = d_{sa} \ V^*_{sa} \qquad (2.2.11)$$

Combination of eqns (2.10) and (2.11) yields:

$$V^*_m \left(\frac{\rho_{sa} - \rho}{\rho_m - \rho}\right)^{\frac{1}{3}} = V^*_{sa} \qquad (2.2.12)$$

By means of (2.2.12) the friction velocity of a particle relative to a certain material m has been reduced to that of a sand particle.

Substitution of eqn (2.2.12) into (2.2.7) yields

$$C_{\ell m} = \frac{4}{3} \frac{Gr}{Re^{*2}} \left(\frac{\rho_m - \rho}{\rho_{sa} - \rho}\right)^{\frac{2}{3}} \qquad (2.2.13)$$

a relationship which yields the lift coefficient of a particle of density ρ_m.

The stream velocity at which the particle is lifted from the boundary or dropped from the stream is herein named "critical lift or sedimentation velocity" and is denoted by Vo (V_{10} in the figure of Appendix II).

/The .....

The experimentally observed values for the five normal cases discussed are reported in Table 1.

By introducing Vo into the expressions of the friction velocity v_* and of the Reynolds number Re*, one gets a new notation:

$$Re^*o = \frac{v_{*o}\, d}{\nu} \qquad (2.2.4) \text{ (repeated)}$$

$$v_{*o} = \left(\frac{fo}{8}\right)^{\frac{1}{2}} Vo \qquad (1.4.7) \text{ (repeated)}$$

For an orderly display of the points representing the five normal cases, one also has to introduce <u>empirically</u> the ratio $\frac{d}{D}$ as a power of $(1 - \frac{d}{D})$, resulting in the following eqn:

$$Re^*m\,\frac{d}{D} = Re^*o\,\left(\frac{\rho_{sa} - \rho}{\rho_m - \rho}\right)^{\frac{1}{3}} \frac{1}{(1 - \frac{d}{D})^{3,5}} = 2\,Gr^{\frac{1}{2}} \qquad (2.2.14)$$

This equation is plotted in Figure 4, and is verified by five experimental points derived from normal cases.
A comparison of (2.2.14) with (2.2.13) yields the lift coefficient for various conditions of material density and particle pipe diameter ratios.

For $\frac{d}{D} \to o$ one gets

$$C_\ell' = C_{\ell,o} = \frac{1}{3} \qquad (2.2.15)$$

For $\frac{d}{D} \neq o$

$$C_\ell' = C_{\ell,\frac{d}{D}} = \frac{1}{3} \cdot \frac{1}{(1 - \frac{d}{D})^7} \qquad (2.2.16)$$

/Values .....

Values C'_λ become very large for $\frac{d}{D} \rightarrow 1$.

Because of (2.2.16), eqn (2.2.14) can also be written as follows:

$$C'_\lambda = \frac{4}{3} \frac{Gr}{Re^{*}o^2} \left(\frac{\rho_m - \rho}{\rho_{sa} - \rho}\right)^{\frac{2}{3}} \frac{1}{\left(1-\frac{d}{D}\right)^7} \qquad (2.2.17)$$

Concluding:

Conditions providing particle lift from the boundary under the action of the stream have been expressed by an experimental correlation of the type (2.2.14) exemplified in the graphical representation of Figure 4.

2.3. Equivalence of the phenomenon of particle lift in transport by saltation or full suspension

Experimental conditions summarizing the occurrence of incipient saltation are represented by the points plotted in Figure 5 for transported material concentrations $x = o$, and $x = 0,10$.

Values of the nominal stream velocity (*) at which saltation occurs are given in Table 1.

For a graphical explanation of the condition of saltation, one is referred, e.g.,to Figure 10-b of Appendix II.

The value of nominal velocity $Vso = Vszo = 2,85$ (m/s) represents on the parabola at $x = o$ the condition of incipient saltation.

/The .....

(*) The nominal stream velocity is defined by the ratio:

$$\frac{\text{Total flow rate (solid and liquid)}}{\text{Cross-sectional area of the pipe}}$$

The nominal stream velocity may differ from the actual nominal stream velocity in the presence of material deposits in the pipe.

The rapid rise of the excess hydraulic gradient is typical of the saltation phenomenon which causes energy loss by impact.

In order to correlate conditions of incipient saltation experimentally, the groups

$$\Phi_{so} = \frac{V^2_{so}}{gd} C_d \quad \text{(for a concentration x = o)} \qquad (2.3.1)$$

and

$$\Phi_{sx = 0,10} = \frac{V^2_{sx = 0,10}}{gd} C_d \quad \text{(for a concentration x = 0,10)} \qquad (2.3.2)$$

have been plotted in Figure 5 against the ratio $\frac{d}{D}$.

The experimental equations representing this correlation are the following:

$$\frac{d}{D} = 0,215\ \Phi^{-\frac{1}{2}}_{so} \quad \text{(for x = o)} \qquad (2.3.3)$$

$$\frac{d}{D} = 0,250\ \Phi^{-\frac{1}{2}}_{sx = 0,10} \quad \text{(for x = 0,10)} \qquad (2.3.4)$$

The experimental values of Vso are those of Table 1, derived from the figures of Appendix II.

In the present analysis the case x = o is of particular interest.

By comparing eqn (2.2.2) with eqn (2.2.8), the condition of equality between the lift force and the drag force can be written along the vertical for v_{*so} as follows:

$$C'_{\ell} \frac{\pi d^2}{4} \frac{v^2_{*so}\,\rho}{2} = C_d \frac{\pi d^2}{4} \frac{v^2_{se}\,\rho}{2}$$

i.e.

$$\frac{Cd}{C'_{\ell}} = \left(\frac{v_{*so}}{v_{se}}\right)^2 \qquad (2.3.5)$$

/Moreover .....

Moreover,

The Froude number of a particle undergoing incipient saltation, i.e. for a stream velocity V = Vso, may be expressed as follows:

$$\frac{V^2_{so}}{gd} = Frs_o = \frac{\rho_m - \rho}{\rho} \quad \frac{Reso^2}{Gr} \qquad (2.3.6)$$

where $Reso = \frac{Vso^d}{\nu}$ and Gr is given by eqn (2.2.6)
Eqns (2.3.5) and (2.3.6) substituted in (2.3.1) yield:

$$\frac{d}{D} = 0{,}215 \left(\frac{1}{C_k' \left(\frac{v_{*so}}{v_{se}}\right)^2} \quad \frac{1}{\frac{Reso^2}{Gr} \frac{\rho_m - \rho}{\rho}} \right)^{\frac{1}{2}} \qquad (2.3.7)$$

The symbols in eqn (2.3.7) have the following meanings:

v_{*so} is the friction velocity providing incipient particle lift for a particle undergoing saltation.

Reso is the particle Reynolds number relative to a stream velocity Vso, providing incipient saltation at zero concentration transported, and from a bed of particles.

V_{se} is the particle settling velocity.

Gr is the particle Grashof number.

/24 .....

The following transformations are applied to eqn (2.3.7):

a) the group $v_{*so}^2 \, Reso^2$ is written as

$$v_{*so}^2 \, Reso^2 = Vso^2 \, Re*so^2 \qquad (2.3.8)$$

where

$$Re*so = \frac{V*so \; d}{\nu} = \left(\frac{f_s}{8}\right)^{\frac{1}{2}} \frac{V_{so} \; d}{\nu} \qquad (2.3.9)$$

with f_s the friction factor of the pipe in condition of incipient saltation.

Then, denoting with λ the ratio

$$\lambda = \frac{f_s}{f_o} \qquad (2.3.10)$$

Re*so can be expressed in function of Re*o as follows:

$$Re*so = \lambda^{\frac{1}{2}} \, Re*o \qquad (2.3.11)$$

b) The effect of particle density already expressed by eqn (2.2.12) is introduced in (2.3.11).

In the case of sand taken as reference material, one gets

$$Re*o^{sand} = \left(\frac{f_o}{8}\right)^{\frac{1}{2}} Vo^{sand}$$

In the presence of any other material, reduction to sand is obtained by means of the factor $\left(\frac{\rho_{sa} - \rho}{\rho_m - \rho}\right)^{\frac{1}{3}}$ by writing:

/Re*m .....

$$Re^*m = Re^*o\left(\frac{\rho_{sa}-\rho}{\rho_m-\rho}\right)^{\frac{1}{3}} = Re^*o^{sand} \qquad (2.3.12)$$

c) C'_λ is expressed by means of (2.2.16), so obtaining

$$\frac{1}{3}\frac{Re^*m}{(1-\frac{d}{D})^{3,5}} = \frac{1}{3}\,Re^*m\,\frac{d}{D} = C'_\lambda\,Re^*m \qquad (2.3.13)$$

Eqns (2.3.8), (2.3.11), (2.3.12) and (2.3.13) substituted in eqn (2.3.7) yield the final expression:

$$2\,Gr^{\frac{1}{2}} = Rem\,\frac{d}{D}\;2x2,67\;\frac{Vso}{v_{se}}\;\frac{d}{D}\left(\frac{\rho\,m-\rho}{\rho}\right)^{\frac{1}{2}}\lambda^{\frac{1}{2}} \qquad (2.3.14)$$

Eqn (2.3.14) becomes identical with (2.2.14) if the factor

$$\varphi = 2x2,67\;\frac{Vso}{v_{se}}\;\frac{d}{D}\left(\frac{\rho\,m-\rho}{\rho}\right)^{\frac{1}{2}}\lambda^{\frac{1}{2}} = 1 \qquad (2.3.15)$$

An approximate evaluation of λ can be obtained from the hydraulic gradients:

i_o, at $V = Vo$

and

$i_{so} = i_o + \Delta i_{so}$ at $V = Vso$,

i.e. by calculating the ratio

$$= \frac{i_o + \Delta i_{so}}{i_o} = \frac{i_{so}}{i_o} \qquad (2.3.16)$$

/values .....

values of λ obtained for the five normal cases are listed in Table No. 2; for anomalous cases $\lambda = 1$.

Numerical calculations have produced φ values which in their average (cf. Table 2, φ average = 0,99) confirm relationship (2.3.15), i.e. the validity of (2.2.14) as a general condition of equilibrium for a particle at the boundary.

Conclusion

The existence of a single condition of equilibrium at the boundary has been proved for incipient movement of a particle followed either by saltation or by full suspension.

The equation $\varphi = 1$ proving this condition also provides a useful relationship among certain parameters typical of the particle and of the stream.

2.4. Discussion of the experimental results of paragraphs 2.2. and 2.3.

The following discussion deals with the conditions of equilibrium of a solitary particle (correlation of Figure 4 with corresponding geometrical situation of Figure 3-B-1) and of a particle belonging to a bed of particles (correlation of Figure 5 and geometrical situation of Figure 3-B-2.)

In Table 3, the Grashof number of the particle with the corresponding Reynolds numbers of the particle at which this is lifted, has been given for normal and anomalous cases.

According to the table, normal cases are those countersigned by a value $\frac{d}{k} > 1$, and
anomalous cases by a value $\frac{d}{k} < 1$.

Of particular interest in the following discussion is the value $\frac{d}{k} = 1$.

This discriminating condition is obtainable either with particles of the same diameter d as the absolute dimension k of the pipe roughness (as in Figure 3-C-1) or with particles forming a bed on a comparatively smoother pipe wall (as in Figure 3-B-2).

/The .....

The latter situation is typical of the normal cases in conditions of incipient saltation, i.e. of a bed of particles altering the relative roughness of the pipe from $\frac{k}{D}$ to an artificial value $\frac{d}{D}$, where often $d \gg k$.

The corresponding (nominal) velocity at which the particle leaves the bed has been indicated with Vso (saltation velocity at zero concentration of transported material).

Introducing as a measure of the "artificial" roughness the symbol

$$k' = d$$

one can write eqn (2.3.16) as follows:

$$\varphi = 2 \times 2{,}67 \; \lambda^{\frac{1}{2}} \frac{Vso}{V_{se}} \frac{k'}{D} \frac{\rho m - \rho}{\rho} = 1 \qquad (2.3.17) \text{ (modified)}$$

valid for particle beds where $d > k$.

Eqn (2.3.16) (modified) again reduces eqn (2.3.16) to (2.2.17) and to Figure 4 because of the position $d = k'$.

Consequently, one can assert that the layer of particles has altered in this instance only the relative coefficient of roughness from $\frac{k}{D}$ to $\frac{k'}{D} = \frac{d}{D}$.

One can expect eqn (2.14) to be valid still when the particle diameter d decreases to dimensions of the pipe roughness k (d=k) as illustrated in Figure 3-C-1).

Continuation beyond this limit, i.e. for $\frac{d}{k} < 1$, should still imply the condition

$$\varphi = 1$$

/For .....

For $d = d' < k$, let us indicate the new stream velocity causing particle removal from the boundary with V'_{so}.

Then the previous expression of φ can be written for $d = d' < k$ as follows:

$$\varphi = \frac{V_{so}}{V_{se}} \quad \frac{k}{D} \quad \text{constant} = \frac{V'_{so}}{V_{se}} \quad \frac{d'}{D} \quad \text{constant} = 1 \qquad (2.4.1)$$

i.e.

$$V'_{so} = V_{so} \frac{k}{d'} \qquad (2.4.2)$$

Consequently, if the position $\frac{d'}{k} < 1$ is obtained through an increase in absolute roughness k, with D constant, the previous condition (2.4.2) implies a proportional increase in the mean saltation velocity of the stream (cf. Figure 3-C-2).

Conclusion

It has been proved that normal and anomalous cases are characterized simply by a different value of the ratio $\frac{d}{k}$.

$\frac{d}{k} > 1$ for normal cases.

$\frac{d}{k} < 1$ for anomalous cases.

The condition $\varphi = 1$ can be extended to the case $\frac{d}{k} < 1$, provided an augmented stream velocity is introduced in eqn (2.3.17) in the form $V'_{so} = V_{so} \frac{k}{d'}$ (where $d' = d < k$).

The following worked example is an application of the theory just discussed.

Let us consider the case $\frac{d}{D} = 0{,}00071$ of Table 1, where

$\rho_{sa} = 2650 \ (\frac{m^3}{kg})$ (sand)

$\rho \quad = 1000 \ (\frac{m^3}{kg})$ (water)

/d .....

$d = 0{,}50 \times 10^{-3}$ (m)

$D = 0{,}700$ (m)

$g = 9{,}8 \ (\frac{m}{s^2})$

$\nu = 10^{-6} \ (\frac{m^2}{s})$

$C_d = 1{,}7$

$f_o = 0{,}0255$

From Table 3,

$Gr = 2{,}03 \times 10^3$

for $f_o = 0{,}0255$ Figure 20 gives:

$\frac{k}{D} = 0{,}003$

$k = 0{,}0003. \quad D = 2{,}10 \times 10^{-3}$ (m)

Consider another pipe with diameter D_1 and absolute roughness $k_1 = d$, so that:

$$\frac{d}{D} = \frac{k_1}{D_1} = \frac{0{,}5 \times 10^{-3}}{D_1} = 0{,}003$$

Then $D_1 = 0{,}166$ (m)

From Figure 5 for

$\frac{d}{D} = 0{,}003, \ \Phi = \frac{Cd \ Vso^2}{gd} = 4250$

i.e.

$$Vso = (\frac{\Phi \ gd}{Cd})^{\frac{1}{2}} = (\frac{4250 \times 9{,}8 \times 0{,}5 \times 10^{-3}}{1{,}7})^{\frac{1}{2}} = 3{,}45 \text{ (m/s)}$$

Because $k_1 = d$ one should expect

$Vso \approx Vo$

/In .....

In fact

from Figure 4:

for $Gr = 2,03 \times 10^3$ and $\rho_{sa} = \rho_m$

$$Vo = \frac{Re^* m d}{d} \nu \left(1 - \frac{d}{D}\right)^{3,5} \left(\frac{8}{f_o}\right)^{\frac{1}{2}} =$$

$$\frac{93 \times 10^{-6}}{0,5 \times 10^{-3}} (1-0,003)^{3,5} \times \left(\frac{8}{0,0255}\right)^{\frac{1}{2}} = \underline{3,25} \quad (m/s)$$

i.e., Vo is in good agreement with Vso.

Keeping $\frac{k_1}{D_1} = 0,003$ constant, the pipe diameter is now increased to its original value $D = 0,700$ m and k_1 to its actual value $k = 2,1 \times 10^{-3}$ m.

Then the mean velocity of the stream must be increased in the ratio

$$\frac{k}{d} = \frac{0,0021}{0,0005} = 4,20$$

i.e.

$$V'_{so} = Vso \ \frac{k}{d} = 3,45 \times 4,20 = 14,50 \text{ m/s}$$

For $V'_{so} = 14,50$ m/s

$$\Phi so = \frac{Vs_o^2 C_d}{gd} = \frac{14,5^2 \times 1,7}{9,8 \times 0,5 \times 10^{-3}} = 72000$$

For $\Phi so = 72000$ one can read in Figure 5 the value $\frac{d}{D} = 0,00071$ in full agreement with the practical value of this ratio.

It is finally of importance to define a lower limit of validity for eqn (2.3.3), in relation to the size of the particle.

/Eqn .....

Eqn (2.3.3) with equation (2.3.1) can be rewritten as follows:

$$\frac{d}{D} = 0{,}215 \left(\frac{gd}{C_d}\right)^{\frac{1}{2}} \frac{1}{V'_{so}} \qquad (2.3.3) \text{ (repeated)}$$

(Note that the symbol Vso is now replaced by V'_{so} because $d < k$)

In the range of the small particles where the Stokes law is valid (i.e. for $Re < 1$), the Stokes equation combined with (2.2.8) yields the following (cf. ref. 7)

$$C_d = \frac{24}{Re} \qquad (2.4.3)$$

with $Re = \frac{d\, v_{se}}{\nu}$

then one can write

$$\frac{d}{D} = 0{,}215 \left(\frac{gd}{\frac{24}{Re}}\right)^{\frac{1}{2}} \frac{1}{V_{so}}$$

Moreover, the expression C_d written above, when introduced in (2.2.8), yields:

$$Gr = 18\, Re \qquad (2.4.4)$$

(2.4.4) introduced into the previous one, gives:

$$\frac{d}{D} = 0{,}215 \left(\frac{gd}{24}\, \frac{Gr}{18}\right)^{\frac{1}{2}} \frac{1}{V_{so}}$$

or

$$\frac{d}{D} = 0{,}215 \left(\frac{gd}{18 \times 24} \times \frac{gd^3}{\nu^2} \frac{\rho_m - \rho}{\rho}\right)^{\frac{1}{2}} \frac{1}{V_{so}}$$

from which, with the position $V_{so} = V'_{so}$

$$V'_{so} = 0{,}01 \frac{gd}{\nu} D \left(\frac{\rho_m - \rho}{\rho}\right)^{\frac{1}{2}} \qquad (2.3.3) \text{ (modified)}$$

valid for $Re < 1$.

/From .....

From eqn (2.3.3)(modified), it would appear that V'_{so} becomes very small with the size of the particle, a condition imposed by the large increase in the drag coefficient C_d.

However, there is a lower limit to V'_{so} fixed by the numerical value m of the Reynolds number of the stream

$$RE = \frac{V'_{so}\, D}{\nu} \geq m$$

at which the friction factor f cannot be considered any more a constant ($\frac{k}{D}$ fixed).

For $RE \ll m$, the boundary layer thickness δ increases and consequently the velocity at the particle (situated as in Figure 3-C-2°) drops.

Consequently, the stream velocity must be increased in proportion in order to be able to dislodge the particle from its pocket.

Taking as an example the case $\frac{d}{D} = 0{,}00071$ from Table 1
for
$f_o = 0{,}0255$ and
$D = 0{,}700$ (m)
one gets
$k = 2{,}10 \times 10^{-3}$ (m)
for
$\frac{k}{D} = \frac{2{,}10}{0{,}700} \times 10^{-3} = 0{,}003$
one can determine, from Figure 20,
$RE = \frac{V^2_{so}\, D}{\nu} = m \approx 10^6$

Being the kinematic viscosity of water

$$\nu = 10^{-6}\ (\frac{m^2}{s})$$

/33 .....

$$V'_{so\ min.} = \frac{\nu}{D} \quad m = 10^{-6} \times 10^{6} \times 0{,}700 = 0{,}7 \ (m/s)$$

Then from (2.3.3) (modified) one gets

$$d_{min} = 100 \frac{V'_{somin}\nu}{gD} \left(\frac{\rho}{\rho_m - \rho}\right)^{\frac{1}{2}} =$$

$$\frac{100 \times 0{,}70 \times 10^{-6}}{9{,}8 \times 0{,}700} \times (2{,}5)^{\frac{1}{2}} = 1{,}6 \times 10^{-5} \ (m)$$

$d = 1{,}6 \times 10^{-5}$ (m) is the minimum diameter which is still applicable to eqn (2.3.3).

3. PARTICLE EQUILIBRIUM CONDITIONS STUDIED BY MEANS OF THE PROFILE OF THE UNDISTURBED STREAM

3.1. The lift on a particle expressed by means of the circulation

The lift force on a body in a two-dimensional flow, discussed in paragraph 1.3, is now extended to the spherical particle.

A pipe of very large diameter D and a particle placed at a distance z_c from the bottom are shown in Figure 6, once in a longitudinal section (Figure 6-A), and once in a transversal section (Figure 6-B) of the pipe.

The velocity at z_c is v_c; the velocity profile across the pipe is assumed to be logarithmic, i.e. for smooth pipes (I) it is expressed by eqns (1.4.1) (Ia) and (1.4.1) (Ib), for rough pipes (II) by eqns (1.4.1) (IIa) and (1.4.1) (IIb).

The velocity gradient in correspondence to the particle is

$$tg\ \gamma = \left(\frac{dv_c}{dz}\right)_{z = z_c} \qquad (3.1.1)$$

The velocity at a point at distance z from the wall is

$$v_z = v_c + (z - z_c) \left(\frac{dv}{dz}\right)_{z = z_c} \qquad (3.1.2)$$

/The .....

The increase in velocity between z_c and z is v_t =

$$(z - z_c) \left(\frac{dv}{dz}\right)_{z = z_c} \qquad (3.1.3)$$

An elementary spherical segment of angular amplitude $d\beta$, latitude β, and distance from the particle centre $z-z_c$ (cf. Figure 6-B), has an elementary area:

$$dS = 2\pi \ (z-z_c) \ (z_1-z_c) \ d\beta$$

and when projected horizontally:

$$dS' = 2\pi(z-z_c) \ (z_1-z_c) \cos\beta \ d\beta \qquad (3.1.4)$$

Then, according to eqn (1.3.4), the amount of circulation enveloping the surface projected (which is $d\beta$ in extent) is:

$$d\Gamma = 2\pi \ (z-z_c)^2 \ (z_1-z_c) \cos \beta \left(\frac{dv}{dz}\right)_{z = z_c} d\beta$$

Writing

$z-z_c = (z_1-z_c) \cos\beta$

and integrating, one obtains

$$\Gamma = 2 \times 2\pi \int_0^{\frac{\pi}{2}} (z_1-z_c)^3 \cos^3\beta \left(\frac{dv}{dz}\right)_{z = z_c} d\beta \qquad (3.1.5)$$

where the factor 2 denotes that integration has been extended to both hemispheres.

From eqns (1.4.1) (I.a) or (1.41) (II.a), i.e. for a particle in the turbulent region ($z_c > \delta$ or $z_c > k$), one obtains:

$$\left(\frac{dv}{dz}\right)_{z = z_c} = \frac{5{,}75 \ v_*}{z_c} \qquad (3.1.6)\ (a)$$

/For .....

For a particle inside the boundary layer one obtains for smooth pipes (I) and from eqn (1.4.1) (I.b):

$$\left(\frac{dv}{dz}\right)_{z = z_c} = 5{,}50 \ \frac{v*}{\delta} = 5{,}50 \ \frac{v_*^2}{\nu} \ ; \ (z_c < \delta) \ ; \ (3.1.6)(I.b)$$

For rough pipes (II) and from eqn (1.4.1) (II.b):

$$\left(\frac{dv}{dz}\right)_{z = z_c} = 8{,}50 \ \frac{v*}{k} = 8{,}50 \ \frac{v*^2}{\nu} \ ; \ (z_c < k); \ (3.1.6)(II.b)$$

Let us consider a particle inside the turbulent region (case a):

Substitution of (3.1.6)(a) into (3.1.5) yields:

$$\Gamma_{zc} = \frac{4\pi \ x \ 5{,}75}{z_c} \ v_* \ (z_1 - z_c)^3 \int_0^{\frac{\pi}{2}} \cos^3 \beta \ d\beta$$

Then, putting $z_1 - z_c = \frac{d}{2}$

and calculating the integral

$$\int_0^{\frac{\pi}{2}} \cos^3\beta \ d\beta = \left(\operatorname{Sin}\beta - \frac{1}{3} \operatorname{Sin}^3\beta\right)_0^{\frac{\pi}{2}} = \frac{2}{3}$$

the final expression of the circulation relative to a particle in the turbulent region (case a) is arrived at:

$$\Gamma_{zc} = \frac{5{,}75}{3} \ \pi \frac{d^3 v_*}{z_c} \qquad (3.1.7((a)$$

By analogy, in the case of a particle inside the boundary layer (case b), expression (3.1.6) (I.b) substituted into (3.1.5) yields, for smooth pipes (I):

$$\Gamma_{zc} = \frac{5{,}50\pi}{3} \ d^3 \ \frac{v_*}{\delta} = \frac{5{,}50\pi}{3} \ d^3 \ \frac{v_*^2}{\nu} \ ; (z_c < \delta) \ (3.1.7)(I.b)$$

/The .....

The same reasoning for rough pipes (II) yields:

$$zc = \frac{8,50}{3}\,\pi d^3\,\frac{v_*}{k} = \frac{8,50\pi}{3}\,d^3\,\frac{v_*^2}{\nu}\,;(z_c<k) \qquad (3.1.7)(II.b)$$

By combining equations (3.1.7) and (1.3.2), one arrives at an expression of the lift force F_{zc} for a stationary particle placed in a stream at a distance z_c from the wall.

This is:

(I) For smooth pipes
in the turbulent region (a)

$$F_{zc} = \frac{5,75}{3}\,\frac{\pi d^3}{z_c}\,v_*^2\,\rho\,(5,50 + 5,75\,\lg\frac{z_c}{\delta});\ (z_c>\delta);\ \underset{(I.a)}{(3.1.8)}$$

inside the boundary layer (b)

$$F_{zc} = \frac{5,50}{3}^2\,\rho\pi\,d^3\,\frac{v_*^2}{\delta^2}\,z_c = \frac{5,50^2\rho\pi\,d^3}{3}\,\frac{v_*^4}{\nu^2}\,z_c;\ (z_c<\delta);$$
$$(3.1.8)(I.b)$$

(II) For rough pipes:
in the turbulent region (a)

$$F_{zc} = \frac{5,75}{3}\,\frac{\pi d^3}{z_c}\,v_*^2\,\rho\,(8,50 + 5,75\,\lg\frac{z_c}{k});\ (z_c>k);$$
$$(3.1.8)(II.a)$$

inside the boundary layer (b)

$$F_{z_c} = \frac{8,50}{3}^2\,\rho\pi d^3\,\frac{v_*^2}{k^2}\,z_c = \frac{8,50}{3}^2\rho\pi\,d^3\,\frac{v_*^4}{\nu^2}\,z_c;\ (z_c<k)$$
$$(3.1.8)(II.b)$$

The previous expressions, when referring to a particle in contact with the wall, i.e. for $z_c = \frac{d}{2}$, yield the following:

/(I.a) .....

(I.a)

$$F_{x\,d/2} = \frac{5,75}{3}\ 2\,\pi d^2\ v_*^2\,\rho\,(5,50 + 5,75\ \lg \frac{d}{2\delta});\ (\frac{d}{2} > \delta\ );$$

(3.1.8) (I.a) (bis)

(I.b)

$$F_{x\,d/2} = \frac{5,50}{3}^2\ \rho\ \frac{\pi d^4}{2}\ \frac{v_*^2}{\delta^2} = \frac{5,50}{3}^2\ \rho\ \frac{\pi d^4}{2}\ \frac{v_*^4}{\nu^2};\ (\frac{d}{2} < \delta\ );$$

(3.1.8) (I.b) (bis)

(II.a)

$$F_{x\,d/2} = \frac{5,75}{3}\ 2\ \pi d^2\ v_*^2\,\rho\,(8,50 + 5,25\ \lg \frac{d}{2k});\ (\frac{d}{2} > k);$$

(3.1.8) (II.a) (bis)

(II.b)

$$F_{x\,d/2} = \frac{8,50}{3}^2\ \rho\ \frac{\pi d^4}{2}\ \frac{v_*^2}{k^2} = \frac{8,50}{3}^2 \rho \frac{\pi d^4}{2}\ \frac{v_*^4}{\nu^2};\ (\frac{d}{2} < k);$$

(3.1.8) (II.b) (bis)

Conclusion

The expressions obtained for the lift force on a particle contain only quantities typical of the stream and of the particle without the presence of any experimental coefficient representing mutual interaction.

They express the lift force as a function of the particle radial distance z_c from the wall, which in the case of contact acquires the value $z_c = \frac{d}{2}$.

/3.2. .....

3.2. The stream potential function for the lift force

The expression for the lift force derived in the previous paragraph is used here for the calculation of its potential function.

Initial conditions must be defined in relation to the lift force on the particle when balancing the force due to gravity.

With the introduction of a parameter ψ, which takes into consideration the geometry of the stream providing equilibrium, equality between lift force and the force due to gravity can be expressed as follows:

$$\psi \; F_{\chi\, d/2} = (\rho m - \rho) \; g \frac{\pi d^3}{6} \quad , \tag{3.2.1}$$

this for $v_* = v_{*o}$ and $z_c = \frac{d}{2}$

The work produced by the lift force when moving the particle upwards is equal to the work done against the force due to gravity, increased by the particle kinetic energy.

The rotational energy imparted to the particle has been neglected in the present study.

If v''_{zc} is the particle forward velocity, this can be related to the local velocity of the stream v_{zc} by a slip coefficient λ ($o < \lambda < 1$) i.e.

$$v''_{zc} = v_{zc} (1 - \lambda) \tag{3.2.2}$$

/The .....

The balance can then be written as follows:

$$\int_{\frac{d}{2}}^{z_1} \psi F_{\lambda zc} \, dz_c = (\rho_m - \rho) \frac{\pi_d^3}{6} g \int_{\frac{d}{2}}^{z_1} dz_c + \frac{1}{2} \rho_m$$

$$\frac{\pi_d^3}{6} v_{zl}^2 (1-\lambda)^2 \qquad (3.2.3)$$

where v_{zl} is the velocity of the stream at a distance $z_1 = z_c$ from the wall, corresponding to the particle centre position at that particular instant.

In the practical calculation of the energy equation (3.2.3), only the case of smooth pipes (I) within the turbulent region (a) and within the boundary layer (b), is worked out in detail.

Corresponding expressions for rough pipes will be derived by inspection.

The initial condition for eqn (3.2.3) can be defined easily by noting that at the origin of the particle trajectory $\lambda = 1$, i.e. the particle is lifted from a position of rest, for which the slip in velocity is 1.

Then the derivative of eqn (3.2.3) against z_c yields for $z_c = \frac{d}{2}$ eqn (3.2.1), from which ψ can be calculated.

Carrying out the calculation in detail for smooth pipes (I)

Case (a)

$F_{\lambda zc}$ is expressed by means of (3.1.8) (I.a), $F_{\lambda \frac{d}{2}}$ by (3.1.8) (I.a)(bis)

v_{zc} by means of (1.4.1) (I.a)

/These .....

These substitutions in (3.2.3) and integration between the limits $z_c = \frac{d}{2}$ and $z_c = z_1$ provide:

$$\frac{\left(5{,}50 \lg \frac{z_c}{\delta} + \frac{5{,}75}{2} \lg^2 \frac{z_c}{\delta}\right)_{\frac{d}{2}}^{z_1}}{5{,}50 + 5{,}75 \lg \frac{d}{2\delta}} = \left(\frac{z_c}{\frac{d}{2}}\right)_{\frac{d}{2}}^{z_1} + \frac{1}{2} \frac{\rho_m}{\rho_m - \rho} \frac{v_*^2}{g \frac{d}{2}}$$

$$(5{,}50 + 5{,}75 \lg \frac{z_1}{\delta})^2 (1 - \lambda)^2 \qquad (3.2.4)(\text{I.a})$$

where with a new symbol ψ'_{Ia}:

$$\psi'_{Ia} = \frac{1}{5{,}50 + 5{,}75 \lg \frac{d}{2\delta}} \qquad (3.2.5)(\text{I.a})$$

The expressions written above are valid in the interval

$$\delta \leqslant \frac{d}{2} \leqslant z_c \leqslant z_1$$

Case (b)

$F_{\lambda zc}$ is expressed by means of (3.1.8) (I.b)

v_{zc} by means of (1.4.1) (I.b), $F_{\lambda \frac{d}{2}}$ by (3.1.8) (I.b) (bis)

Substitution in eqn (3.2.3) and integration (after division of both members by $(\frac{d}{2\delta}^2)$ yield:

$$\frac{1}{2}\left[\left(\frac{\frac{z_c}{\delta}}{\frac{d}{2\delta}}\right)^2\right]_{\frac{d}{2}}^{z_1} = \left(\frac{\frac{z_c}{\delta}}{\frac{d}{2\delta}}\right)_{\frac{d}{2}}^{z_1} + \frac{1}{2} \frac{\rho_m}{\rho_m - \rho} \frac{v_{*o}^2}{g \frac{d}{2}} \overline{5{,}50}^2 (\frac{z_1}{\delta})^2 (1 - \lambda)^2$$

(3.2.4)(I.b)

where $\psi'_{Ib} = \frac{1}{\frac{d}{2\delta}}$ with a new symbol ψ'_{Ib} : (3.2.5)(I.b)

The expressions written above are valid in the interval

$$0 \leqslant \frac{d}{2} < z_c \leqslant z_1 \leqslant \delta$$

/A .....

A first remark about eqns (3.2.4) (I.a) and (3.2.4) (I.b) is that the derivatives of their left-hand members coincide at the point $z_c = \frac{d}{2} = \delta$

This means that it is possible to continue the two functions, one into the other, without discontinuity in the value of the lift forces when moving from the laminar to the turbulent region of the flow.

Equivalent expressions for rough pipes (II) can be derived by inspection of the previous ones (I), by replacing the constant 5,50 with the new constant 8,50 and δ with k.

Consequently, for rough pipes (II):

Case (a): (inside the turbulent region)

$$\frac{(8{,}50 \lg \frac{z_c}{k} + \frac{1}{2} \cdot 5{,}75 \lg^2 \frac{z_c}{k})_{\frac{d}{2}}^{z_1}}{8{,}50 + 5{,}75 \lg \frac{d}{2k}} = \left(\frac{z_c}{\frac{d}{2k}}\right)_{\frac{d}{2}}^{z_1} + \frac{1}{2} \frac{\rho_m}{\rho_m - \rho} \frac{v_*^2}{g \frac{d}{2}}$$

$$(8{,}50 + 5{,}75 \lg \frac{z_1}{k})^2 (1 - \lambda)^2 \qquad (3.2.4)(II.a)$$

where:

$$\psi'_{IIa} = \frac{1}{8{,}50 + 5{,}75 \lg \frac{d}{2k}} \qquad (3.2.5)(II.a)$$

The expressions written above are valid in the interval

$$k \leqslant \frac{d}{2} \leqslant z_c \leqslant z_1$$

/Case (b) .....

Case (b): (inside the boundary layer).

$$\frac{1}{2}\left[\left(\frac{\frac{z_c}{k}}{\frac{d}{2k}}\right)^2\right]_{\frac{d}{2}}^{z_1} = \left(\frac{\frac{z_c}{k}}{\frac{d}{2k}}\right)_{\frac{d}{2}}^{z_1} + \frac{1}{2}\frac{\rho_m}{\rho_{m-p}}\frac{v_{*o}^2}{g\frac{d}{2}}\overline{8,50}^2\left(\frac{z_1}{k}\right)^2(1-\lambda)^2 \qquad (3.2.4)(II.b)$$

where

$$\Psi'_{IIb} = \frac{1}{\frac{d}{2k}} \qquad (3.2.5)(II.b)$$

Conclusion

Two energy equations, one for smooth pipes and one for rough pipes, have been established from consideration of equilibrium at the boundary and from the expression of the lift force calculated by means of the circulation around the particle.

The initial condition of these energy equations has been defined in relation to the geometrical position of the particle centre and to the critical friction velocity providing equilibrium between the forces on the particle.

3.3. Discussion of the stream potential function

A graphical representation of the stream potential function for smooth (I) and rough (II) pipes is shown in Figures 7 and 8 respectively.

In the diagram of Figure 7 the first members of the following eqns are plotted:

/43 .....

$$\left(5{,}50 \lg \frac{z_c}{\delta} + \frac{5{,}75}{2} \lg^2 \frac{z_c}{\delta}\right)_{\frac{d}{2}}^{z_1} = \frac{1}{\psi_{Ia}'} \left[\left(\frac{z_c}{\frac{d}{2}}\right)_{\frac{d}{2}}^{z_1} + \frac{1}{2} \frac{\rho_m}{\rho_m - \rho} \cdot \frac{v_{*o}^2}{g \frac{d}{2}} \left(5{,}50 + 5{,}75 \lg \frac{z_1}{\delta}\right) (1 - \lambda)^2\right] \qquad (3.2.4)(I.a) \text{ (modified)}$$

and

$$\frac{1}{2}\left[\left(\frac{z_c}{\delta}\right)^2\right]_{\frac{d}{2}}^{z_1} = \frac{1}{\psi_{Ib}'} \left[\left(\frac{\frac{z_c}{\delta}}{\frac{d}{2\delta}}\right)_{\frac{d}{2}}^{z_1} + \frac{1}{2} \frac{\rho_m}{\rho_m - \rho} \frac{v_{*o}^2}{g \frac{d}{2}} \left(5{,}50 \frac{z_1}{\delta}\right) (1-\lambda)^2\right] \qquad (3.2.4)(I.b) \text{ (modified)}$$

where ψ_{Ia}' and ψ_{Ib}' are given by (3.2.5) (I.a) and (3.2.5)(I.b) respectively, and represent initial conditions.

Denoting with u_I the function shown in Figure 7, one obtains:

Inside the boundary layer, i.e. for $o < z_1 < \delta$:

$$u_{Ib} = \frac{1}{2} \left(\frac{z_1}{\delta}\right)^2 \qquad (3.3.1)(I.b)$$

and in the turbulent region, i.e. for $z_1 > \delta$:

$$u_{Ia} = \frac{1}{2} + 5{,}50 \lg \frac{z_1}{\delta} + \frac{5{,}75}{2} \lg^2 \frac{z_1}{\delta} \qquad (3.3.1)(I.a)$$

The preceding considerations can be extended to the case of rough pipes (II) and the corresponding expressions obtained.

$$\left(8{,}50 \lg \frac{z_c}{k} + \frac{5{,}75}{2} \lg^2 \frac{z_c}{k}\right)_{\frac{d}{2}}^{z_1} =$$

$$\frac{1}{\psi_{IIa}'} \left[\left(\frac{z_c}{\frac{d}{2}}\right)_{\frac{d}{2}}^{z_1} + \frac{1}{2} \frac{\rho_m}{\rho_m - \rho} \frac{v_{*o}^2}{g \frac{d}{2}} \left(8{,}50 + 5{,}75 \lg \frac{z_1}{k}\right) (1-\lambda)^2\right]$$

(3.2.4)(II.a) (modified)

/and .....

and

$$\tfrac{1}{2}\left[\left(\frac{z_c}{k}\right)^2\right]_{\frac{d}{2}}^{z_1} = \frac{1}{\psi'_{IIb}}\left[\left(\frac{\frac{z_c}{k}}{\frac{d}{2k}}\right)_{\frac{d}{2}}^{z_1} + \tfrac{1}{2}\,\frac{\rho_m}{\rho_{m-\rho}}\,\frac{v_{*o}^2}{g\frac{d}{2}}\,(8{,}50\,\frac{z_1}{k})(1-\lambda)^2\right]$$

(3.2.4)(II.b) (modified)

where ψ'_{IIa} and ψ'_{IIb} are given by (3.2.5) (II.a) and (3.2.5) (II.b) respectively .

Denoting the function shown in Figure 8 by u_{II}, one obtains:

Inside the boundary layer, i.e. for $o < z_1 < k$:

$$u_{II} = \tfrac{1}{2}\,(\frac{z_1}{k})^2 \qquad (3.3.1)(II.b)$$

and inside the turbulent region, i.e. for $z_1 > k$:

$$u_{II} = \tfrac{1}{2} + 8{,}50\ \lg\frac{z_1}{k} + \frac{5{,}75}{2}\ \lg^2\frac{z_1}{k} \qquad (3.3.1)(II.a)$$

The representation shown in Figure 7 and 8, of the first members of eqn (3.2.4) (modified) is particularly suitable for a graphical description because it is independent of initial conditions, which have been transferred to the second members as factors $\frac{1}{\psi'_{Ia}}$, $\frac{1}{\psi'_{Ib}}$, $\frac{1}{\psi'_{IIa}}$, and $\frac{1}{\psi'_{IIb}}$.

If, in a discussion, the above factors are returned to the first members, the initial slope of the geometrical tangent is always equal to one, as the following expressions of the derivative will prove.

(a) For smooth pipes:

$$\lim_{z_c \to \frac{d}{2}} \frac{d}{dz_c}\ (5{,}50\ \lg\frac{z_c}{\delta} + \frac{5{,}75}{2}\ \lg^2\frac{z_c}{\delta})\psi'_{Ia} = 1 \qquad (I.a)$$

/lim .....

$$\lim_{z_c \to \frac{d}{2}} \frac{d}{d_{zc}} \left(\left[\frac{z_c}{\frac{d}{2}\delta} \right]^2 \right) + Ib = 1 \qquad \text{(I.b)}$$

and similarly for rough pipes.

In the following, only the case of rough pipes (II) will be discussed in detail because of its practical interest.

Conclusions may nevertheless be extended to the case of smooth pipes without further analysis.

The function u_{II} of Figure 8 has a representation which uses either $\frac{z_c}{k}$ or $\frac{d}{2k}$ as current variable.

The value $\frac{d}{2k}$ corresponds to the initial position of the particle centre with the particle somewhere in contact with the wall.

The curve has a point of inflexion in F, i.e. for $\frac{z_c}{k} = 1$ and $\frac{d}{2k} = 1$.

The curve lies entirely below its tangent within the turbulent region($\frac{z_c}{k} > 1$ or $\frac{d}{2k} > 1$) and above its tangent inside the boundary layer region.

Considering the second member of eqns (3.2.4)(II.a) or (II.b) (modified), its first (bracketed) term covers the increase in geodetic height, its second (bracketed) term the increase in kinetic head of the particle.

The condition of particle equilibrium which has been expressed from an experimental point of view by eqn (2.2.14), is here discussed again in relation to the potential function.

/The .....

The following conventions are introduced for a correct evaluation of the term $(1 - \frac{d}{D})$ of eqn (2.2.14).

The crest of the pipe irregularities is taken as origin of the pipe diameter D, so that for all particles of dimensions $\frac{d}{2k} \leq 1$,

the term $1 - \frac{d}{D} = 1$.

This convention can be transferred to the case of smooth pipes by putting $D = D' - 2\delta$, δ being the boundary layer thickness and D the pipe geometrical diameter.

Then one can rewrite eqn (2.2.14) in a slightly modified form as follows:

$$\frac{4Gr}{Re_{*o}^2} \frac{(1 - \frac{d}{D})^7}{\left(\frac{\rho_{sa} - \rho}{\rho_m - \rho}\right)^{3/2}} = 4 \frac{gd}{v_{*o}^2} \frac{\rho_m - \rho}{\rho} \frac{(1 - \frac{d}{D})^7}{\left(\frac{\rho_{sa} - \rho}{\rho_m - \rho}\right)^{3/2}} = 1 \quad (2.2.14) \text{ (modified)}$$

Considering a direction vector indicator t, tangent to the curve at a point Q, this indicator represents the condition of equilibrium for a particle with a diameter d_Q (in the case of the figure $\frac{d_Q}{2k} = 20$), provided the friction velocity v_{*o} satisfies eqn (2.2.14).

The geometrical condition that the indicator is a tangent at Q is automatically verified for $v_* = v_{*o}$ by the value assumed by factor ψ'_{IIa}, as previously explained.

The curve u_{II} divides the plane into an upper region characterized by values $v_* < v_{*o}$, and a lower region characterized by values $v_* > v_{*o}$ (this with the convention of measuring the angle of the indicator from the Y axis).

/A .....

A particle will be stable at the boundary only in the upper region where the force due to gravity exceeds the lift force.

In the lower region it will be forced to leave the boundary for the stream because of excess lift force.

However the tendency to stability or instability for small variations of the friction velocity around its critical value v_{*o}, i.e. for $v_* = v_{*o} + \Delta v_{*o}$ or $v_* = v_{*o} - \Delta v_{*o}$, where Δv_{*o} is a rather small quantity, changes considerably with the size of the particle, i.e. with the value $\frac{d}{2k}$.

Let us consider the phenomena in a pipe of very large diameter such that $\frac{d}{D} \approx o$ (whatever value of d is considered), or in a large conduit of rectangular section of considerable depth and infinite width.

Let the roughness k of the wall or of the conduit bottom be a constant, while the particle diameter is made to vary in the following ranges:

1) $\frac{d}{2k} \gg 1$

2) $\frac{d}{2k} \approx 1$

3) $\frac{d}{2k} \ll 1$

for k constant.

1) For $\frac{d}{2k} \gg 1$, as at point Q, for $v_* = v_{*o} + \Delta v_{*o}$ the indicator does not intersect the curve u_{II} further to the right and consequently the force due to gravity can never exceed the lift force once the particle is in the stream.

/Conditions .....

The particle therefore is carried away in full suspension.

2) For $\frac{d}{2k} \approx 1$ as at point R, one might have instability of the equilibrium even for $v_* = v_{*_o}$ because the indicator tangent to the curve leaves the curve above (see also Figure 8, detail A).

Consequently, for $v_* = v_{*_o}$ the particle is likely to leave the boundary.

If the directed indicator t_R is shifted parallel to itself, it determines another point of tangency P on u_{II}. Its ordinate PT = PS + ST represents the maximum total height reached by the particle, where TS is the geodetic and $\overline{PS}$ the kinetic fraction of the total height. Because the indicator t_R intersects the curve u_{II} further down at U, definitely at this point and probably even before, the force due to gravity will exceed the lift force and the particle will begin a downwards movement towards the boundary. When reaching the wall practically all of its kinetic energy will be lost on impact. However, instability at the boundary will force the particle back into the stream, giving rise to a well known phenomenon of recurrent trajectories called "saltation".

Saltation is a transport phenomenon typical of a particle with dimensions not much different from the pipe roughness.

/If .....

If $\frac{d}{2k} < 1$, saltation can occur even in the condition of equilibrium critical velocity $v_* = v_{*o}$.

If $\frac{d}{2k} > 1$, i.e. with a particle centre in a position to the right of point F, the friction velocity providing saltation must exceed its critical value somewhat, i.e.

$$v_* = v_{*o} + \Delta v_{*o}$$

3) The case $\frac{d}{2k} << 1$, deals with particles well inside the boundary layer of the stream.

The particle could be placed in the pocket between two contiguous irregularities of a solid contour or the boundary could be made of a bed of coarse particles, with smaller particles of the same or a different material embedded in between (river beds).

Denoting with v_{*od} the particle corresponding critical velocity (i.e. that one calculated for a particle diameter $d << 2k$), the following assumption is introduced.

Whatever the value of the pipe roughness k may be, the critical velocity v_{*od} providing equilibrium of the forces on the particle is considered invariant, i.e. depending on the particle diameter only and not on the depth of the pocket in which the particle is placed (cf. Figure 3-C case 2^o).

Then the friction velocity (at the crest of the irregularities of height k), can be expressed as follows:

$$v_{*k} = \frac{k}{d} \; v_{*od} \qquad (3.3.2)$$

/This .....

linear
This is subject to the assumption that a distribution of velocity takes place inside the pocket (cf. Figure 3-C-2 section S - S).

By means of eqn (2.2.14) (modified), according to the conventions $1 - \frac{d}{D} = 1$, the putting of the critical friction velocity v_{*od} (i.e. relative to a particle of dimension d) can be related to the critical friction velocity v_{*ok} of a particle with dimensions $d' = k$ (i.e. equal to the pipe roughness), as follows:

$$\frac{v_{*od}}{v_{*ok}} = \left(\frac{d}{k}\right)^{\frac{1}{2}} \qquad (3.3.3)$$

Elimination of v_{*od} between eqns (3.3.2) and (3.3.3) yields

$$\frac{v_{*k}}{v_{*ok}} = \left(\frac{k}{d}\right)^{\frac{1}{2}} \geqslant 1 \qquad (3.3.4)$$

For a correct interpretation of eqn (3.3.4), the meaning of symbols is repeated in the following.

v_{*k} is the friction velocity (at the crest of the irregularities) which can lift a particle of size d ($d<k$) to lift from a pocket of height k.

v_{*ok} is the friction velocity (satisfying eqn (2.2.14) (modified))relative to a particle of the same diameter d' as the pipe roughness k.

This velocity v_{*ok} in a pipe originally smooth but covered with a solid deposit of these particles $d' = k$, would lift these from the bed.

In the case of a pipe covered with grains of coarse sand of size k, entrailing particles of fine sand of size d,

/the .....

the above expression (3.3.4) proves that the removal of fine sand is possible only after some grains of the coarse sand have been swept away by the stream.

This is so because $v_{*ok} < v_{*k}$.

However, eqn (3.3.4) may not hold when the finer particles are lighter than the coarse material (e.g. fine coal placed between coarse sand).

Denoting the densities relative to the material of size k and d by ρ_k and ρ_d ($\rho_k > \rho_d$; $k > d$), one obtains by again using eqns (2.2.14) (modified) and (3.3.2)

$$\frac{v_{*k}}{v_{*ok}} = \left(\frac{k}{d}\right)^{\frac{1}{2}} \left(\frac{\rho d - \rho}{\rho_k - \rho}\right)^{\frac{1}{6}} \gtrless 1$$

For $\frac{v_{*k}}{v_{*ok}} = 1$, both the large particles with diameter k and the smaller particles with diameter $d < k$ are lifted from the boundary with the same friction velocity.

The discriminating condition is given by

$$\frac{k}{d}\left(\frac{\rho d - \rho}{\rho_k - \rho}\right)^{\frac{1}{3}} = 1.$$

In the case of fine coal and coarse sand in water

$\rho_d - \rho = 0{,}40$; $\rho_k - \rho = 1{,}65$

$$\frac{k}{d} = \left(\frac{1{,}65}{0{,}40}\right)^{\frac{1}{3}} = 1{,}60$$

$$d_{coal} = \frac{k}{1{,}60}$$

Removal of particles by the mechanics of erosion, as just described, produces two kinds of material transport in

/practice .....

practice (see Figure 9A):

1) The fine particles have an indicator which, being tangent to u_{II}, e.g. at P (where at P, $d = \frac{k}{2}$,) gives an intersection with curve u_{II} which is far away (and not representable on the scale of Figure 9A), if any intersection is possible.
(Note that the slope of the indicator at P fixes the friction velocity v_{*k} at the crest of the pipe irregularities, this being the friction velocity able to lift the fine particles of sand from the pockets made by the larger particles, which are assumed to form a fixed matrix, e.g. by glueing them together).

Consequently, the small particles travel a considerable distance inside the stream before dropping to the boundary if full suspension is not achieved (as in the case of dust).

The coarse particles have an indicator which is tangent to u_{II} at F and consequently they hardly move away from the boundary (intersection with u_{II} very near to F).

Conclusion

A stream potential function has been established for smooth and rough pipes.

The stream potential function is divided by a point of inflexion into two branches, one covering the boundary layer flow region ($\frac{d}{2k} < 1$,) and one the turbulent flow region $\frac{d}{2k} > 1$ of the stream.

/The .....

The stream potential is defined as a function of both $\frac{d}{2k}$, a parameter representing the initial position of the particle, and $\frac{z_c}{k}$, the variable, representing the geodetic height reached by the particle in its trajectory. Moreover the additional condition is valid:

$$\frac{d}{2k} \leq \frac{z_c}{k} \leq z_1$$

The stream potential function has a geometrical tangent at the origin of the particle trajectory which implies a condition of equilibrium for the vertical forces acting on the particle. This condition is expressed by a critical friction velocity $v_* = v_{*o}$.

Particle equilibrium for $v_* = v_{*o}$ is stable in the region $\frac{d}{2k} > 1$

A single particle of dimensions $\frac{d}{2k} \gg 1$ when the friction velocity exceeds its critical value somewhat ($v_* > v_{*o} + \Delta v_{*o}$) is likely to be transported by the stream in full suspension.

For a single particle of dimension $\frac{d}{2k} \approx 1$, but still with $\frac{d}{2k} > 1$, an excess friction velocity ($v_* = v_{*o} + \Delta v_{*o}$) is causes particle saltation, i.e. a short trajectory is followed.

The saltation tendency increases for increased instability of the equilibrium at the boundary, i.e. in the region near and to the left of point F, where still $\frac{d}{2k} \approx 1$, but with a value for $\frac{d}{2k} < 1$.

Here particles are saltation prone even for values of friction velocity $v_* = v_{*o} + \delta v_{*o}$ and differing very little from equilibrium.

/The .....

The equilibrium of a particle well inside the boundary layer($\frac{d}{2k} \ll 1$) in the presence of a rigid boundary of the wall asperities has also been expressed.

A particle leaves the pocket between two irregularities because of the high value reached by the friction velocity at the crest of the irregularities, the velocities at the particle and at the crest having been related by means of the ratio $\frac{d}{k}$.

The particle, when pushed outside the boundary layer, travels deep into the stream and returns to the boundary after a long trajectory, or may not return at all (full suspension).

Finally, the removal mechanism of particles embedded in a collapsible boundary of larger particles such as small particles of sand entrained in coarse sand, has been made dependent primarily on the removal by scouring of the coarse fraction.

Two kinds of transport trajectories have been forecast: one short-spanned for the coarse sand, one long-spanned for the fine sand, with deep penetration into the stream and the possibility of full suspension (powder).

3.4. The artificial boundary corresponding to solid deposits - formation of dunes and ripples

The discussion has been concerned so far with the mechanics of a single particle and its behaviour in relation to the boundary condition of roughness.

Conduits of very large diameter or canals of great depth and infinite width, compared to particle diameter, were assumed.

/The .....

The equilibrium of a particle when situated in a bed of other similar particles will be studied under the same conditions.

If k is the original roughness of the boundary, let us assume two instances in which a bed will contain particles:

1) with particle size much greater than k

   $(\frac{d}{2k} \gg 1)$ (Figure 9-B-1) and

2) with particle size much smaller than k $(\frac{d}{2k} \ll 1)$ (Figure 9-B-2)

Suppose that case 1 corresponds to point Q of Figure 8, i.e. to a particle with ratio $\frac{d}{2k} = 20$.

If v_{*ol} is the critical friction velocity for $d = d_1$ (where $\frac{d_1}{2k} = 20$), one obtains from eqn (2.2.14) (modified)

$$v_{*ol} = v_{*ok} \left(\frac{d_1}{k}\right)^{\frac{1}{2}} = v_{*ok} (10)^{\frac{1}{2}} = 3{,}3\ v_{*ok}$$

For $v_* < v_{*ol}$ particles will pile up at the boundary in a single-double layer, etc., restricting the free area of the pipe until the decrement in stream velocity causes an increase in bed height to such an extent that it balances with its reduction in area the decrement in stream velocity.

At this stage the condition $v_* = v_{*ol}$ will be verified again.

The roughness of the pipe corresponds more or less to that of a canal with a bed of roughness d_1 (cf. Figure 9-B-1).

/Flow .....

Flow on a particle bed of the type shown involves a friction factor $f_1 > f_k$, f_k being the friction factor relative to the initial roughness of the pipe k.

Case 2, dealing with particles much finer than the pipe roughness k, can be discussed along the same lines.

For a friction velocity v_* smaller than the friction velocity which is able to raise a particle from its pocket, particles will be deposited between the humps of the irregularities, building up a bed of particles.

Denoting by v_{*o2} the critical friction velocity typical of the size of the particle, this will ultimately be reached through the decrement of the free area.

From eqn (2.2.14) (modified), one can express v_{*o2} as follows:

$$v_{*o2} = v_{*ok} \left(\frac{d}{k} 2 \right)^{\frac{1}{2}}$$

under the condition $\frac{d}{D} \to 0$

The flow takes place along a bed of fine particles with a friction factor f_2 considerably smaller than f_k ($f_2 < f_k$). (cf. Figure 9-B-2).

In describing the modifications of the bed profile caused by velocity disturbances, one may mention ripples and dunes.

Ripples are herein defined as undulations having a height of only a few particle diameters.

Dunes are undulations having a height of many particle diameters.

/The .....

The presence of a large or small roughness as in cases 1 and 2 must be associated with the magnitude of the velocity gradient at the wall.

In the presence of solid deposits, the particle dimension d replaces the pipe roughness k. Consequently the smaller $\frac{d}{D}$, the greater will be the velccity gradient at the boundary, in other words for $\frac{d}{D} \to 0$ the velocity profile will approach the rectangular shape more and more.

This is expressed graphically in Figure 9A by increasing the slope of the fundamental curve u_{II} in the ratio $\frac{D_2}{D} = 4$ for u_{II2} and in the ratio $\frac{D_1}{D} = \frac{1}{4}$ for u_{III}, being D_2 and D_1, two new pipe diameters.

For d = k = constant, let us have two velocity disturbance functions of the pipe length L: $\Delta\, v_{*o}\,(L)$ and $\delta v_{*o}\,(L)$, being Δ of one order of magnitude greater than δ.

Then one can express velocity conditions at F in both cases as follows

$$\frac{v_*}{v_{*o}} = \frac{v_{*o} \pm \Delta\, v_{*o} \pm \delta v_{*o}}{v_{*o}} = 1 \pm \Delta \pm \delta$$

The different slopes of the potential function at F can simply be eliminated by introducing an amplification factor β of the disturbance.

In case 1 , i.e. for a bed of particles with large ratio $\frac{d}{D_1}$, because of the low value of the velocity gradient, β appears in the denominator as $\frac{1}{\beta}$.

/In .....

In case 2, i.e. for a very small ratio $\frac{d}{D_2}$ a large value of the velocity gradient, β is a multiplier.

In symbols:

case 1: $\frac{v_{*1}}{v_{*o1}} = 1 \pm \frac{1}{\beta}\Delta \pm \frac{1}{\beta}\delta$ $\qquad (D_1 = \frac{D}{4})$

case 2: $\frac{v_{*2}}{v_{*o2}} = 1 \pm \beta\Delta \pm \beta\delta$ $\qquad (D_2 = 4D)$

In Figure 9A the indicator t at F must be thought of as moving once in the region of solid deposits, once in the region of particle movement, and once in a position where it is the tangent of curve u_{II}.

The three positions of the indicator correspond to the value

in case 1:

$1 - \frac{1}{\beta}\Delta - \frac{1}{\beta}\delta$

$1 + \frac{1}{\beta}\Delta + \frac{1}{\beta}\delta$

and 1

in case 2:

$1 - \beta\Delta - \beta\delta$

$1 + \beta\Delta + \beta\delta$

and 1.

Assume that the term $\frac{1}{\beta}\Delta$ is of the same order of magnitude as δ, then in case 1 one may write

$$\frac{v_{*1}}{v_{*o1}} = 1 \pm \delta$$

/The .....

The indicator corresponding to the small excess velocity $\frac{v_{*1}}{v_{*ol}} = 1 + \delta$ will produce a particle movement of very short span, which ultimately produces a ripple in the bed.

Consequently, in case 1 the most likely configuration is that of a bed with superimposed ripples.

In case 2, β is large and so both terms of the second member are of importance in the previous eqn, i.e.

$$\frac{v_{*1}}{v_{*ol}} = 1 \pm \beta\Delta \pm \beta\delta$$

The indicator, when corresponding to the large velocity excess $1 + \beta\Delta + \beta\delta$, will produce with its term $\beta\Delta$ particle movement of a long trajectory on which a movement of shorter span due to $\beta\delta$ may be superimposed.

Consequently, in case 2 the most likely configuration of the bed is that of dunes (term $\beta\Delta$) and ripples (term $\beta\delta$).

Dunes are therefore formed only in the case of relatively small particles, i.e. for a small value of the ratio $\frac{d}{D}$.

They may or may not have a superimposed ripple configuration.

As is well known, the stream lifts particles on the positive slope of the dune (disturbance with + sign) and deposits them on the negative slope of the dune (disturbance with - sign).

If the friction velocity is further increased by an increase of the flow rate, the indicator in themiddle

/position .....

position of tangency turns clockwise, i.e. moves into the zone below curve u_{II} where equilibrium is not possible any longer.

In symbols, whenever

$$| v_{*1} | \cdot | 1 \pm \beta\Delta + 1 \pm \beta\delta | > v_{*o}$$

the dune will disappear completely because the stream will pick up particles on both slopes of the dune.

This description is in agreement with the experimental observation.

Conclusion

The formation of dunes and ripples is ascribed to disturbances of the critical friction velocity typical of the bed of particles forming the boundary of the stream.

The presence of dunes with the possibility of superimposition of ripples, is likely to occur in beds of small sized materials, i.e. when large velocity gradients occur at the boundary (velocity profile approaching a rectangular shape).

The formation of ripples is confined to deposits of larger particles with lower boundary velocity gradients.

The particle pipe diameter ratio $\frac{d}{D}$ is the critical parameter controlling either of these phenomena.

/3.5. .....

3.5. The particle lift in a flow belonging to the smooth wall turbulence and to the transition regimes

The laws for smooth-wall flow and for the transition flow in sand-roughened pipes of the Nikuradse type can be represented as a function of the so-called "roughness" or "wall number".

$$Re^*_* = \frac{v^* d}{\nu} \qquad (2.2.4) \quad \text{(repeated)}$$

already introduced in paragraph 2.2.

Indicating the friction factors relative to smooth and rough wall flows with f_{sm} and f_{rg}, the following well-known relationships are valid (cf. reference 2):

1) for smooth pipes and for the smooth-wall flow of sand-roughened pipes:

$$\frac{1}{f_{sm}^{\frac{1}{2}}} = 2{,}0 \lg \left(RE\, f_{sm}^{\frac{1}{2}}\right) - 0{,}8 \qquad (3.5.1)\ (I)$$

11) for rough pipes in the fully rough-wall turbulence region:

$$\frac{1}{f_{rg}^{\frac{1}{2}}} = 2{,}0 \lg \frac{D}{2d} + 1{,}74 \qquad (3.5.1)\ (II)$$

being $RE = \frac{VD}{\nu}$

i.e. the Reynolds number of the pipe.

Subtraction of (I) from (II) yields:

$$\frac{1}{f_{rg}^{\frac{1}{2}}} - \frac{1}{f_{sm}^{\frac{1}{2}}} = 1{,}74 + 2{,}0 \lg \frac{D}{2d} - 2{,}0 \lg \left(RE\, f_{sm}^{\frac{1}{2}}\right) + 0{,}80 =$$

$$2{,}54 + 2 \lg \frac{D}{2d} \frac{1}{f_{sm}^{\frac{1}{2}}} \frac{1}{RE}$$

/With .....

With

$$\left(\frac{f_{sm}}{8}\right)^{\frac{1}{2}} V = v^*$$

substitution into the second member of the above expression yields:

$$\frac{1}{f_{rg}^{\frac{1}{2}}} - \frac{1}{f_{sm}^{\frac{1}{2}}} = 1{,}02 - 2 \lg \frac{v^* d}{\nu} \qquad (3.5.2)$$

The graphical representation of this well-known equation is shown in Figure 22 of appendix III (cf. ref. 8).

The curve, representing the friction factor as a function of the Reynolds number(indicated by a continuous line), consists of three distinct parts.

The horizontal part applies to values of $Re^* \geqslant 70$, representing the condition of full rough-wall turbulence (case II).

The sloping straight line applies to flow under smooth-wall conditions (case I). Rough pipes behave in this region like smooth-wall pipes.

The curved branch represents transition conditions between the smooth and rough cases.

This portion is not derived from theoretical considerations, but is derived from Nikuradse's experimental results.

The prolonged horizontal branch intersects the experimental transition line at a point corresponding to a wall number $Re^*_d = 3{,}20$ i.e.

$$Re^*_d = \left(\frac{f_{rg}}{8}\right)^{\frac{1}{2}} \frac{Vd}{\nu} = \frac{v_{*d}}{\nu} = 3{,}20$$

/In .....

In considering the condition for smooth pipes,

i.e.

$$Re^* = \left(\frac{f_{sm}}{8}\right)^{\frac{1}{2}} \frac{V\delta}{\nu} = \frac{v_* \delta}{\nu} = 1$$

one obtains for $Re^* d = 3{,}20$ at the end of the transition region, $d = 3{,}20$.

Moreover, for $d = \frac{\delta}{5{,}50}$, $Re^* \frac{1}{5{,}50} = 0{,}183$.

Let us calculate the lift force on a particle, first as related to the experimental lift coefficient and secondly as related to the circulation.

According to eqns (1.3.1) and (2.2.15) and for

$v_c = v_*$, $C_\ell = \frac{1}{3}$

$$F_\ell = C_\ell \frac{\pi d^2}{4} \frac{v_c^2 \rho}{2} = \frac{1}{3} \frac{\rho \pi d^2}{4} \frac{v_*^2}{2} \qquad (3.5.3)\ (A)$$

The lift force on the same particle expressed by means of the circulation around a particle inside the boundary layer is given by (3.1.8) (I.b) (bis) i.e.

$$F_\ell = \frac{5{,}50^2}{3} \rho \frac{\pi d^2}{2} \left(\frac{d}{\delta}\right)^2 v_*^2 \qquad (3.5.4)$$

For a particle placed at a distance $\frac{d}{2} = \frac{\delta}{5{,}50 \times 2}$ from the wall, eqn (3.5.4) becomes

$$F_\ell = \frac{1}{3} \rho \frac{\pi d^2}{4} \frac{v_*^2}{2} \qquad (3.5.3)\ (B)$$

an expression which was also given as (3.5.3) (A).

Noting that eqn (2.2.14) was derived from the experimental expression of the lift force given by (1.3.1), the following interpretation of (2.2.14) is possible:

/Because .....

Because of the identity of (3.5.3) (A) and (3.5.3) (B), i.e. because of the equality of the theoretical and experimental values of the lift force, one can state that eqn (2.2.14) is still valid up to a distance

$$z_c = \frac{d}{2} = \frac{\delta}{5,50 \times 2}$$

from the wall.

Considering that the wall number relative to δ is

$$\frac{v_* \delta}{\nu} = 1,$$

then for $d_* = \frac{\delta}{5,50}$ the wall number will be:

$$\frac{v_* d_*}{\nu} = v_* \frac{\frac{\delta}{5,50}}{\nu} = 0,182$$

being

$$d_* = \frac{\delta}{5,50}.$$

If eqn (3.5.4) is assumed to provide the correct expression for the lift of a particle in the range

$$0 < Re^*_d < \frac{1}{5,50} = 0,182,$$

then in this range, i.e. for $d \leqslant d_* = 0,182\delta = \frac{\delta}{5,50}$,

$$F_\ell = \frac{1}{3} \frac{\pi d^2}{4} \left(\frac{d}{d_*}\right)^2 v_*^2 \qquad (3.5.5)$$

Considering a new critical velocity

$$v_{**o} = \frac{d}{d_*} v^*_o \qquad (3.5.6)$$

/able .....

able to produce lift on a particle at the boundary, this velocity which is replacing v_{*o} in eqns (2.2.14) (mod.) when $d < d_*$, allows us to rewrite this equation as follows:

$$4 \frac{\rho m - \rho}{\rho} \frac{gd}{v_{**o}^2} \left(\frac{\rho sa - \rho}{\rho m - \rho}\right)^{\frac{2}{3}} = 1 \qquad (3.5.7)$$

valid for $d < d_* = \frac{\delta}{5,50}$

Eqn (3.5.6) can be compared with eqn (2.4.2) and found to be the analogous one for the smooth-wall case, i.e. with a particle at the boundary of a smooth pipe, and within the boundary layer.

One need only to replace k with d_* and $\dot{V}so$ with v_{*o}. Given the wall number Re* , eqn (2.2.14) (modified) supplies the corresponding particle diameters d by substitution of v_{*o} with $v_{*o} = Re^* \cdot \frac{\nu}{d}$ into the said equation.

In the case of sand, i.e. for $\frac{\rho m - \rho}{\rho} = 1,65$, one obtains the following diameters:

$Re^* = \frac{v_{*o} d}{\nu}$	sand 70	32	1	$\frac{1}{5,50}$
d (mm)	0,425	0,054	0,058	0,0214

These are the diameters of the particles which are lifted from the boundary at the corresponding Reynolds or wall numbers Re*.

/Conclusion .....

Conclusion

The validity of the formula determining the critical friction velocity has been extended in the region of partially rough wall turbulence and smooth wall turbulence up to a distance $\frac{d_*}{2} = \frac{\delta}{5,50 \times 2}$ from the wall, where δ is the thickness of the boundary layer in a smooth-wall flow, for $Re^* = 1$.

For a particle smaller than d_*, a formula analogous to the one giving particle lift when placed inside a pocket of two successive irregularities, has also been established for smooth-wall pipes.

4. SUMMARY

The conditions of particle lift from a boundary, on account of fluid superficial forces, have been investigated experimentally and theoretically.

The experimental approach consisted of a correlation of results obtained from an analysis of some experiments reported in technical literature.

Boundary conditions giving particle lift followed by transport in full suspension or in saltation were found to be exactly equivalent.

They have been expressed by an experimental correlation between the particle Grashof number and a particle Reynolds number in which the particle diameter and the friction velocity of the stream appear.

The correlation was found to be applicable to particle beds, to a solitary particle, and in general to particles of a diameter at least of the size of the pipe irregularities.

/The .....

The analysis was further extended to particles of dimensions smaller than the irregularities of the pipe.

In this second instance it was found that the stream velocity providing particle lift is the stream velocity relative to a particle of the size of the irregularities multiplied by the ratio $\frac{\text{pipe absolute roughness}}{\text{particle diameter}}$.

The experimental analysis was carried out with consideration of stream characteristics in the section of the particle, i.e. in the section of the disturbed flow.

The theoretical analysis again considered particle equilibrium at the boundary, and studied it with the use of well-known expressions describing the velocity distribution in smooth (I) and rough (II) pipes.

The lift force was expressed by means of the circulation around the particle.

Expressions of the lift force were obtained for smooth (I) and rough pipes (II), in the turbulent region (a) and inside the boundary flow region (b) of the stream.

A stream function as a potential of the lift force was obtained for (I) and (II), for both the turbulent (a) and laminar flow (b) regions.

A detailed discussion has been carried out for rough pipes (II) in relation to the cases of:

(a) a solitary particle and the phenomenon of its transport in full suspension; and

(b) the saltation of a particle from a bed of particles.

/(c) .....

(c) The saltation of particles with the formation of dunes, the formation of dunes with superimposed ripples.

It was found that the formation of dunes with superimposed ripples is probably possible when the particle size allows a large velocity gradient at the boundary (rectangular velocity profile).

Finally, the phenomenon of particle lift and the relevant expression of the friction critical velocity have been investigated within the transition region and the smooth-wall region of turbulent flow.

A.C. BONAPACE
PRINCIPAL RESEARCH OFFICER

PRETORIA.
8/10/73
/KW

5. LIST OF SYMBOLS (S.I.A. Units used)

c	strength of the vortex	$\frac{m^2}{s}$
C_d	coefficient of drag	-
C_ℓ	generic coefficient of lift	-
$C_{\ell m}$	coefficient of lift relative to a particle with density ρ_m	-
$C_{\ell sao}$	coefficient of lift relative to a particle of sand for $\frac{d}{D} \longrightarrow 0$	-
$C'_\ell = C_{\ell m \frac{d}{D}}$	coefficient of lift for a particle of an unspecified material for $\frac{d}{D} \neq 0$	o
D	pipe diameter	(m)
d	particle diameter, symbol of differentiation	(m)
$f, f_o, f_s, f_{rg}, f_{sm}$	friction factor for a stream with mean velocity V, Vo, Vso, for rough-wall and smooth-wall pipes respectively	-
F_d	drag force	(N)
F_g	force due to gravity	(N)
F_ℓ	lift force on a particle	(N)
$F_{\ell z_c}$	lift force on a particle when at at distance z_c from the wall	(N)
F_{lvc}	accelerating force on a particle in the direction of the stream, i.e. in the direction of v_c	(N)(Newton)

/Frs .....

Frs	Froude number of a particle in the presence of a stream velocity Vso ($Frs = \frac{Vso^2}{gd}$)	-
Fr*	Froude number of a particle in the presence of a frictional velocity v_* $Fr^* = \frac{v_*^2}{gd}$	-
Gr	Grashof number of a particle: $Gr = \frac{gd^3}{\nu^2} \frac{\rho_m - \rho}{\rho}$	
g	acceleration due to gravity	(m/s^2)
H	liquid head	(m)
i	hydraulic gradient of the stream	-
i_o	hydraulic gradient of the stream at V = Vo	-
k	absolute roughness of a pipe	(m)
k'	absolute roughness for d = k	(m)
p	ratio ($\frac{d}{D} = p$ or $\frac{k}{D} = p$)	-
R	hydraulic radius	(m)
RE	pipe Reynolds number ($RE = \frac{VD}{\nu}$)	-
Re*, Re*o	Reynolds number of a particle for the frictional velocity v_* and v_{*o} respectively, ($Re^* = \frac{v_{*d}}{\nu}$; $Re^*o = \frac{v_{*od}}{\nu}$)	-
Re*so	frictional velocity v_{*so} ($Re^*so = \frac{v_{*so}d}{\nu}$)	-

/Res .....

Res	Reynolds number of a particle for a stream mean velocity Vso ($Res = \frac{Vso\,d}{\nu}$)	-
Re	Reynolds number of a particle settling in an undisturbed fluid ($Re = \frac{v_{se}\,d}{\nu}$)	-
$Re_{m\frac{d}{D}}$	Reynolds number providing particle lift at the boundary for $\frac{d}{D} \neq o$ and $\rho_m \neq \rho_{sa}$, and for a frictional velocity v_{*o}.	-
S'	area	(m^2)
s	velocity slip $o<s<1$	-
u_I	stream potential function relative to smooth pipes	-
u_{II}	stream potential function relative to rough pipes	-
V	mean velocity of the stream (in presence of particle deposits, V is defined by flowrate(solid and liquid) divided by the pipe unrestricted section)	-
Vo	critical sedimentation velocity	($\frac{m}{s}$)
Vso, Vsx	mean velocity of the stream at which saltation occurs and for a transported concentration of solid x = o and x ≠ o respectively	-

/Vso' .....

V_{so}'	mean velocity of the stream causing particle lift at the boundary when $d < k$	$(\frac{m}{s})$
v	local fluid velocity	$(\frac{m}{s})$
v_c	local fluid velocity relative to particle centre, in undisturbed conditions	$(\frac{m}{s})$
v_{se}	settling velocity of a particle	$(\frac{m}{s})$
v_t	tangential velocity; also increment in velocity across a particle	$(\frac{m}{s})$
v_z v_{zc}	local velocity at distances z and z_c from the wall respectively	$(\frac{m}{s})$
v_δ	local fluid velocity at a distance δ from the wall	$(\frac{m}{s})$
v_*, v_{*o}	frictional velocity at the wall for stream velocities of V and Vo respectively $\left(V^* = (\frac{f}{8})^{\frac{1}{2}} V;\quad V^*o = (\frac{fo}{8})^{\frac{1}{2}} Vo\right)$	$(\frac{m}{s})$
v_{*so}	frictional velocity relative to a stream mean velocity Vso $\left(v_{*s} = (\frac{fs}{8})^{\frac{1}{2}} Vso\right)$	$(\frac{m}{s})$
v_z'	particle upward velocity (i.e. in the direction z)	$(\frac{m}{s})$

/v_{zc}'' .....

v''_{zc}	particle forward velocity (i.e. in the direction v_z)	$(\frac{m}{s})$
z, z_1	a distance from the wall	(m)
z_c	distance from the wall of particle centre	(m)
x	volumetric solid concentration ($o < x < 1$)	-
β	latitude	-
Γ	circulation around a particle	$(\frac{m}{s})^2$
γ	angle corresponding to the slope of the velocity profile	-
Δ	Finite increment	-
δ	thickness of the boundary layer for smooth pipes	(m)
δ_o	distance from the wall beyond which logarithmic profile representation fails	(m)
λ	ratio f_s/f_o	
μ	viscosity	$\frac{kg}{ms}$
ν	kinematic viscosity	$(\frac{m}{s})^2$
ρ_m ρ_{sa}	density of an unspecified material and of sand respectively	$(\frac{kg}{m^3})$
ρ	density of the fluid	$(\frac{kg}{m^3})$
τ_*	shear stress at the wall	$(\frac{N}{m^2})$

/angle .....

φ	angle factor	-
ϕ_{so} ϕ_{sx}	non-dimensional group representing conditions of incipient saltation for a transported concentration x = o and x ≠ o respectively $\phi_{so} = \frac{V_{so}^2}{gd} C_d$; $\phi_{sa} = \frac{V_{sx}^2 C_d}{gd}$	
$\curlywedge$	constant representing initial conditions	-
$\curlywedge$Ia, $\curlywedge$Ib $\curlywedge$IIa $\curlywedge$IIb	constants representing initial conditions for smooth (I) and rough (II) pipes for a particle diameter $\frac{d}{2} > k$ (a) and $\frac{d}{2} < k$ (b) respectively	-

SUFFIXES

sa, m	refer the symbol to sand or an unspecified material
s	refers symbol to saltation
o, x	means in the presence of a solid transported concentration x = o; x ≠ o respectively
ℓ	means lift
d	means drag
rg	means rough wall
sm	means smooth wall

/6. .....

6. REFERENCES

1 Bonapace, A.C.
The hydraulic transport ofgranular materials of uniform size composition in horizontal pipes.
Coal, Gold and Base Minerals of Southern Africa.
August to December, 1968.

2 Prandtl, L.
Stroemungslehre
F. Vieweg & Sohn. Braunschweig 1949.
2.1 Chapter III, paragraph 11, pages 155-156.

3 Durand, R. and Condolios, E.
Experimental investigation on the transport of solids in pipes.
Le Journees d'Hydraulique, Societé Hydrotechnique de France. Grenoble, June, 1952.

4 Soleil and Ballade
Hydraulic transport of solids in public works.
Le Journee d'Hydraulique, Societé Hydrotechnique de France. Grenoble, June, 1952.

5 **Woster,** R.C.
The hydraulic transport of solids.
Extracts from the proceedings of a colloquium on the hydraulic transport of coal (November, 1952).
National Coal Board - Scientific Department, England.

6 Worster, R.C. & Dennis, D.F.
Hydraulic transport of solid materials in pipes.
Proceedings of the Institution of Chemical Engineers, London, 1955. Volume 169, pages 563-586.

/7. .....

7 Bonapace, A.C.
The drag coefficient of a particle and the voids fraction in a fluidisation or sedimentation assembly of particles.
Paper B5. Hydro Transport 2 (The second Internasional Conference on Hydraulic Transport of Solids in Pipes) 20-22 Sept. 1972.
British Hydromechanics Research Association, Cranfield, England.

8 Ackers, P.
Resistance of fluids flowing in channels and pipes.
Department of Scientific Industrial Research, Hydraulic Research Paper No. 1. 1958. England.

/Appendix .....

APPENDIX I

A WORKED EXAMPLE

As is well known, the propagation of coal dust explosions, e.g. in the tunnel of a mine, depends on the circumstance that the wind caused by the explosion continuously feeds the flame front with particles of coal by removing them from the surroundings.

Special experimental tunnels have been built for the study of the phenomenon of explosion propagation.

In this kind of investigation it is often of importance to determine the critical stream velocity at which a solid particle of a certain diameter is lifted from the bottom of the tunnel (boundary).

Let us assume the following data:

Tunnel diameter	$D = 1{,}000$	(m)
Material	coal	
Particle diameter	$d = 10^{-4}$	(m)
Density of coal	$\rho_m = 1400$	(kg/m^3)
Medium	air	
Density of air	$\rho = 1{,}20$	(kg/m^3)
Kinematic viscosity of the air at 20^oC	$1{,}5 \times 10^{-5}$	$(\frac{m^2}{s})$

/Density .....

Density of sand (as reference density) $\rho_{sa} = 2650 \quad (\frac{kg}{m^3})$

The Grashof number of the particle is

$$Gr = \frac{d^3 g}{\nu^2} \quad \frac{\rho_{m-} \rho}{\rho} = 50,5$$

The initial stream velocity is required at which the coal particle is brought from the boundary into suspension.

From eqn (2.2.14) being $(1 - \frac{d}{D})^{3,5} \approx 1$ one obtains:

$$2\ Gr^{\frac{1}{2}} \approx Re^*o \left(\rho \frac{\rho_{sa-} \rho}{m- \rho} \right)^{\frac{1}{3}}$$

and

$$Re^*o = 2 \left(\frac{\rho_{m-} \rho}{\rho_{sa-} \rho} \right)^{\frac{1}{3}} Gr^{\frac{1}{2}} = 2 \times 0,81 \times 7,1 = 11,5$$

From eqn (1.4.7) for

$$\frac{v^*o\, d}{\nu} = \frac{Vo\, d}{\nu} \left(\frac{fo}{8} \right)^{\frac{1}{2}} = 11,5$$

$$v_{*o} = 11,5 \frac{\nu}{d} = \frac{11,5 \times 1,50 \times 10^{-5}}{10^{-4}} = 1,72 m/s$$

Assume an absolute roughness of the tunnel walls equal to:

$$k = k' = d = 10^{-4} \ (m)$$

Then for

$$\frac{d}{D} = \frac{k'}{D} = 10^{-4}$$

/fo .....

fo is determined from Figure 20, i.e.

$$f_o = 0{,}012$$

$$\left(\frac{f_o}{8}\right)^{\frac{1}{2}} = 0{,}0387$$

and

$$Vo = \frac{1{,}72}{0{,}0387} = 44{,}5 \text{ m/s}$$

which is the required critical stream velocity.

In the case of a rougher finishing of the tunnel wall, e.g. for

$$k_1 = 10^{-3} \text{ (m)}$$

the new velocity Vo'' can be calculated as follows:

Keeping $k = 10^{-4}$ (m) constant, consider a tunnel of reduced diameter, e.g. with

$$D_1 = 0{,}10 \text{ m},$$

i.e. such that

$$\frac{k}{D_1} = \frac{d}{D_1} = 10^{-3}$$

Corresponding to

$$\frac{k}{D_1} = 10^{-3}$$

one reads in Figure 20

$$f_{o1} = 0{,}019$$

/and .....

and

$$\left(\frac{f_{o1}}{8}\right)^{\frac{1}{2}} = 0,049$$

Then

$$V_{o1} = \frac{v_{*o}}{\left(\frac{f_{o1}}{8}\right)^{\frac{1}{2}}} = \frac{1,72}{0,049} = 35 \quad (m/s)$$

which is the critical velocity for $D_1 = 0,10$ (m).

Supposing an increase in the tunnel diameter and in the absolute roughness in the same proportion, i.e. fixing $D = 1,000$ (m) and $k_1 = 10^{-3}$ (m) and $d = 10^{-4}$ (m). one gets

$$\frac{k_1}{D} = 10^{-3}$$

$$\frac{k_1}{d} = 10$$

Then the stream velocity which provides particle lift must have a tenfold value, i.e.

$$V_{o2} = V_{o2} \frac{k_1}{d} = 35 \times 10 = 350 \text{ (m/s)}.$$

This is the stream velocity which is able to dislocate a particle with $d = 0,1 \times 10^{-3}$ m from its position between two irregularities of the conduit, as shown in Figure 3-C.

Consequently, an increase in roughness involves a proportional increase in the critical velocity of the stream in agreement with that already discussed in paragraph (2.4).

A simple method to prevent propagation explosions in tunnels could be that of an artificial increase in certain sections of the tunnel of the roughness of the wall.

/The .....

The tunnel could be lined, e.g., in these sections with a sheet metal corrugated profile.

Care should be taken to insure that small coal particles are always contained in the pockets of the corrugated contour.

/Appendix II .....

APPENDIX II

DERIVATION OF THE EXPERIMENTAL QUANTITIES USED IN THE PREVIOUS ANALYSIS

In this appendix the methods used to define the main parameters of the previous analysis, contained in Tables No. 1, 2, 3, are discussed.

From the review of this appendix it is, for instance, possible to trace the numerical values of the critical sedimentation velocity and saltation velocity of Tabel 1 in their original experimental presentation.

Because figures and analytical expressions given in this appendix have been exhaustively discussed elsewhere (cf. reference 1), they are presented without proof but in sufficient detail to allow a geometrical reconstruction and interpretation of all these diagrams.

The figures of this appendix(*) are reproductions of the figures of the previously mentioned work (cf. reference No. 1) with the original numbers in brackets next to the new numbers of the figures.

The analytical expressions are written in the original symbols (which may sometimes differ from those used sofar): this has been done in order to simplify the interpretation of the figures.

/A .....

(*) Except when the contrary is stated explicitly.

A conversion list of the old symbols into the ones used in the preceding text is given at the end of this appendix. Consequently the interpretation of the figures is straightforward and so are the analytical expressions.

Figures 10-a, 11-a, 12-a, 13-a, 14-a, 15-A and 16-A, describe experiments with the hydraulic transport of solids of uniform size composition as obtained by the various experimenters; figures 10-b, 11-b, 12-b, 13-b, 14-b, 15-B and 16-B describe the same experiments with the interpretation given by the author.

The values of critical sedimentation velocity and saltation velocity given in Table 1 can be obtained from the second group of figures (b or B figures).

In this second group of figures the excess hydraulic gradient is plotted against the nominal velocity of the stream V(*)

The experiments refer to volumetric concentrations of various solids of constant size, conveyed in water.

Moreover, small letters (a or b) refer to normal cases, capital letter (A or B) to anomolous cases.

Taking as an example of normal cases figure 10-b, the curves of constant volumetric concentration represent the excess hydraulic gradient as a function of the nominal velocity V.

/The .....

(*) by definition:

1) Excess hydraulic gradient = the total hydraulic gradient minus the hydraulic gradient of a nominal flow of pure liquid.
2) Nominal flow = the volumetric flow of solid + liquid.
3) Nominal velocity = the volumetric flow divided by the empty section of the pipe.

The points plotted are verification points simply transferred from figure 10-a.

The family of parabolae represents the transport of particles in sliding and rolling motion, i.e. as a separate phase, moving in more or less definite contact with the pipe wall.

The parabolic law introduced expresses the fact that although some of the particles may advance in fully suspended conditions and others in sliding and rolling motion, on the whole they can be looked upon as progressing with only a fraction of their weight effective.

This fraction is unity at zero nominal velocity and zero at the vertex of the parabola.

The parabola x = o represents the excess energy loss due to stationary material deposits in the pipe, i.e. for no particle transport (x = o).

Denoting with V_{lo} and V_{lx} the critical sedimentation velocities for no particle transport (x=o) and for particle transport ($x \neq o$), with i_{oo} and i_{ox} the excess hydraulic gradient at nominal velocity V = o, for concentrations x = o $x \neq o$ respectively, and with h a parameter defined later, one can express the position of the vertex of a parabola as follows:

$$V_{lx} = V_{lo} \left(\frac{i_{oo} + hx}{i_{oo}}\right)^{\frac{1}{2}} \qquad (1)$$

an equation which relates V_{lx} to V_{lo} through i_{oo} and h.

V_{lo} .....

V_{lo} is the critical sedimentation velocity appearing in the correlation of Figure 4 of the previous analysis.

Denoting an auxiliary variable with z so that

$$o < z = \frac{V_{zo}}{V_{lo}} < 1 \quad \text{for } x = o \tag{2.a}$$

and

$$o < z \ \frac{Vzx}{V_{lx}} < 1 \text{ for } x \neq o \tag{2.b}$$

the excess hydraulic gradient at a point of nominal velocity Vzo and Vzx can be expressed as follows:

$$i_{zo} = i_{oo} \left(1 - \frac{Vzo}{V_{lo}}\right)^2 \quad \text{for } x = o \tag{3.a}$$

and

$$i_{zx} = i_{ox} \left(1 - \frac{Vzx}{V_{lx}}\right)^2 \quad \text{for } x \neq o \tag{3.b}$$

Being

$$i_{ox} = i_{oo} + hx \tag{4}$$

one gets finally

$$i_{zx} = (i_{oo} + hx) \left(1 - \frac{Vzx}{V_{lx}}\right)^2 \tag{5}$$

This is the general eqn of a parabola of the family.

The values of i_{oo} for sand and coal have been correlated experimentally in Figure 17, as a function of the ratio $\frac{d}{D}$.

/Introducing .....

Introducing the concept of mechanical friction coefficient f_f for a material with particles in physical contact, and that of the mechanical power required for conveying these loose aggregates of particles (irrespective of the hydraulic power dissipated by the stream because of its flow) one arrives at the following equation:

$$i_{oo}{}^{h} = k \qquad (6)$$

where k is a constant depending only on the kind of material transported.

The values of h, i_{oo} and k, together with the friction coefficient values f_f (as experimentally determined by the author) are grouped in Table 4.

Values of k have been given in this table for coal and sand, the two materials covered by the experiments.

Conclusion

The construction of the family of parabolae is possible through the knowledge of the sedimentation critical velocity V_{lo}, the excess hydraulic gradient i_{oo} and the parameter h.

The energy loss due to saltation of the particle has been calculated as loss due to unelastic impact of the particles with the pipe wall.

With reference to Figure 10b, saltation begins at various solid concentrations along the locus of incipient saltation.

Selecting for instance the parabola x = 0,10, the tangent to the energy loss curve has a discontinuity at point M, a fact explained by a change in the mechanism of energy dissipation.

/Denoting.....

Denoting with x_s and x_f the fraction of particles saltating and progressing in sliding and rolling motion according to the model of reduced weights previously introduced, and with i_{sl} and i_{fl} the excess energy due to saltation and sliding and rolling motion for a unitary solid concentration respectively, one can write the following system of equations:

$$x_s + x_f = x \tag{7}$$

$$x_s\, i_{sl} + x_f\, i_{fl} = i \tag{8}$$

where i is the total excess hydraulic gradient.

Assuming that along a segment-like MP only the number of saltating particles but not their kinetic energy may vary, the required unknown i_{sl} and x_s are expressed as follows:

$$x_s = \frac{\Delta i_s}{i_{sl}} \tag{9}$$

$$i_{sl} = \frac{i_f}{1 + \dfrac{x\, i_{fl} - i}{\Delta i_s}} \tag{10}$$

The numerical values of the symbols can be obtained graphically from Figure 10-b i.e.

$\Delta i_s = 0{,}021$ i.e. the segment $\overline{MQ}$

$x i_{fl} = 0{,}035$ i.e. the segment $\overline{SR}$, i.e. $x \dfrac{i_f}{x}$

$i \quad = 0{,}050$ i.e. the segment $\overline{PR}$

$i_f \quad = 0{,}035$ i.e. the segment $\overline{SR}$

/Then .....

Then one obtains

$$i_{sl} = \frac{0,0350}{1+\frac{0,035 - 0,05}{0,021}} = 1,20$$

$$x_s = \frac{0,021}{1,20} = 0,0175$$

Values of i_{sl} for the five normal cases have been correlated in Figure 18 in a representation

$$\frac{i_{sl}}{\beta} = 0,65 \ \phi_{szo}^{\frac{2}{3}} \qquad (11)$$

where

$$\phi_{szo} = \frac{C_d}{gd} \ V_{szo}^2 \qquad (12)$$

$$\beta = \frac{D-d}{d} \ \frac{\rho_m - \rho}{\rho} \qquad (13)$$

In this correlation the group ϕ_{szo} incorporates, besides known quantities, the saltation velocity at zero concentration Vszo, while β groups the other parameters.

$\frac{D - d}{d}$ expresses the particle trajectory length and $\frac{\rho_m - \rho}{\rho}$ the influence of the material density on the particle trajectory.

In the case of Figure 10-b

$$\beta = \frac{0,150 - 0,00042}{0,00042} \times \frac{2650 - 1000}{1000} = 590$$

/Vszo .....

Vszo = 2,83 m/s (i.e. the value written in Table 1)

$C_d = 2,0$

i.e. $\phi_{szo} = 3950$

Moreover

$$\frac{i_{si}}{\beta} = \frac{1,20}{590} = 0,00205$$

corresponding to the point where $\frac{d}{D} = 0,0028$ of Figure 18.

In order to complete the graphical analysis, points like T, M, P of figure 10-b must be constructed once the family of parabolae has been plotted.

This is done by means of the following correlations (determined through a graphical analysis only):

$$\frac{\Delta i_s}{\beta x} = 0,135 \quad \phi_{szo}^{-\frac{2}{3}} \qquad (13)$$

of Figure 19;

$$\frac{\Delta Vszx}{Vszx} = 0,55 \; \phi_{szo}^{-0,185} \qquad (14)$$

of Figure 20.

(In Figure 10-b: $\Delta V_{szx=0,10} = V_{m} - V_{szo} = 0,25$ (m/s)

With the previously established expression it is possible to discuss the anomalous cases of Figures 15-A and 15-B and 16-A and 16-B.

/Anomalous .....

Anomalous cases are typical for their small ratio $\frac{d}{D}$.

In figures 15B(*) and 16-B the set of points connected by continuous lines was transferred directly from 15-A and 16-A.

Consequently they represent true experimental results.

The dotted lines have been constructed in the light of the theory developed in this work.

Considering at first Figure 16-B, the saltation velocity Vszo for concentration x = o was determined from Figure 5.

In fact, for

$\frac{d}{D} = 0{,}00071$, $\phi_{szo} = 72000$, and x = o

i.e.

Vszo = 14,40 (m/s)

for x = 0,10 $\phi_{szx = 0,10} = 100\ 000$

$V_{szx = 0,10} = 17{,}10$ m/s

The position of point R_1 was fixed by means of

Vszx = ,10 = 17,10 m/s.

It is easily recognizable that the locus x = 0,10 attains a maximum between T_1 and R_1.

Beyond R_1 (i.e. for V > Vszx = 0,10) the particle proceeds in full suspension, while at R_1 the slope of the curve is negative.

/It .....

(*) Note that Figure 15-B is missing in the original work of Reference No. 1.

It was assumed that at the point of maximum (i.e. at Q_1) all the particles should proceed in saltation, a fact expressed by

$$x = x_s = 0,10$$

Consequently, at Q_1 the loss in hydraulic gradient due to saltation corresponding to

$$x = x_s = 0,10$$

can be calculated simply by means of expression (13)

$$\frac{\Delta is}{\beta\ x} = \frac{i_{sl}}{\beta} = \frac{0,096}{2300 \times 0,10} = 0,000415.$$

The value $\frac{i_{sl}}{\beta} = 0,000415$ was obtained from the diagram of Figure 18 for $\Phi_{szo} = 72000$ (i.e. the point indicated by a cross).

Consequently the vertical segment $Q_1Q_1' = 0,096$ represents the loss due to saltation for $x = 0,10$ and analogous segments $\frac{1}{2}\ Q_1Q_1'$ and $\frac{3}{2}\ Q_1Q_1'$ for $x = 0,05$ and $x = 0,15$ loci.

It was also assumed that along the arc R_1Q_1 the concentration of the particles proceeding in saltation should increase from R_1 to Q_1, i.e. for decreasing nominal velocity, and that the fraction progressing in full suspension should consequently decrease.

This means:

at Q_1 $x = x_s = 0,10$

along R_1Q_1

$x_s + x_{su} = 0,10$

/Similarly .....

Similarly, along the arc Q_1T_1 some particles must have separated from the saltating phase and proceed at the boundary by a sliding and rolling motion, i.e. along Q_1T_1

$x_f + x_s = 0,10.$

This assumption is justified by a steady decrease of the excess hydraulic gradient for decreasing nominal velocities.

Similar considerations are obviously applicable to the loci $x = 0,15$ and $x = 0,050$ as well.

The maxima of the three curves, i.e. $x = 0,05$,

$x = 0,10$ and $x = 0,15$, were joined by a locus providing conditions of incipient motion by sliding and rolling.

This locus terminates at S on the $x = o$ locus,

where

$Vs = V_{lo} = 4,85$ m/s.

At S another parabola is superimposed in the velocity range $o < V < 4,85$ m/s. It represents excess hydraulic gradient due to stationary material deposits.

Although the deposition of particles originates for the locus $x = o$ at $Vszo = 14,40$ m/s, between this value and $Vs = V_{lo} = 4,85$ the decrease in nominal velocity causes accumulation in the form of dunes on which particles proceed by saltation.

/The .....

The following assumptions have been tacitly introduced in the description of the phenomenon, e.g. along arc $Q_1 R_1$.

a) The group $\emptyset_{szx}$ remains constant because the decrease in nominal velocity is compensated for by the reduction of the free area of the pipe.

b) $\emptyset_{szx}$ = constant means that the saltation energy relative to a particle is constant too (cf. Figure 18).

c) The hydraulic radius R of the free section decreases from point R_1 to Q_1 because of the accumulation of solid deposits.

d) The saltating fraction increases from zero at R_1 to $\frac{x_s}{x} = 1$ at Q_1.

In the range

$$o < V < V_s = V_{lo} = 4,85 \text{ m/s}$$

for x = o, the excess hydraulic gradient of the pipe due to material deposits increases up to a value $i_{oo} = 0,112$ at V = o.

Analogously, for x = 0,10

$$i_{ox} = 0,10 = i_{oo} + hx = 0,0146$$

at V = 0.

/The .....

The value $i_{oo} = 0,112$ has been determined from Figure 17 for $\frac{d}{D} = 0,00071$; the constant h from relationship (6), i.e.

$$h = \frac{k}{i_{oo}} = \frac{0,0257}{0,112} = 0,23.$$

The vertices of the parabolae of the family, e.g. those in S' and Q', do not obey relationship (1) i.e.

$$V_{1x} = V_{1o} \left(\frac{ioo+hx}{ioo}\right)^{\frac{1}{2}}$$

which should have been strictly applied in the tracing of the curves.

It was decided to keep the position of maxima at Q_1, as in the original figure of reference 1.

However, in Figure 15-B the vertices of the parabolae obey the previous relationship written above, i.e. the vertices are correctly placed.

The small error introduced in Figure 16-B is insignificant in the interpretation of the diagram.

Finally, the critical sedimentation velocity was determined by means of Figure 4 as follows:

The Grashof number of the particle for $d = 0,5 \times 10^{-3}$(m) is

$$Gr = 2030$$

Being $\left(1 - \frac{d}{D}\right)^{3,5} \approx 1$

/95 .....

$$\frac{\rho_m - \rho}{\rho_{sa} - \rho} = 1$$

one reads in Figure 4

$$Re^* \left(\frac{f_o}{8}\right)^{\frac{1}{2}} \frac{V_{lo} d}{\nu} = 92$$

with $\nu = 10^{-6} \frac{m^2}{s}$

for $\frac{k'}{D} = \frac{d}{D} = 0{,}00071$ one gets $f_o = 0{,}0115$

$$V_{lo} = \frac{92 \times 10^{-6}}{0{,}5 \times 10^{-3}} \left(\frac{8}{0{,}0115}\right)^{\frac{1}{2}} = 4{,}85 \text{ m/s}$$

It should be noticed that in the above scheme of calculation the pipe absolute roughness k' introduced is that corresponding to the particle diameter $k' = d = 0{,}5 \times 10^{-3}$ m and not to that of the pipe irregular ities $k = 2{,}1 \times 10^{-3}$ (m), because the particle is now removed from a bed of similar other particles.

It is also worth while noting an interesting difference between Figure 15-B and 16-B in relation to the excess hydraulic gradient due to material deposits in the pipe.

In Figure 15-B this excess gradient between points R_1 and Q_1 is simply zero, while in Figure 16-B it is zero at R_1 and equal to the segment $Q_1' Q_1''$ = 0,0525 at Q_1''.

For the same particle diameter $d = 0{,}5 \times 10^{-3}$(m)the pipe roughness in Figure 15-B is $k = 0{,}70 \times 10^{-3}$ (m), i.e. $\frac{d}{k} = 0{,}70$, and in Figure 16-B $k = 2{,}1 \times 10^{-3}$ (m) i.e. $\frac{d}{k} = 0{,}24$.

/These .....

These two cases can be discussed according to the following extreme conditions:

a) that of $d \approx k$, approximately reproduced by the example of Figure 15-B.

b) $d \ll k$, approximately reproduced by the example of Figure 16-B.

The case $d \approx k$ causes particle saltation without the formation of dunes.

The case $d \ll k$ causes particle saltation with the formation of dunes.

This is in agreement with the discussion relative to Figure 9.

The presence of dunes causes a considerable kinetic loss of head due to periodic variation of the pipe section, i.e. of the actual stream velocity.

The excess loss represented in Figure 16-B by the segment $Q_1' Q_1''$ is attributed to this phenomenon.

The velocity disturbance required for the formation of dunes is particularly localized along the perimeter of the solid deposits layer, where there is a discontinuity between particle roughness and pipe roughness.

/List .....

LIST OF SOME NEW SYMBOLS USED IN APPENDIX II

Symbols listed under heading "Appendix II" are symbols already used in the work of reference 1.

Corresponding symbols of the text are also given under the heading "Text".

Symbol App. II	Text	Description of Symbol	Dimensions
f_f	-	Mechanical friction coefficient of the material in water.	-
h	-	Parameter characterizing a parabola of the family.	-
i_{oo}	-	Hydraulic gradient excess relative to a pipe with stationary deposits of material in the condition $V \rightarrow 0$ and $x = o$.	-
i_f	-	Hydraulic gradient excess required for transport of particle in sliding and rolling motion.	-
i_{sl}	-	Hydraulic gradient excess representing loss due to saltation (for $x_s = 1$).	-
Δi_s	-	Hydraulic gradient excess due to saltation (used in graphical representation).	-
i_{ox}	-	Hydraulic gradient excess for a concentration x and stream velocity $V \rightarrow o$.	-

/98 .....

Symbol App. II	Symbol Text	Description of Symbol	Dimensions
i_{zo}, i_{zx}	-	Hydraulic gradient excess for stream mean velocities Vzo, Vzx respectively.	-
k	-	Constant of expression $i_{oo}h = k$	-
V_{lo}	Vo	Stream sedimentation critical mean velocity for x = o (Nominal)	$(\frac{m}{s})$
Vszo	Vso	Stream saltation mean velocity for x = o (Nominal)	$(\frac{m}{s})$
Vzo	-	Stream mean velocity for x = o $(o < Vzo < V_{lo})$ (Nominal)	-
Vszx	-	Stream saltation mean velocity for $x \neq o$ (Nominal) $(o < Vszx < V_{lx})$	$(\frac{m}{s})$
Vzx	-	Stream mean velocity for $x \neq o$ $(1 < Vzx < V_{lx})$ (Nominal)	$(\frac{m}{s})$
x_s	-	Volumetric solid concentration transported in saltation $(o < x_s < x)$	-
x_f	-	Volumetric solid concentration transported in sliding and rolling motion $(o < x_f < x)$	-

/99 .....

Symbol App. II	Symbol Text	Description of Symbol	Dimensions
x_{su}	-	Volumetric solid concentration transported in full suspension ($o < x_{su} < x$)	-
z	-	A parameter $o < z < 1$: (for $x \neq o$ $o < z = \frac{Vzx}{V_{lx}} \leqslant 1$	-
		for $x = o$ $o < z = \frac{Vzo}{V_{lo}} \leqslant 1$)	-
ϕ_{szo}	ϕ_{so}	Non-dimensional group defined by $\phi_{szo} = \frac{Vszo^2}{gd} C_d$	
ϕ_{szx}	ϕ_{sx}	Non-dimensional group defined by $\phi_{szx} = \frac{Vszx^2}{gd} C_d$	

Note: Figure numbers of Appendix II in brackets refer to original figures of Reference No. 1.

/Appendix III .....

APPENDIX III

Figure 21:

Friction factors of pipes for turbulent flow
(from ref. No. 8.)

Figure 22:

Roughness functions
(from ref. No. 8.)

/101 .....

TABLE 1

SUMMARY OF EXPERIMENTAL QUANTITIES USED IN THE ANALYSIS

(Cfr. Appendix 2)

of ments	$\frac{d}{D}$ (Reference)	Particle Dia. d ($\times 10^{-3}$ m)	Pipe Dia. D (m)	Material & Density (kg/m^3)	Pipe Friction Factor f_o	Sedimentation Critical VEL. V_o (m/s)	Saltation Critical VEL. V_s (m/s)	Particle Settling VEL. (in water) v_{se} (m/s)
and & dolios	0,0028	0,42	0,150	Sand 2650	0,0135	4,92 (e)	2,85 (e)	0,06
and & dolios	0,0136	2,04	0,150	Sand 2650	0,0135	7,10 (e)	2,22 (e)	0,27
orster Dennis	0,166	12,7	0,076	Coal 1400	0,020	2,43 (e)	0,76 (e)	0,40
orster Dennis	0,250	38,0	0,150	Coal 1400	0,016	3,90 (e)	0,96 (e)	0,72
orster	0,330	12,7	0,038	Coal 1400	0,026	0,85 (e)	0,305 (e)	0,40
& e	0,00086	0,5	0,580	Sand 2650	0,0205	- ($d < k$)	(c) 12,0 (for clear pipe)	0,073
& e	0,00071	0,5	0,700	Sand 2650	0,0255	- ($d < k$)	(c) 14,50 (for clear pipe)	0,073

tes: (e) means experimentally determined

(c) means calculated from equations available in the text

TABLE 2

EXPERIMENTAL VALUE OF φ

Grad. Vo o	Excess Hydr. Gradient (Due to solid deposits) Δi_{so}	$\lambda^{\frac{1}{2}} = \left(\frac{i_o + \Delta i_s}{i_o}\right)^{\frac{1}{2}}$	$\varphi = 2 \times 2{,}67\ \lambda^{\frac{1}{2}} \frac{V_{so}}{V_{se}} \frac{d}{D} \left(\frac{\rho_m - \rho}{\rho}\right)^{\frac{1}{2}}$ (Tabulated values φ average = 0,99)	
07	0,012	$1{,}11^{\frac{1}{2}} = 1{,}055$	0,96	$\frac{d}{D} > \frac{k}{D}$
09	0,0135	$1{,}17^{\frac{1}{2}} = 1{,}08$	0,83	$\frac{d}{D} > \frac{k}{D}$
72	0,0067	$1{,}10^{\frac{1}{2}} = 1{,}05$	1,12	$\frac{d}{D} > \frac{k}{D}$
85	0,0063	$1{,}075^{\frac{1}{2}} = 1{,}037$	1,17	$\frac{d}{D} > \frac{k}{D}$
27	0,00433	$1{,}17^{\frac{1}{2}} = 1{,}08$	0,92	$\frac{d}{D} > \frac{k}{D}$
	-	1 (*)	0,97	$\frac{d}{D} < \frac{k}{D}$
	-	1 (*)	0,97	$\frac{d}{D} < \frac{k}{D}$

so = Vo

ry deposit present at incipient saltation.

TABLE 3

NUMERICAL VALUES LEADING TO CORRELATION OF FIGURE 4

$\frac{d}{D}$ (Reference)	$\frac{d}{k}$	$Gr = \frac{\rho_m - \rho}{\rho} \frac{gd^3}{\nu^2}$	$Re^*m \frac{d}{D} = (\frac{f_o}{8})^{\frac{1}{2}} \frac{Vod}{\nu}\left(\frac{\rho_{sa}-\rho}{\rho_m-\rho}\right)^{\frac{1}{3}} \frac{1}{(1-\frac{d}{D})^{3,5}}$
0,333	330	78000×10^3	3950 (e)
0,250	830	215000×10^3	28000 (e)
0,165	206	78000×10^3	4400 (e)
0,0136	136	138×10^3	620 (e)
0,0028	35	$1,16 \times 10^3$	86 (e)
0,00086	0,70	$2,03 \times 10^3$	92 (c) (For f_o = 0,0115 i.e. for $\frac{k'}{D} = \frac{d}{D}$)
0,00071	0,24	$2,03 \times 10^3$	92 (c) (For f_o = 0,0115 i.e. for $\frac{k'}{D} = \frac{d}{D}$)

Note: (c) calculated
(e) experimental

$\nu_{water} = 10^{-6}$ $(\frac{m^2}{s})$

/Table 4 .....

TABLE 4

(Relative to Appendix II)

TYPICAL PARAMETERS FOR THE DETERMINATION OF THE FAMILY OF PARABOLAE

Material	$\frac{d}{D}$ (Reference)	h	i_{oo}	$k = i_{oo}{}^{h}$	Aver.Value $k = i_{oo}{}^{h}$	f_f	a (*)
Sand	0,0028	0,44	0,060	0,02650	0,0257	0,50	32,1
Sand	0,0136	0,96	0,026	0,02500			
Coal	0,165	0,26	0,014	0,00365			
Coal	0,250	0,30	0,011	0,00330	0,0035	0,28	32,0
Coal	0,330	0,35	0,010	0,00350			

(*) a is a proportionality constant

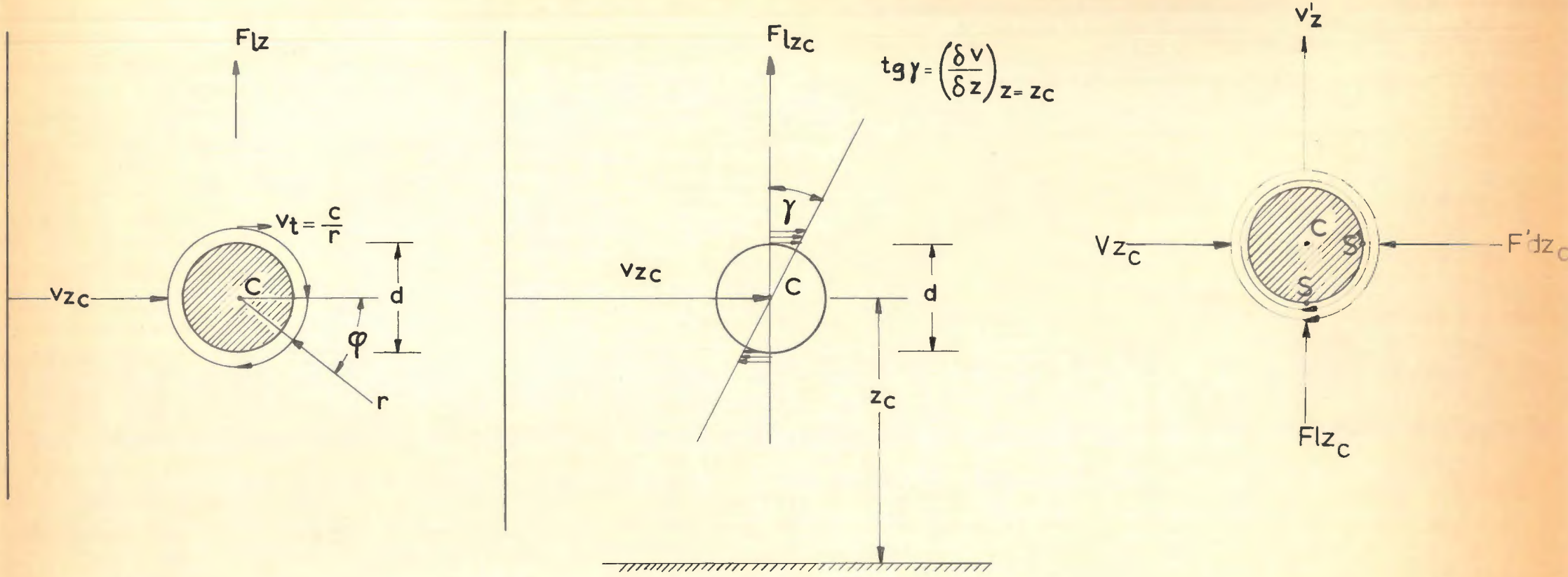

1–A 1–B 1–C

THE LIFT FORCE ON A PARTICLE EXPRESSED BY MEANS OF THE CIRCULATION

FIG. 1

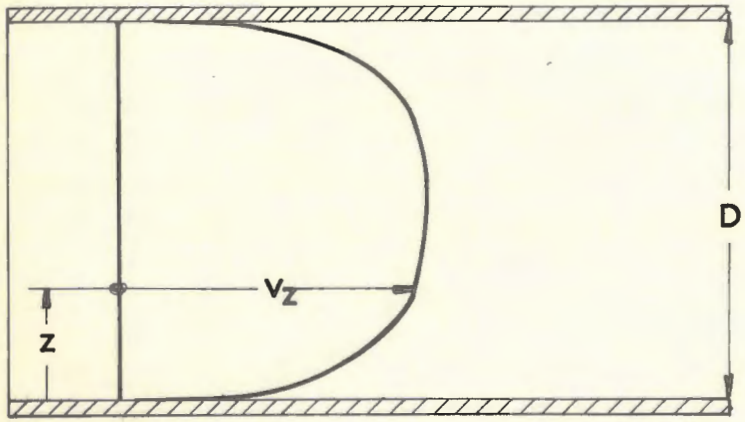

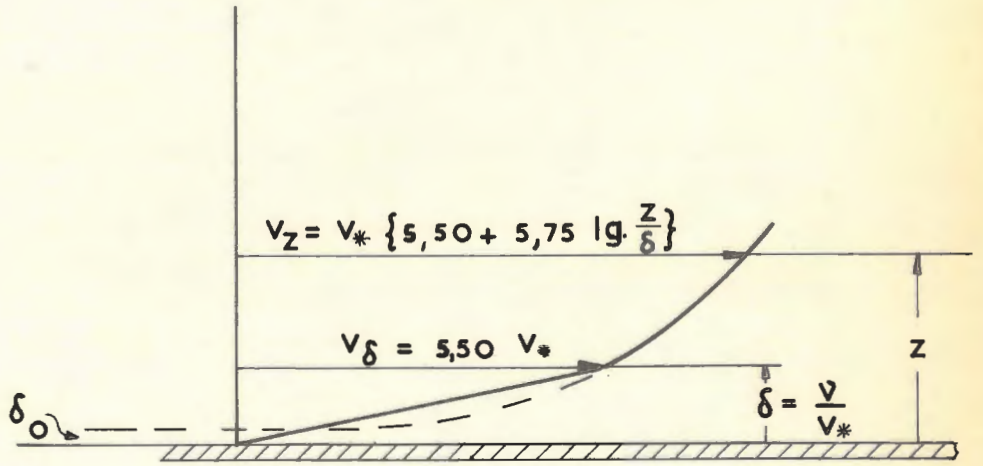

2 – A

2 – B

VELOCITY PROFILE IN A PIPE

FIG. 2

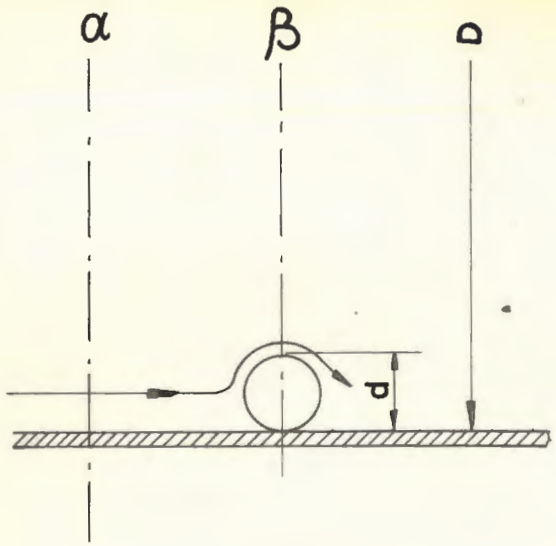

3 – A

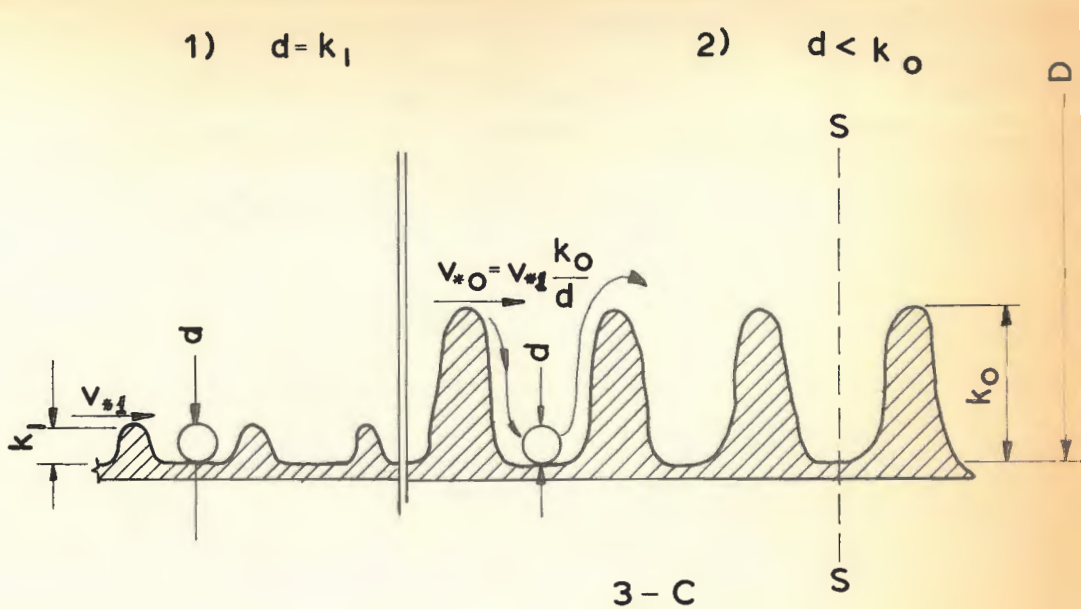

3 – C

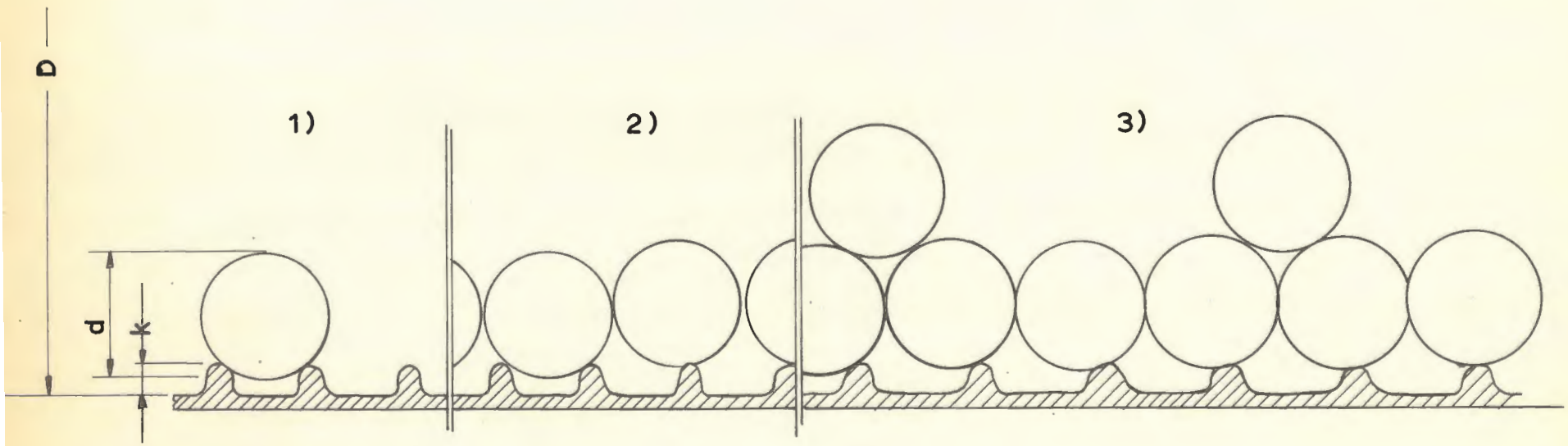

3 – B

VARIOUS BOUNDARY CONDITIONS FOR PARTICLE DEPOSITS

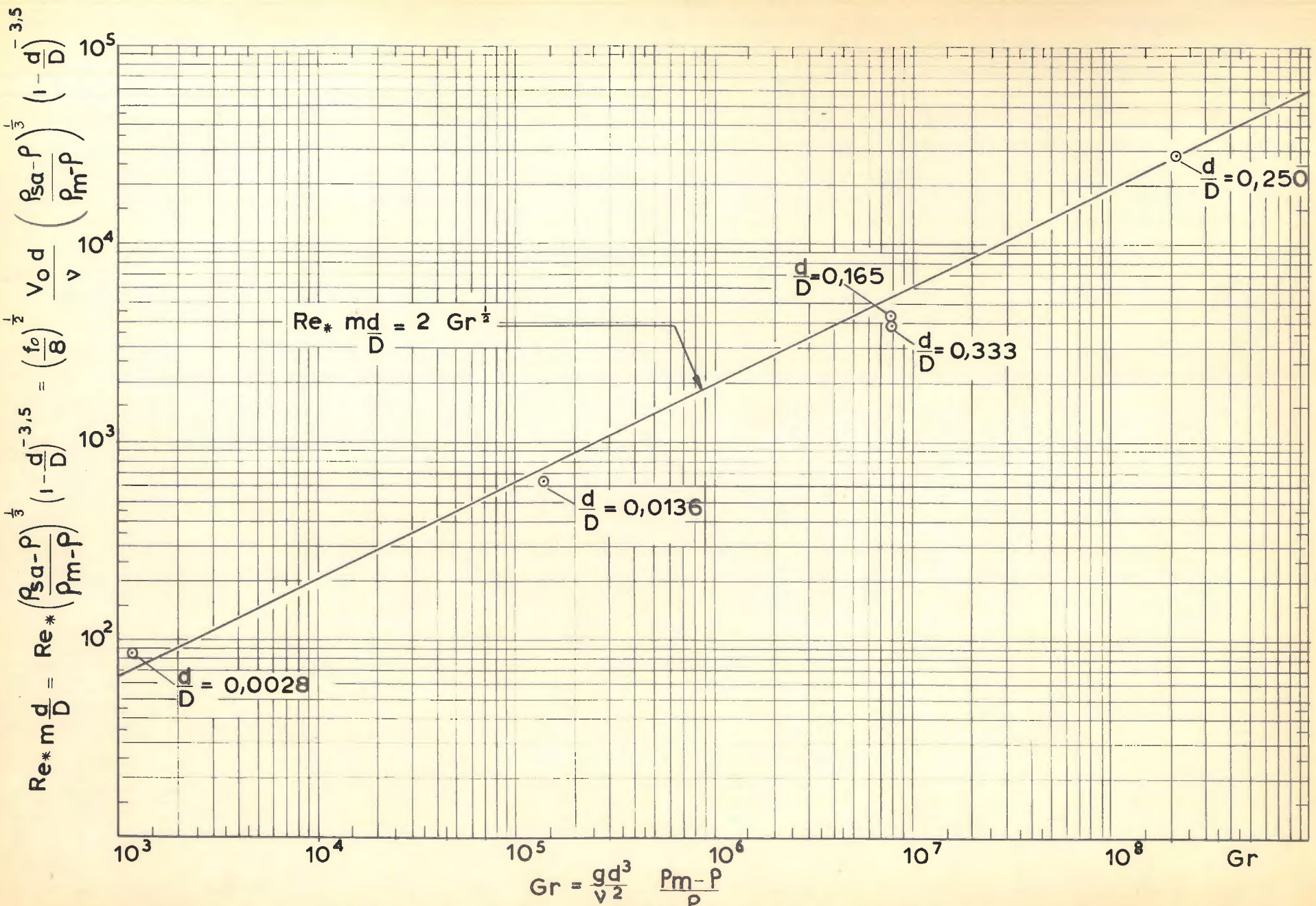

EXPERIMENTAL CORRELATION DEFINING THE CRITICAL SEDIMENTATION VELOCITY V_o

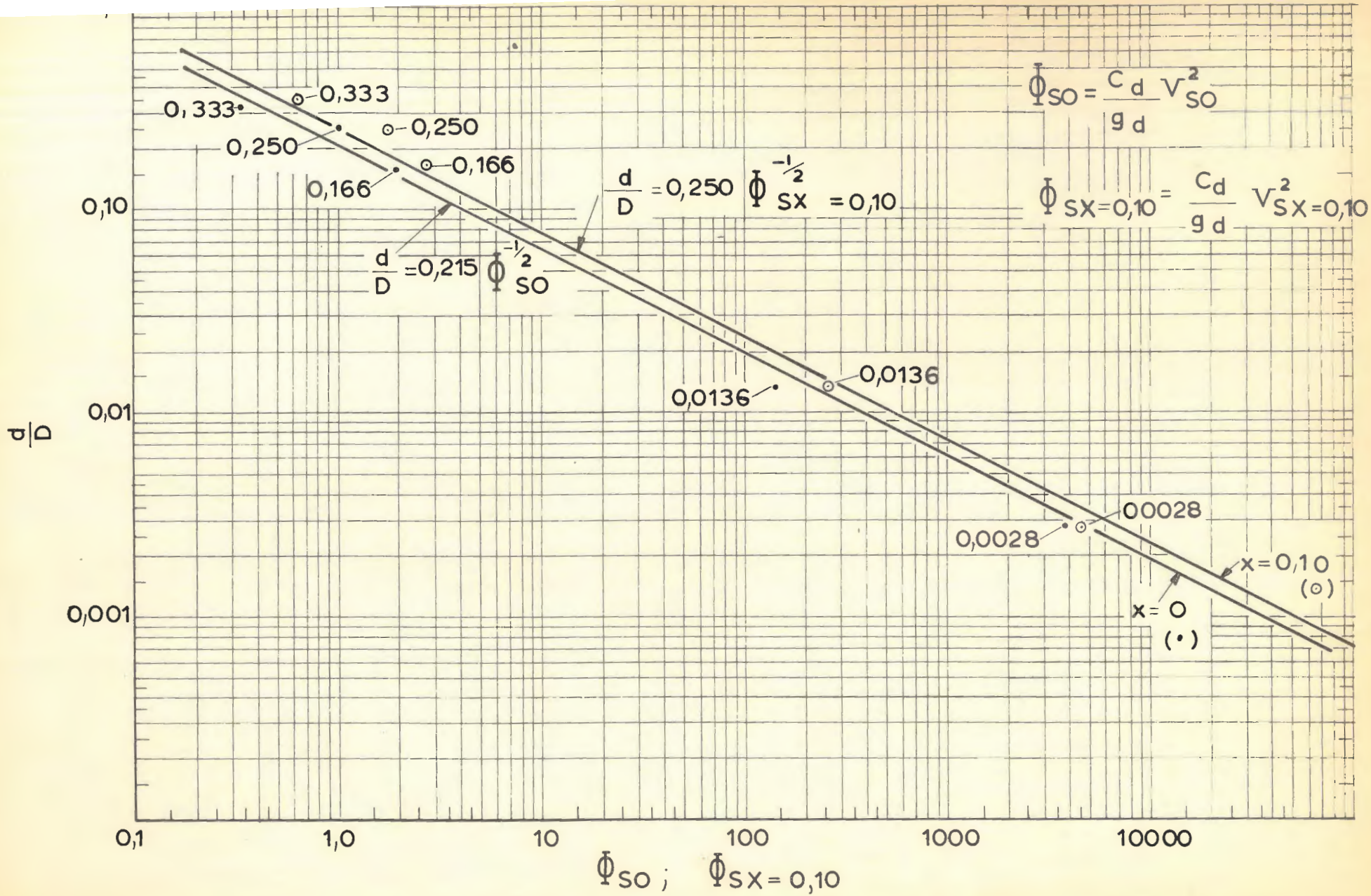

EXPERIMENTAL CORRELATION DEFINING CONDITIONS OF SALTATION.

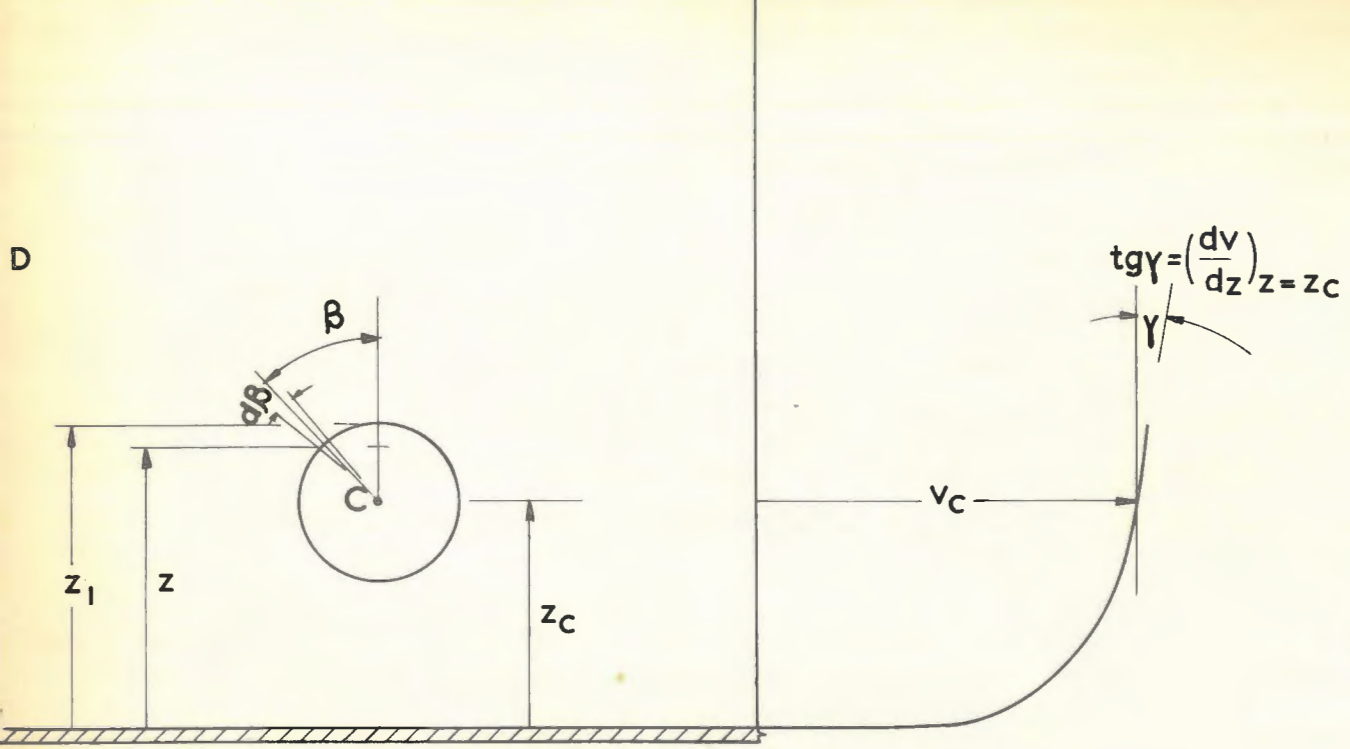

6 — A

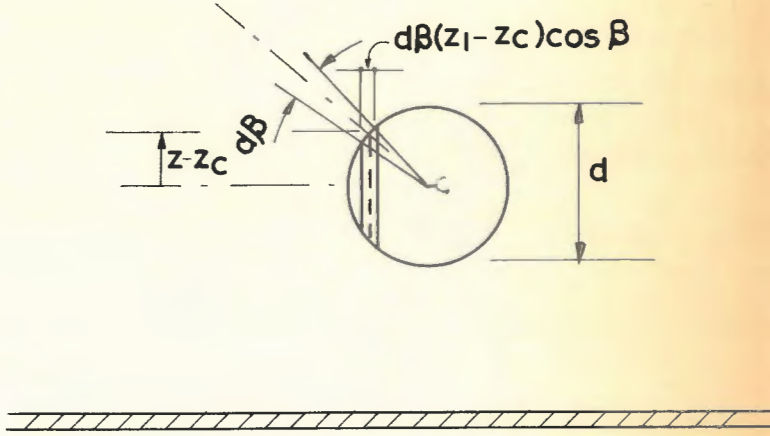

6 — B

CALCULATION OF THE CIRCULATION AROUND
A SPHERICAL PARTICLE
FIG. 6

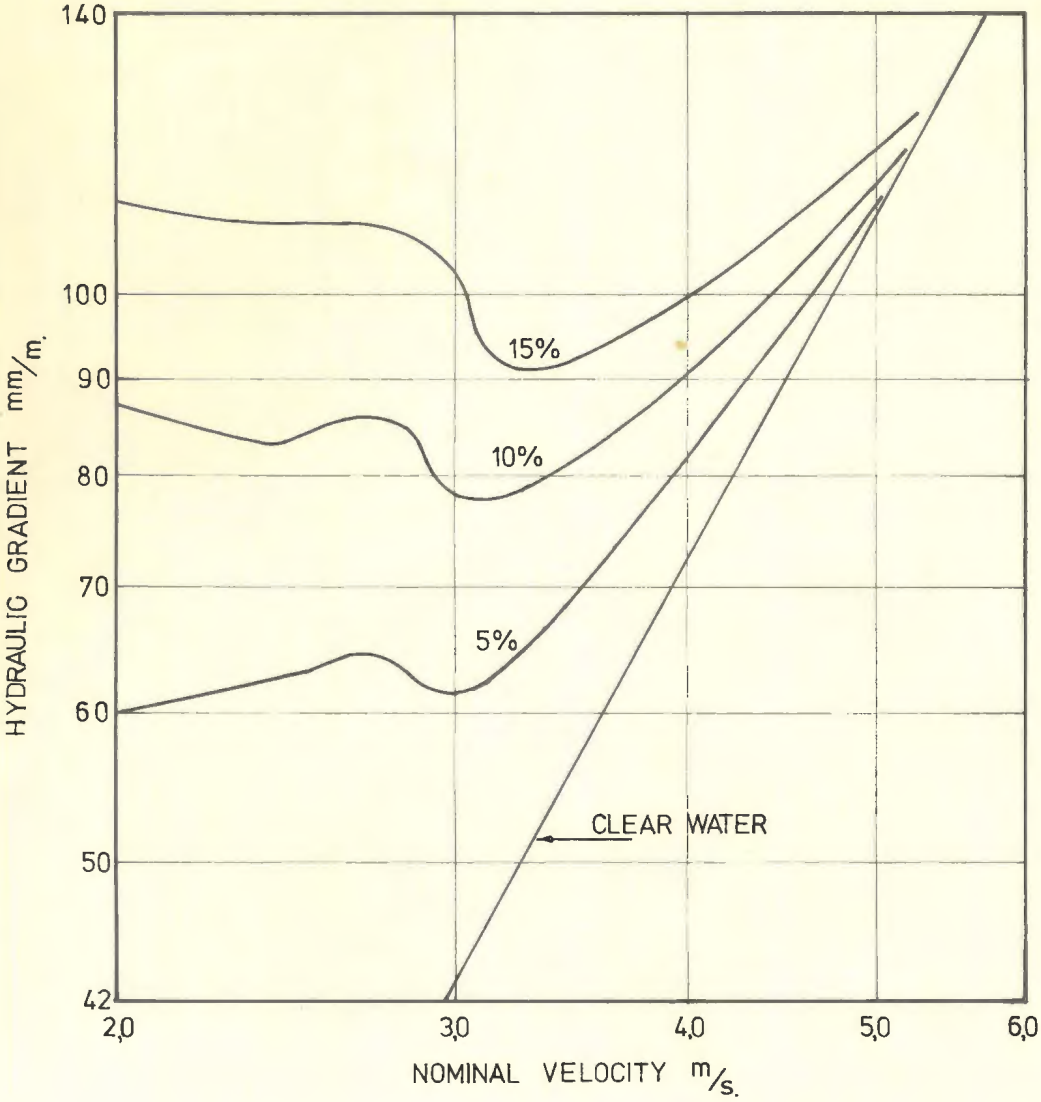

HYDRAULIC GRADIENT–VELOCITY CURVES OBTAINED BY DURAND. R. AND CONDOLIOS E.

(MATERIAL : SAND ; VOL. CONC. 5; 10; 15; %;
PARTICLE DIAMETER: d = 0,42 mm;
PIPE DIAMETER: D = 150 mm.)

FIG. 10-a; (2 a).

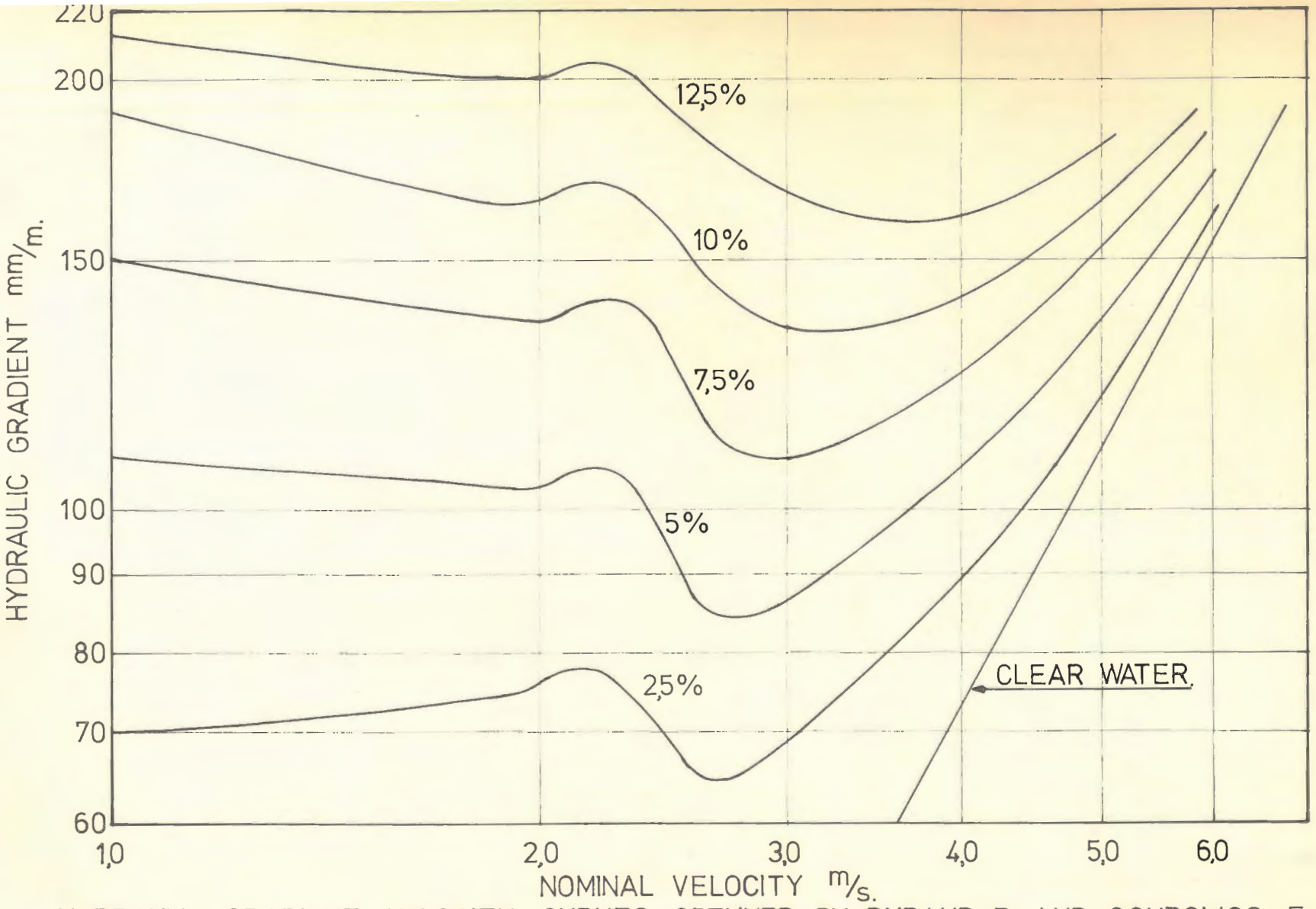

HYDRAULIC GRADIENT VELOCITY CURVES OBTAINED BY DURAND R. AND CONDOLIOS E.

(MATERIAL: SAND VOL. CONC. 12,5 ; 10; 7,5 ; 5; 2,5%
PARTICLE DIAMETER d = 2,04 mm.
PIPE DIAMETER D = 150 mm.)

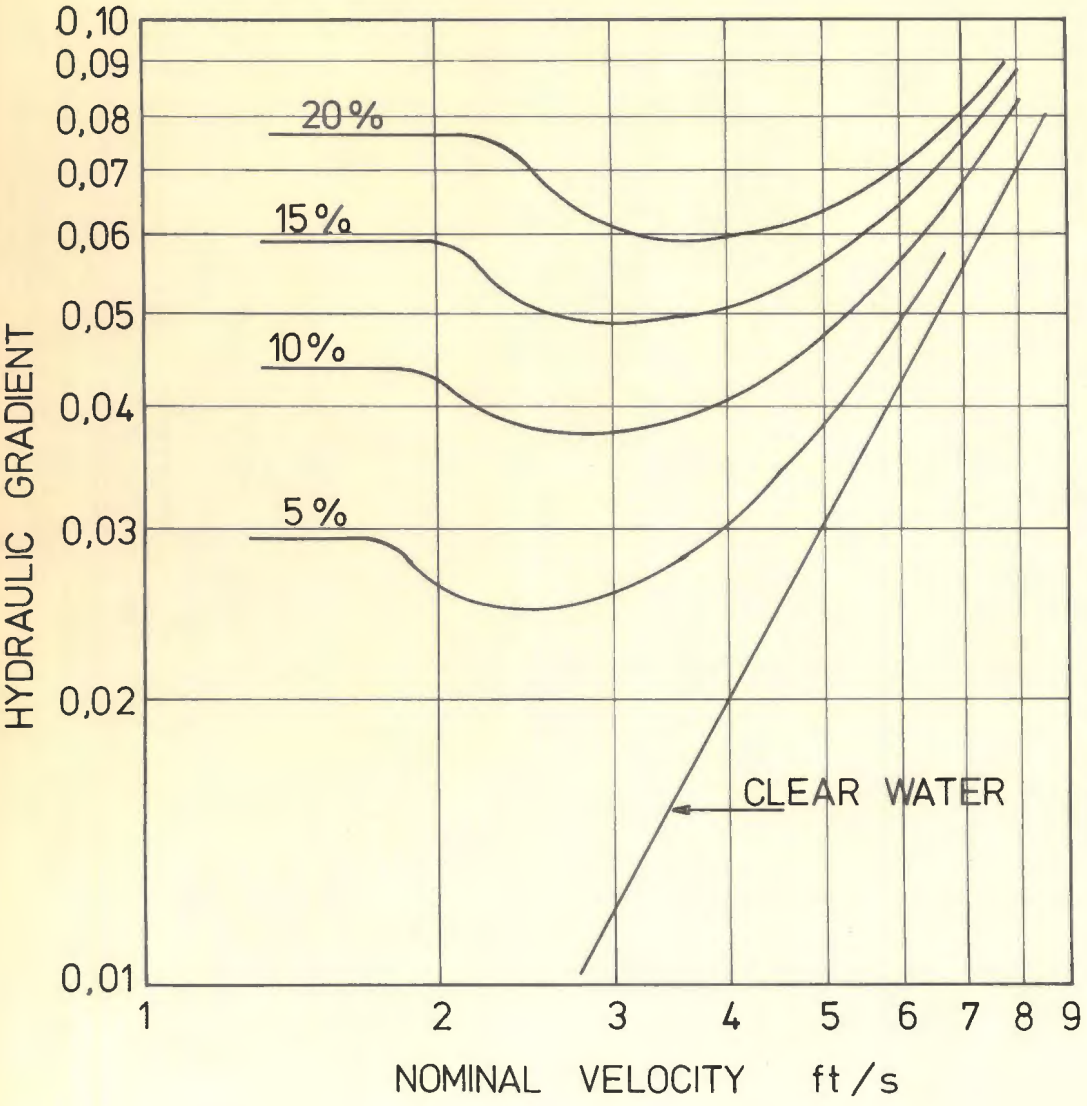

HYDRAULIC GRADIENT - VELOCITY CURVES
OBTAINED BY WORSTER R. AND DENNY D.
MATERIAL: COAL (VOL. CONC. 15;10;5 %)
PARTICLE DIAMETER : d = 12,7 mm (1/2")
PIPE DIAMETER : D = 76 mm (3")

FIGURE 12 - a; (4 a)

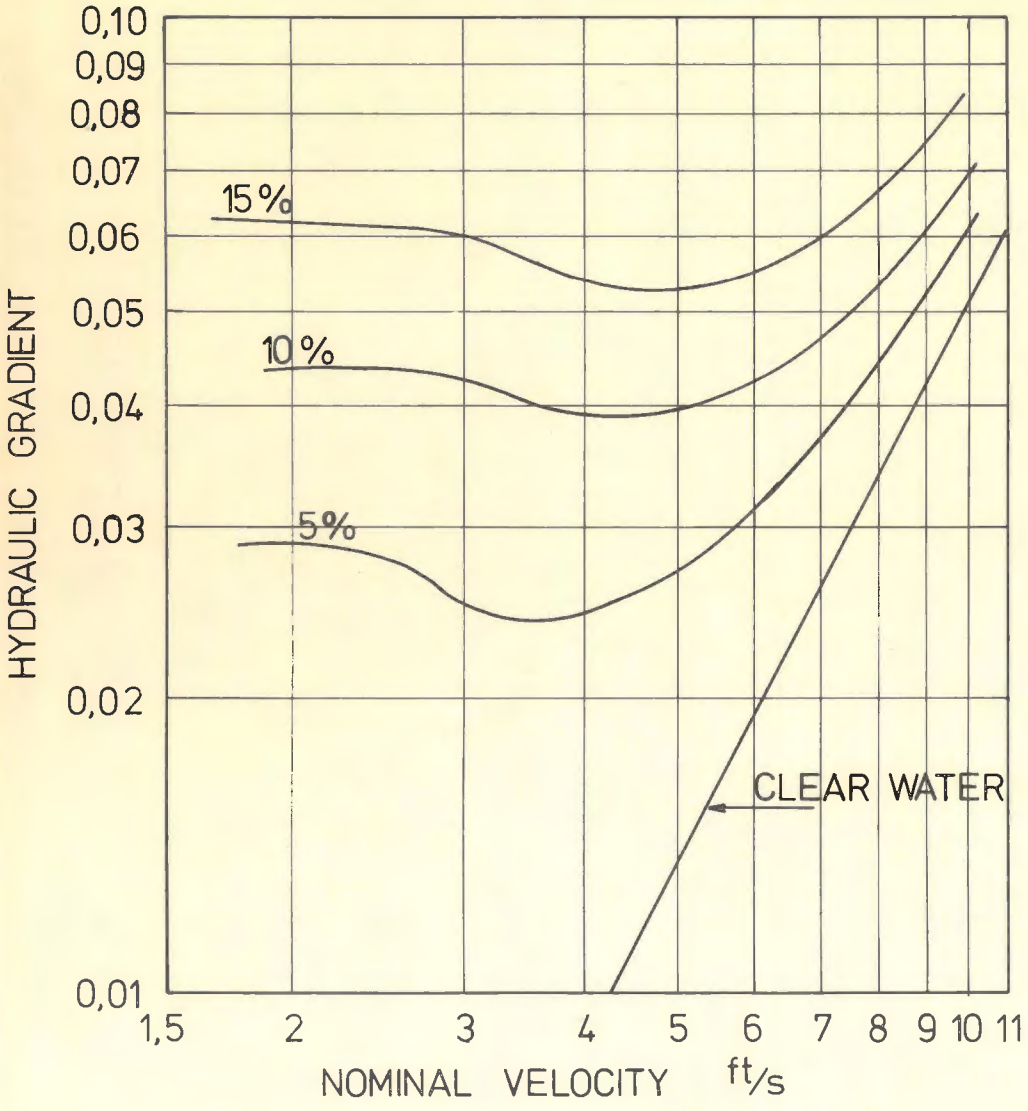

HYDRAULIC GRADIENT – VELOCITY CURVES
OBTAINED BY WORSTER R. AND DENNY D.
MATERIAL : COAL (VOL. CONC. 15 ; 10 ; 5 %)
PARTICLE DIAMETER : d = 38 mm (1 1/2")
PIPE DIAMETER : D = 152 mm (6")

FIGURE 13 – a ; (5 a)

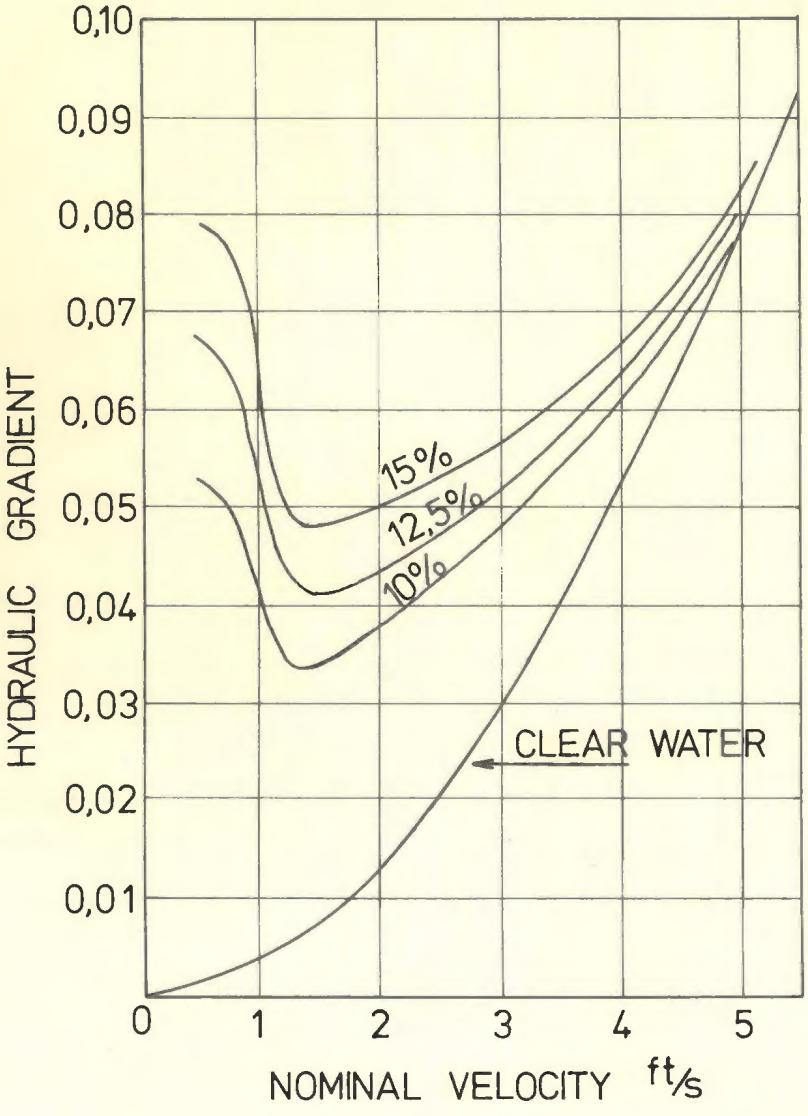

HYDRAULIC GRADIENT – VELOCITY CURVES
OBTAINED BY WORSTER R. AND DENNY D.

MATERIAL : COAL (VOL. CONC. 15 ; 12,5 ; 10 %)
PARTICLE DIAMETER : d = 12,7 mm (1/2")
PIPE DIAMETER : D = 38,0 mm (1 1/2")

FIGURE 14 – a ; (6 a)

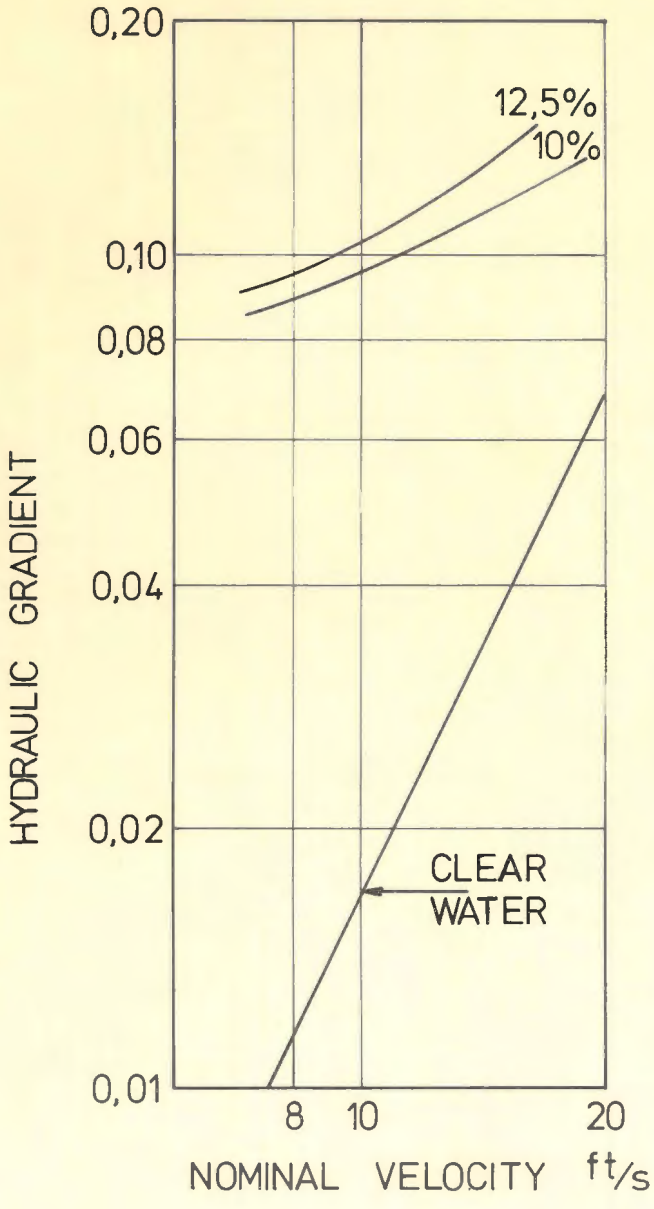

HYDRAULIC GRADIENT - VELOCITY CURVES
OBTAINED BY SOLEIL AND BALLADE
MATERIAL : SAND (VOL. CONC. 12,5 : 10 %)
PARTICLE DIAMETER d = 0,5 mm
PIPE DIAMETER D = 580 mm

FIGURE 15 - A (7)

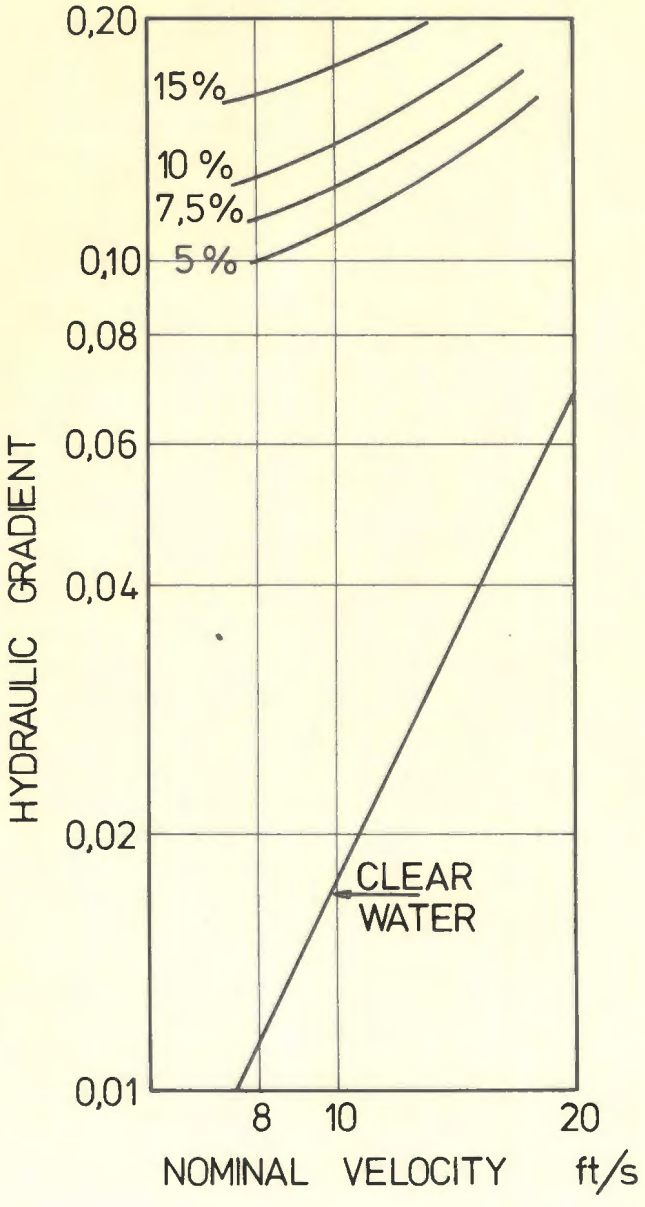

HYDRAULIC GRADIENT VELOCITY CURVES
OBTAINED BY SOLEIL AND BALLADE

MATERIAL: SAND (VOL. CONC. 15 ; 10 ; 7,5 ; 5 %)
PARTICLE DIAMETER d = 0,5 mm
PIPE DIAMETER D = 700 mm

FIGURE 16 - A ; (8)

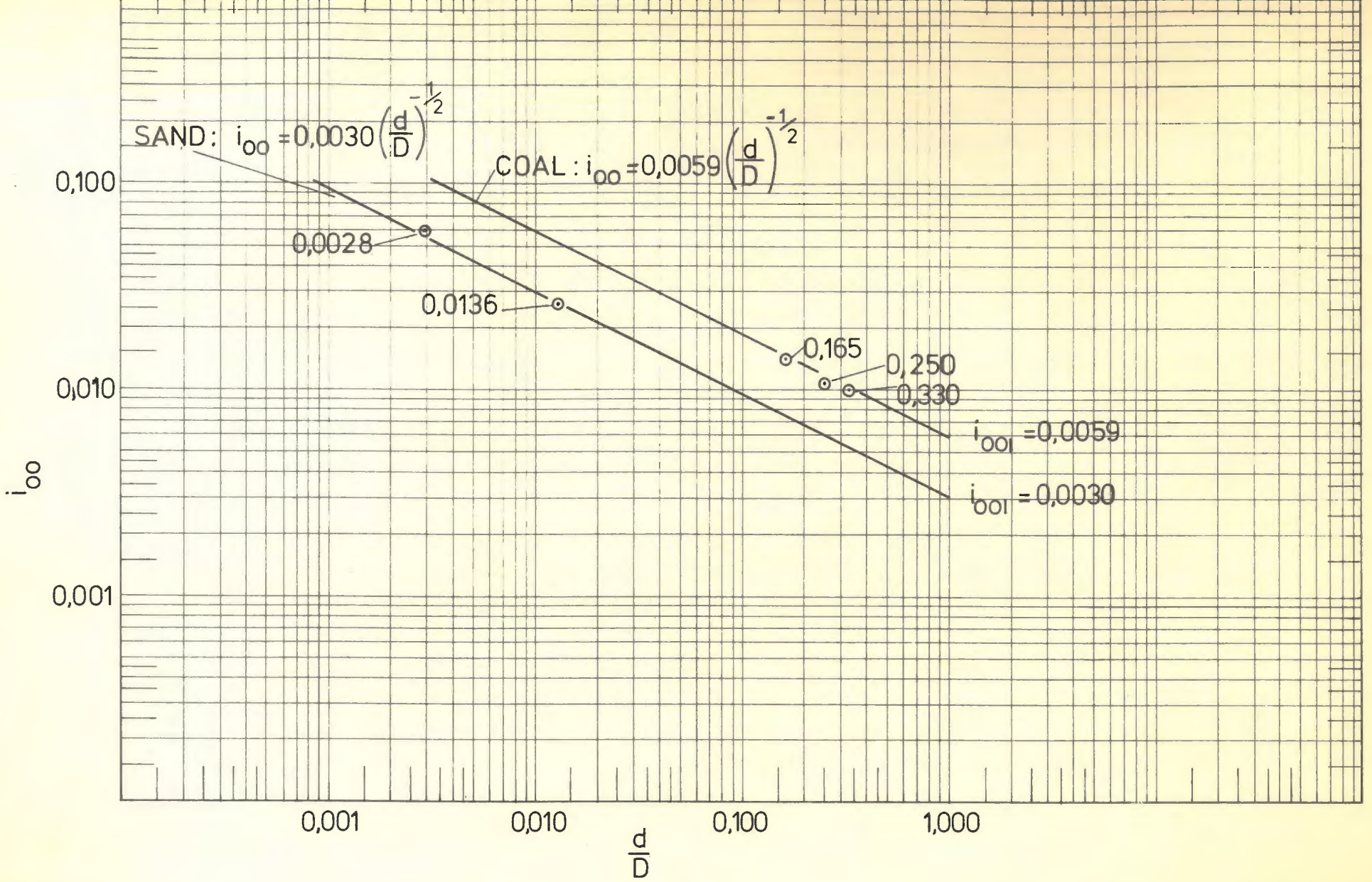
SAND: $i_{oo} = 0{,}0030\left(\frac{d}{D}\right)^{-1/2}$
COAL: $i_{oo} = 0{,}0059\left(\frac{d}{D}\right)^{-1/2}$
0,100
0,010
0,001
i_{oo}
0,0028
0,0136
0,165
0,250
0,330
$i_{oo1} = 0{,}0059$
$i_{oo1} = 0{,}0030$
0,001
0,010
0,100
1,000
$\frac{d}{D}$

FIGURE 17;(10)

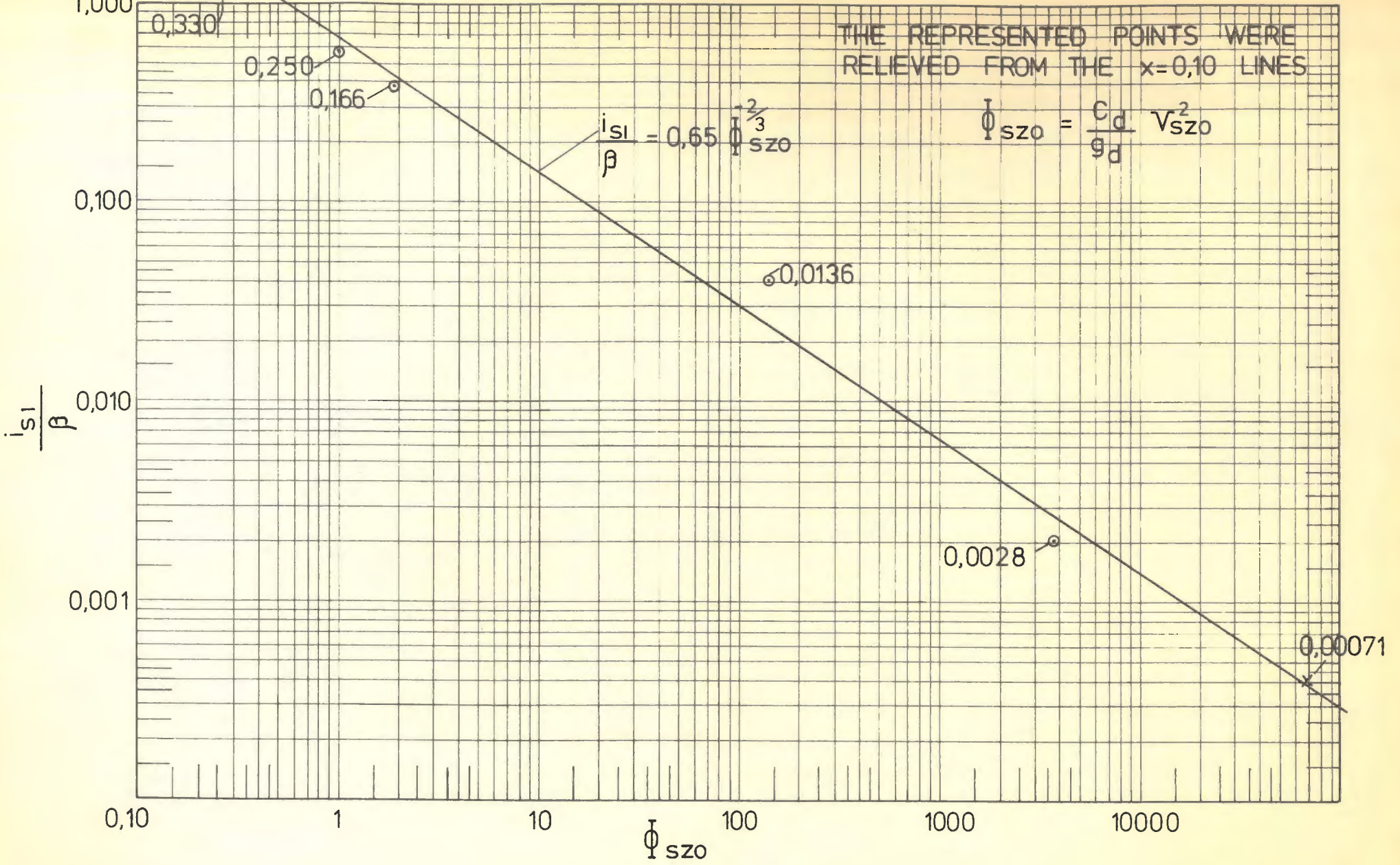
1,000
0,100
0,010
0,001
0,330
0,250
0,166
0,0136
0,0028
0,00071
THE REPRESENTED POINTS WERE RELIEVED FROM THE x=0,10 LINES
$\frac{i_{SI}}{\beta} = 0,65\,\Phi_{SZO}^{-\frac{2}{3}}$
$\Phi_{SZO} = \frac{C_d}{g_d}\,V_{SZO}^2$
$\frac{i_{SI}}{\beta}$
0,10
1
10
100
1000
10000
Φ_{SZO}

FIGURE 18;(12)

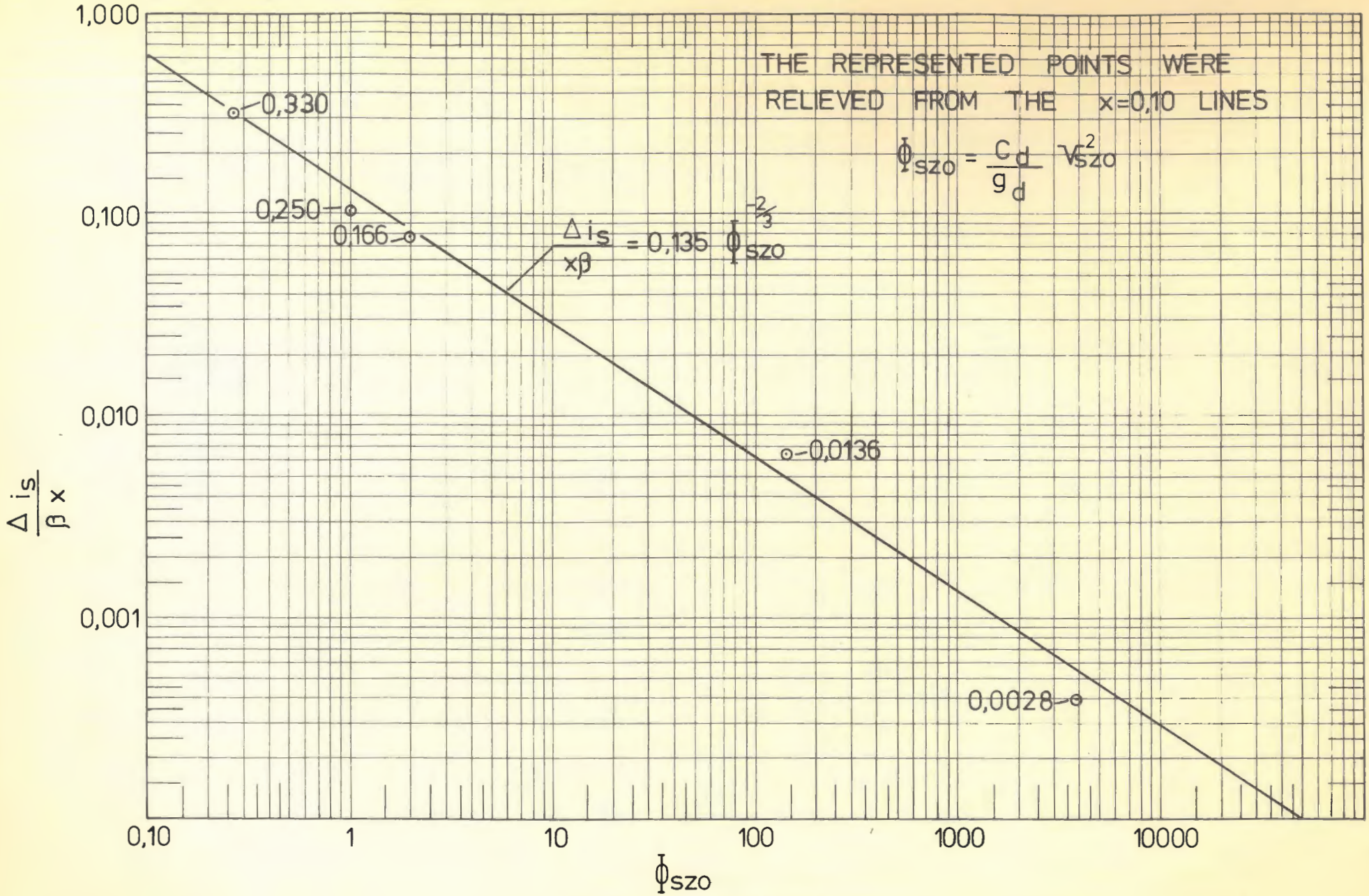
THE REPRESENTED POINTS WERE
RELIEVED FROM THE x=0,10 LINES
$\Phi_{szo} = \frac{C_d}{g_d} V_{szo}^2$
$\frac{\Delta i_s}{x\beta} = 0,135\ \Phi_{szo}^{-\frac{2}{3}}$
0,330
0,250
0,166
0,0136
0,0028
1,000
0,100
0,010
0,001
$\frac{\Delta i_s}{\beta x}$
0,10
1
10
100
1000
10000
Φ_{szo}

FIGURE 19;(13)

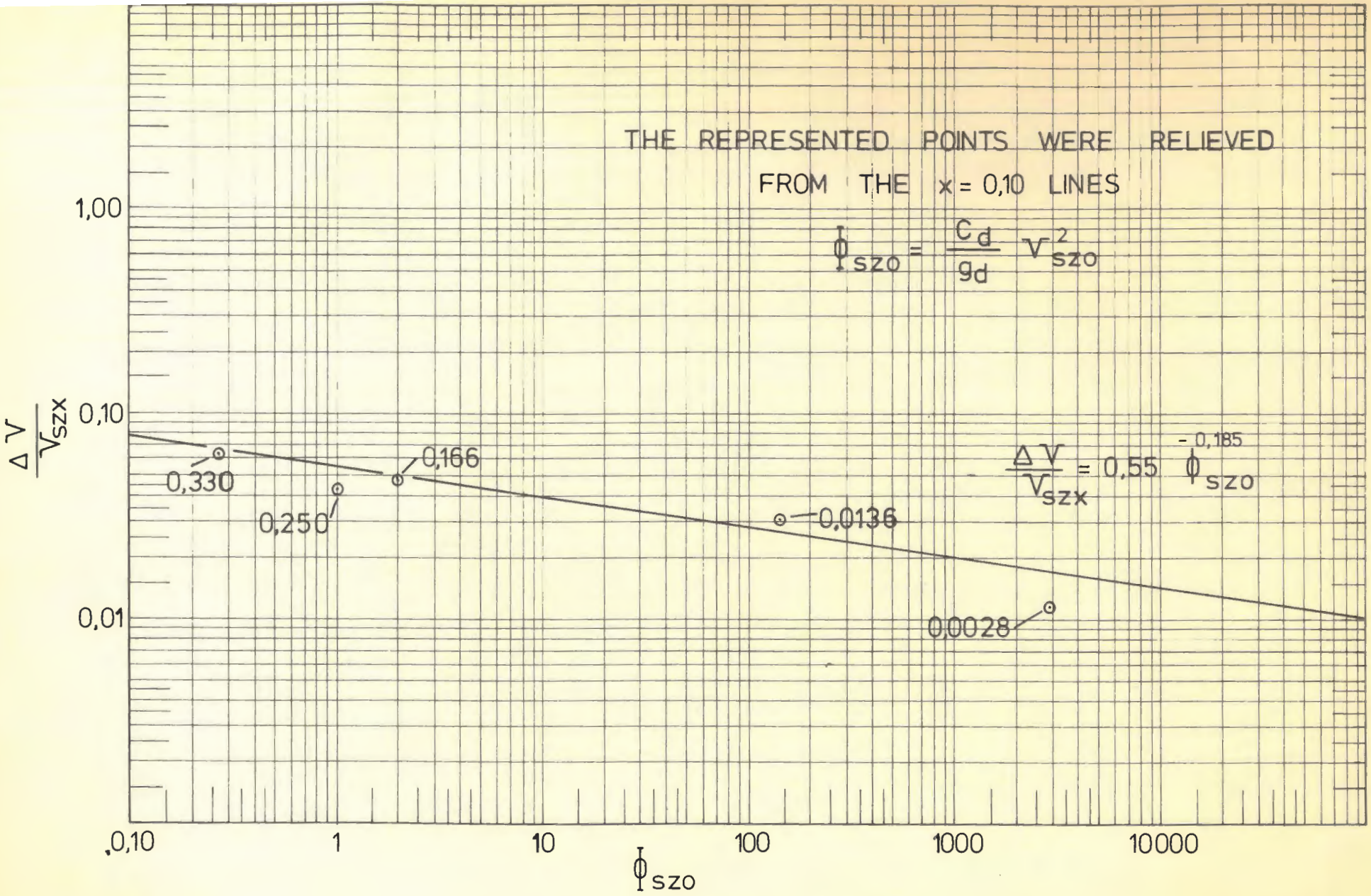
THE REPRESENTED POINTS WERE RELIEVED
FROM THE x = 0,10 LINES
$\phi_{szo} = \frac{C_d}{g_d} V^2_{szo}$
$\frac{\Delta V}{V_{szx}} = 0,55\ \phi_{szo}^{-0,185}$
$\frac{\Delta V}{V_{szx}}$
1,00
0,10
0,01
0,330
0,250
0,166
0,0136
0,0028
0,10
1
10
100
1000
10000
ϕ_{szo}

FIGURE 20;(14)

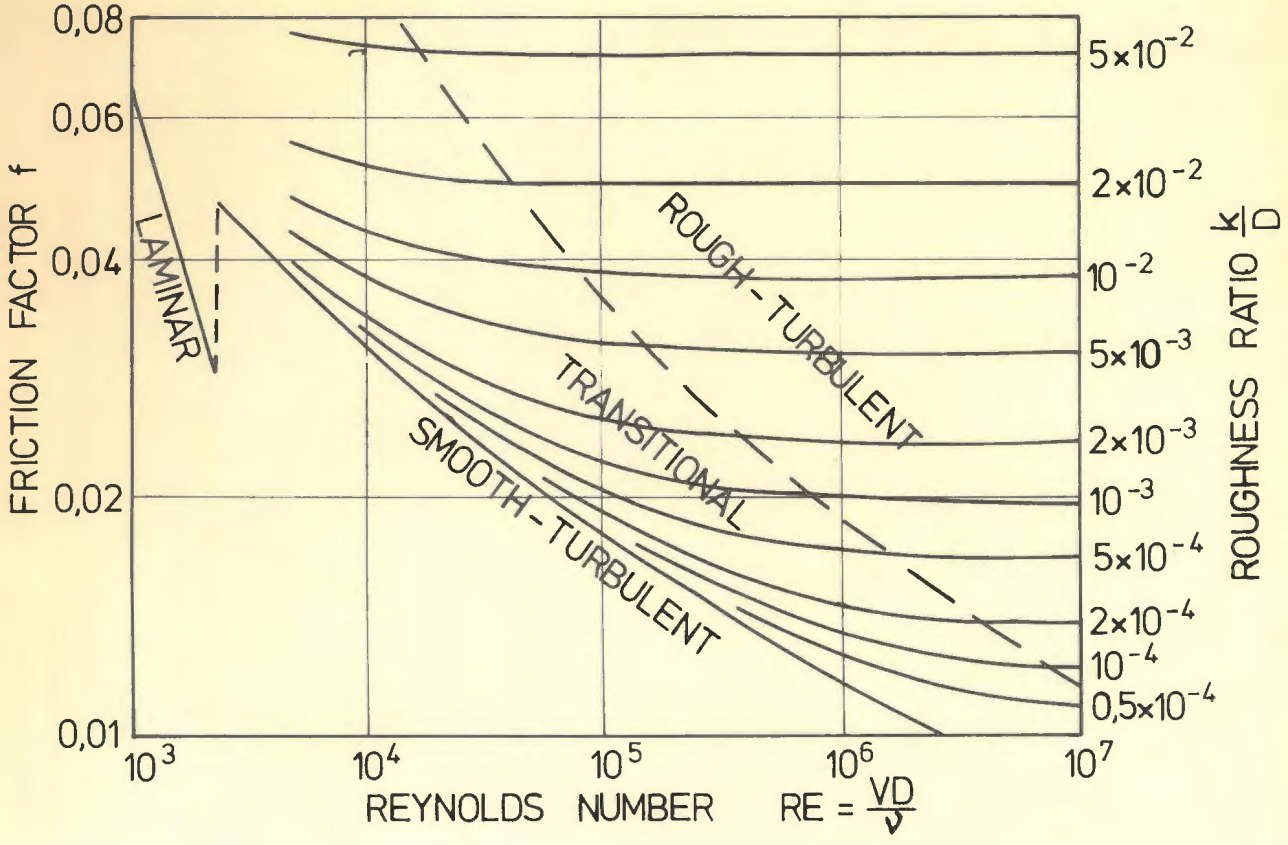

FRICTION FACTOR AS FUNCTION OF RE AND ROUGHNESS RATIO (COLEBROOK - WHITE)

FIGURE 21

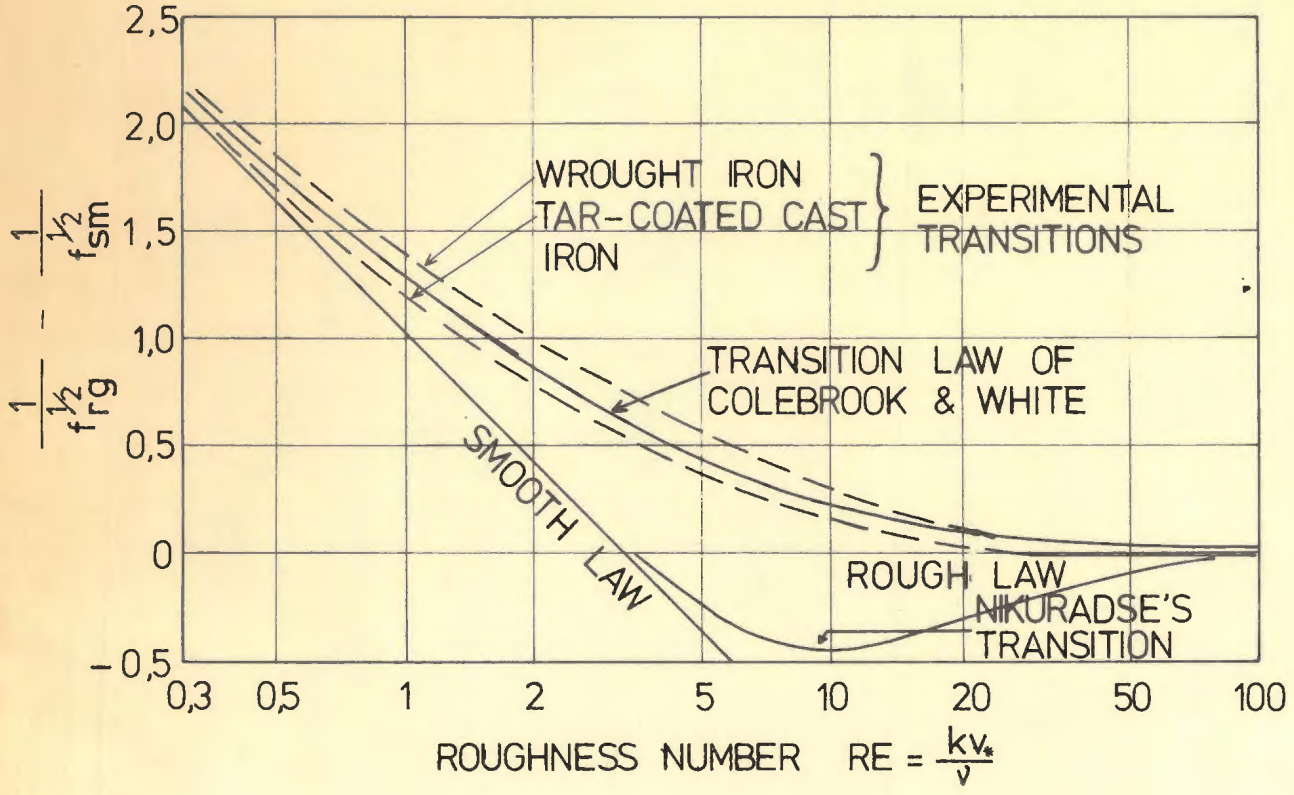

ROUGHNESS FUNCTIONS

FIGURE 22

δ IS THE THICKNESS OF THE BOUNDARY LAYER $\delta = \frac{\nu}{v_*}$

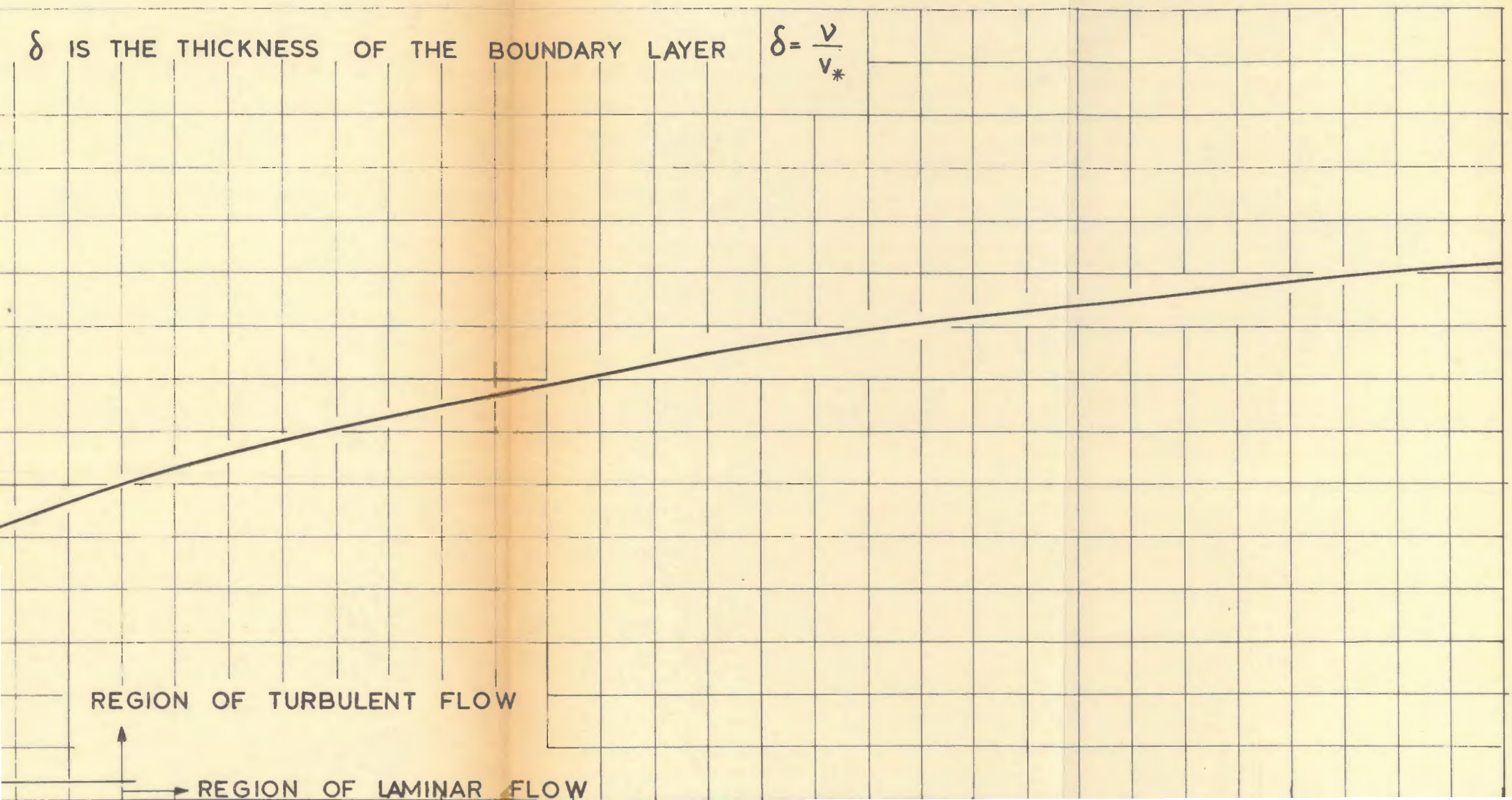

IS THE PIPE ABSOLUTE ROUGHNESS

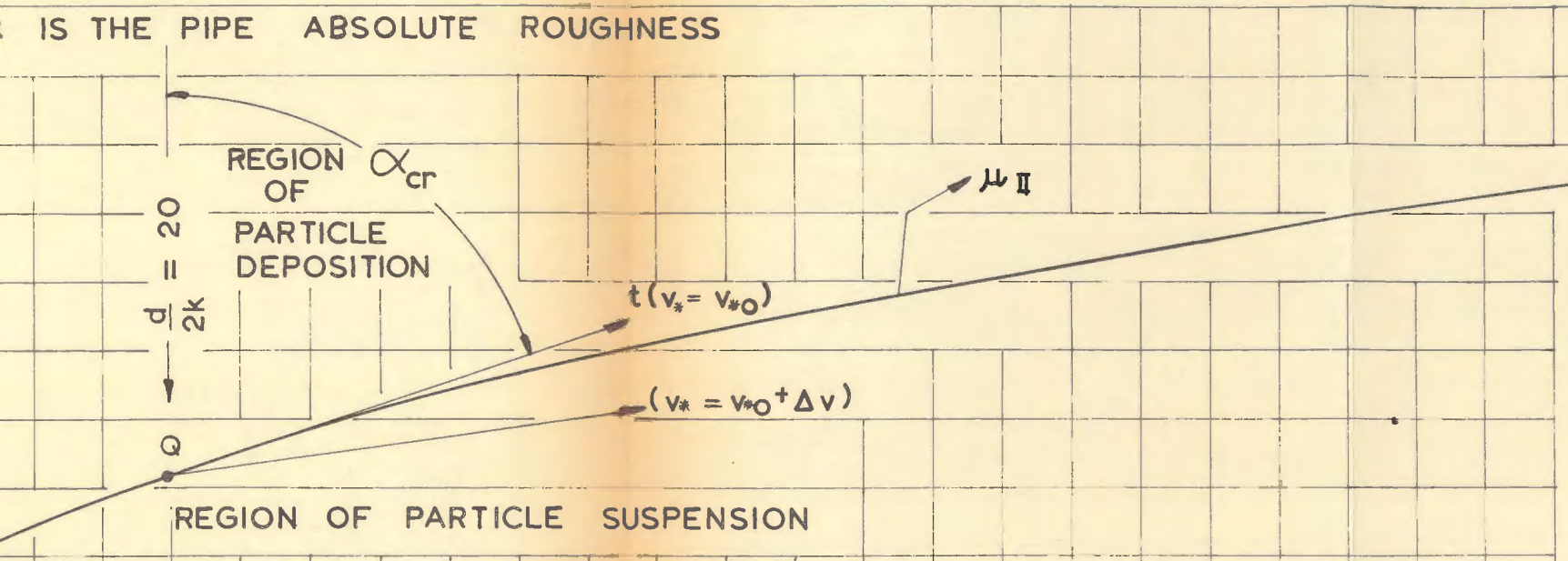

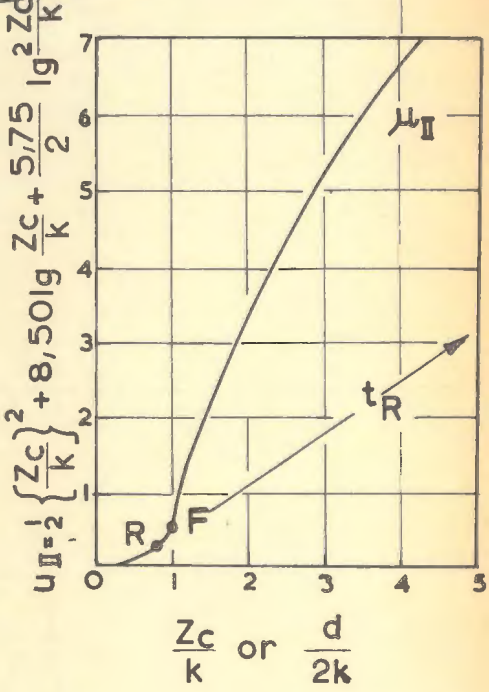

DETAIL A

ON OF TURBULENT FLOW (a)

$\frac{d}{D}$)

u_{II} (for $\frac{k}{D} = \frac{d}{D}$)

u_{II_1} (for $\frac{k}{D_1} = \frac{4d}{D}$)

R TANGENT To u_{II} AT F

ICATOR TANGENT To u_{II} AT P

1)

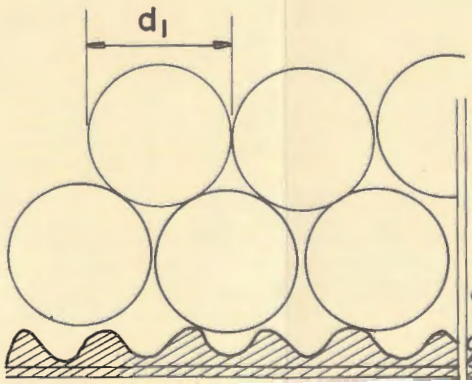

2)

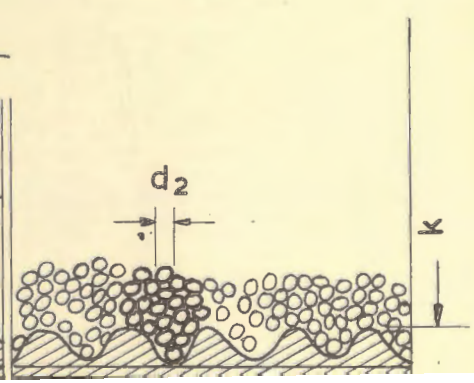

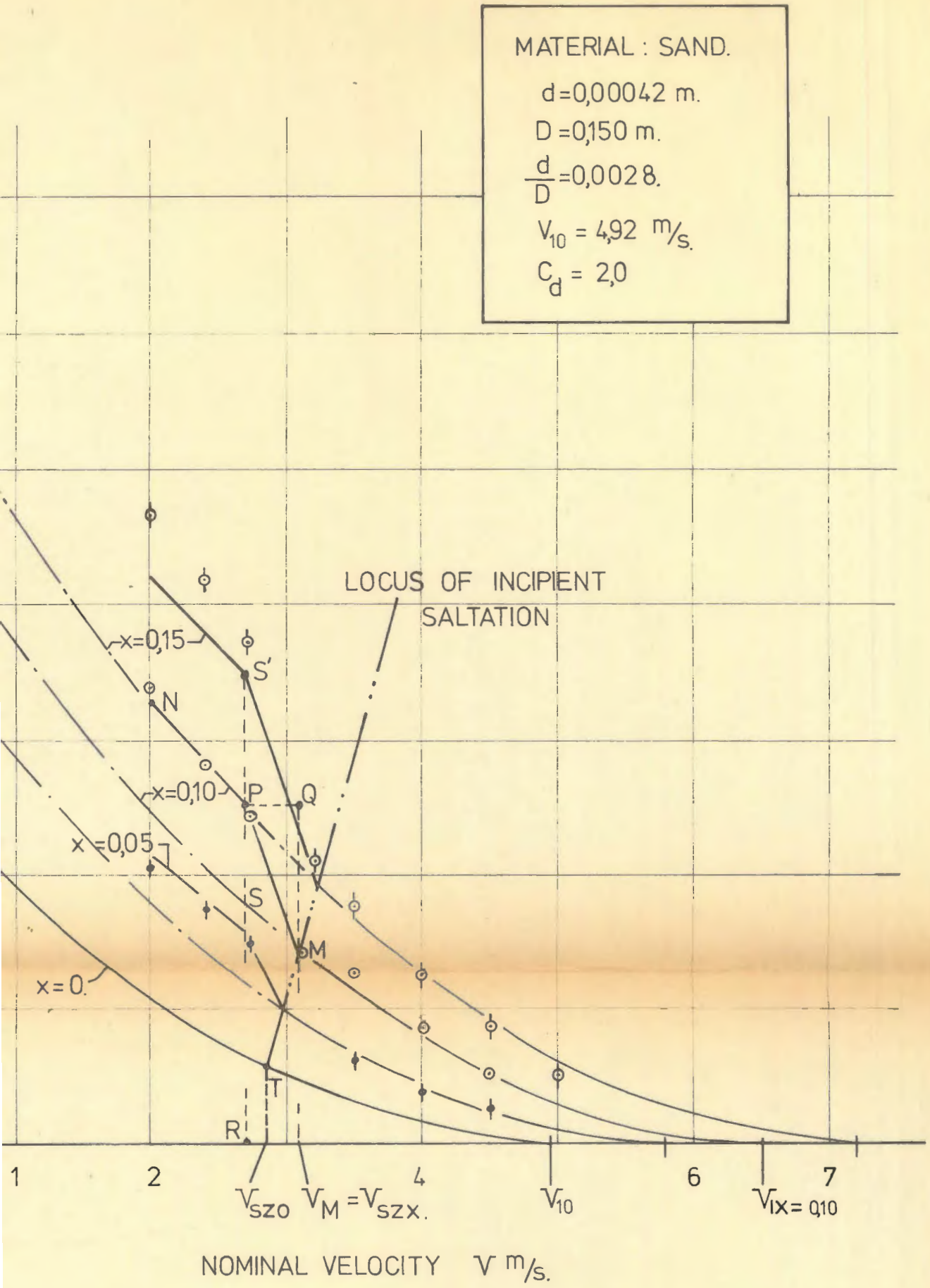

OF FIGURE 10-a REPLOTTED IN A REPRESENTATION: HYDRAULIC ESS VERSUS NOMINAL VELOCITY.

FIGURE 10-b;(2b).

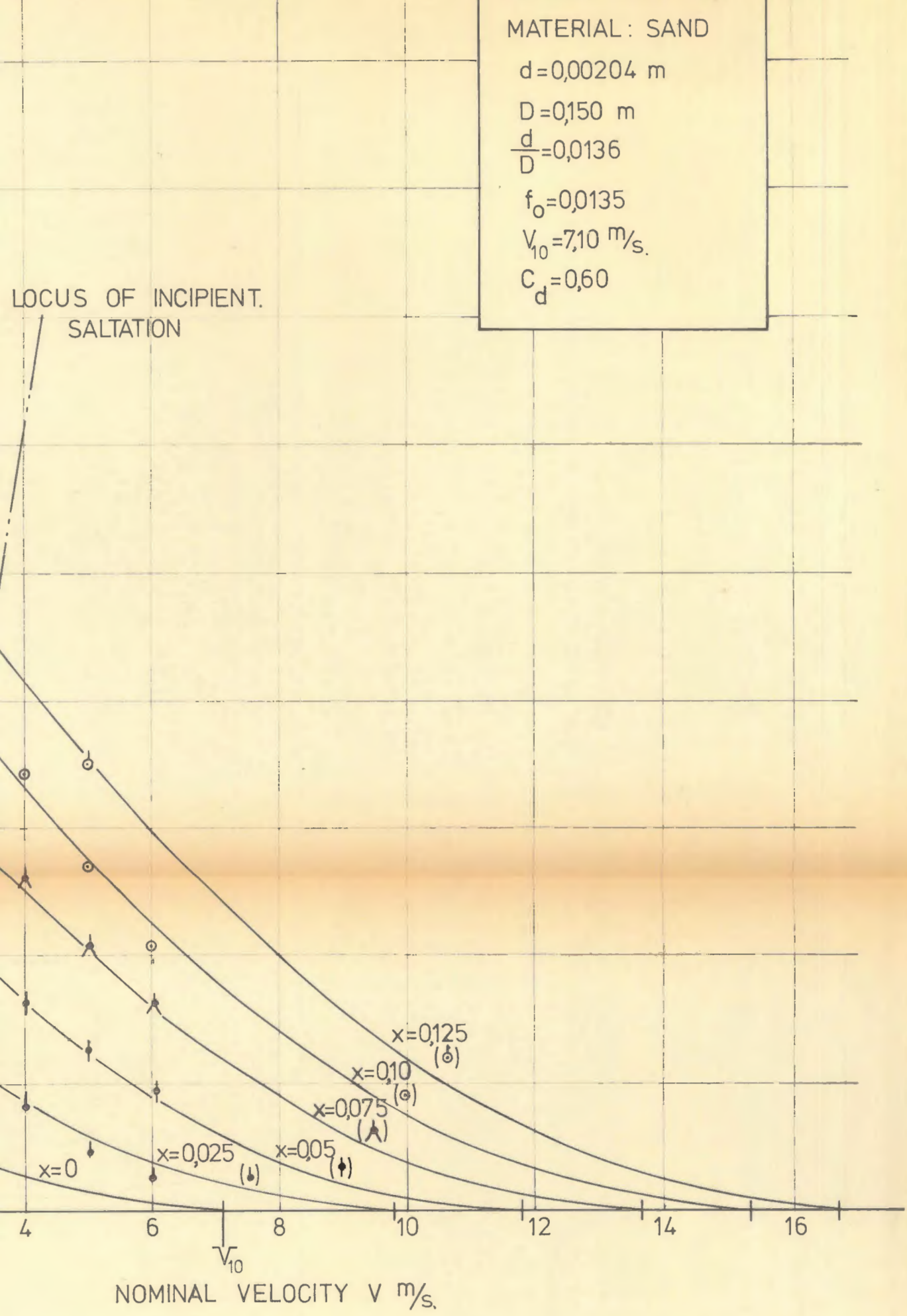

E 11-a REPLOTTED IN A REPRESENTATION : HYDRAULIC GRADIENT EXCESS
ITY

FIGURE 11-b; (3b)

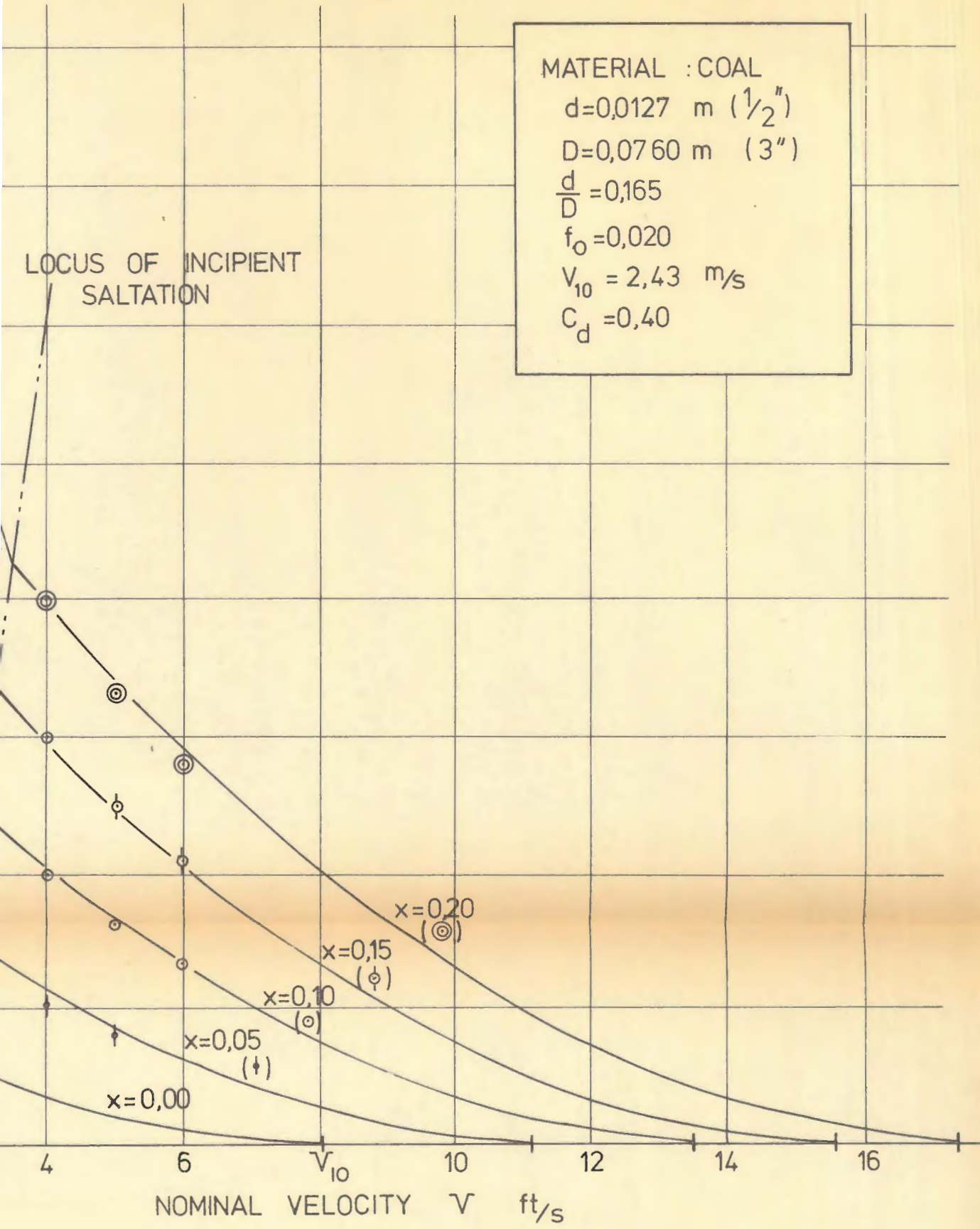

RE 13-a REPLOTTED IN A REPRESENTATION : HYDRAULIC
RSUS NOMINAL VELOCITY.

FIGURE 12 - b : (4 b)

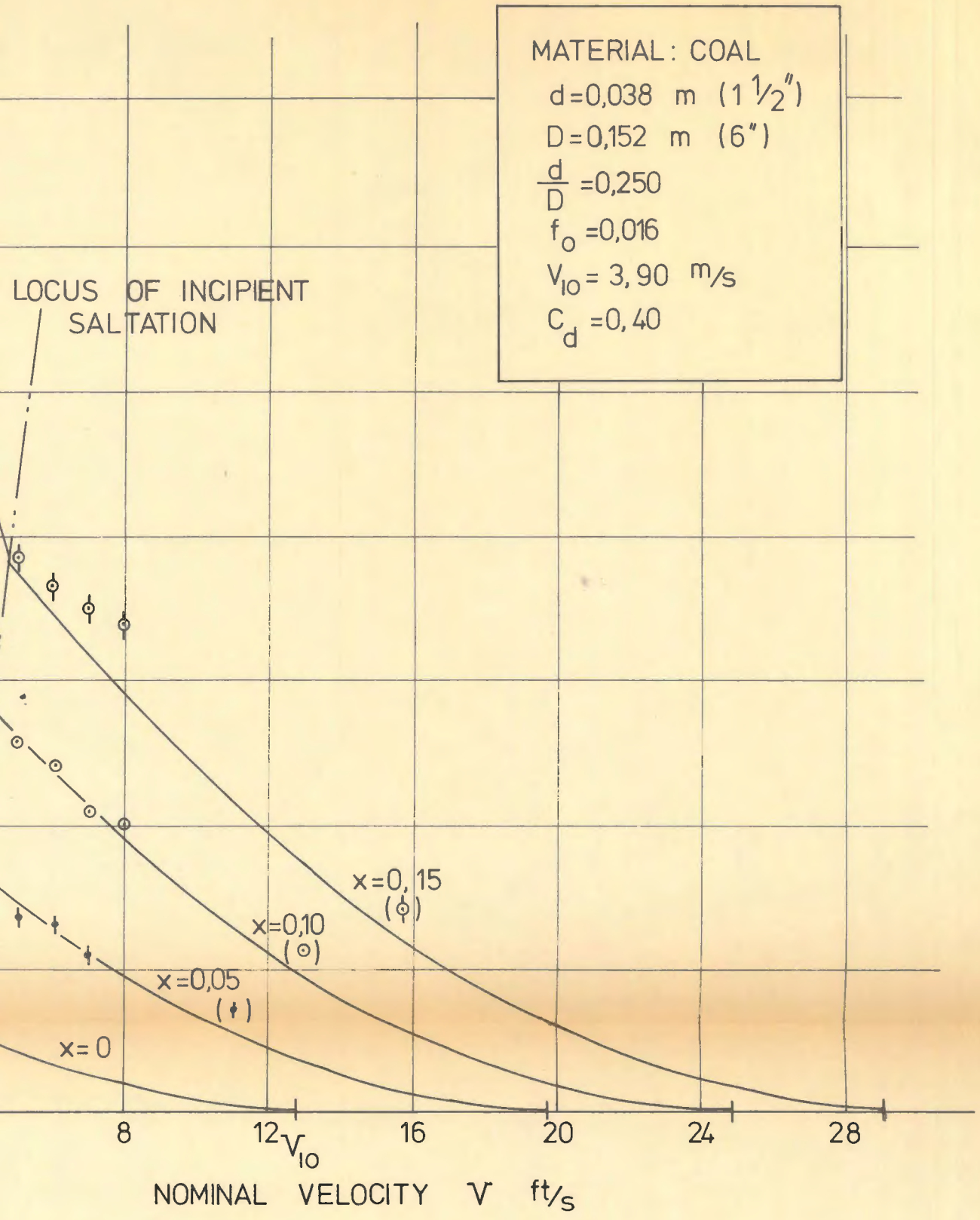

OF FIGURE 13-a REPLOTTED IN A REPRESENTATION: HYDRAULIC XCESS VERSUS NOMINAL VELOCITY

FIGURE 13-b ; (5b)

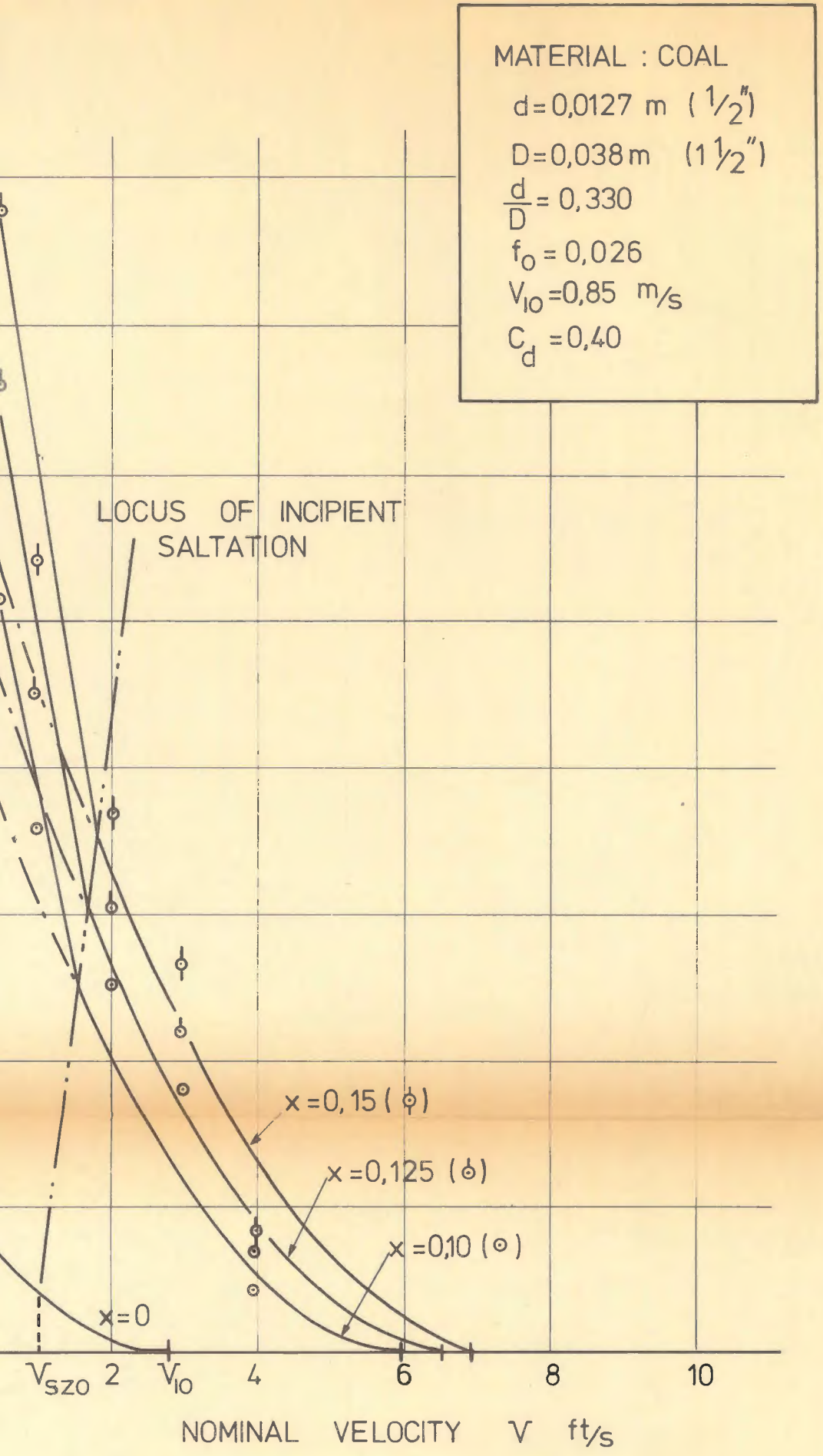

XPERIMENTS OF FIGURE 14-a REPLOTTED IN A REPRESENTATION: YDRAULIC GRADIENT EXCESS VERSUS NOMINAL VELOCITY.

FIGURE 14 – b;(6 b)

ETATION OF EXPERIMENTAL RESULTS LEADS TO
SION THAT NO DUNES ARE PRESENT

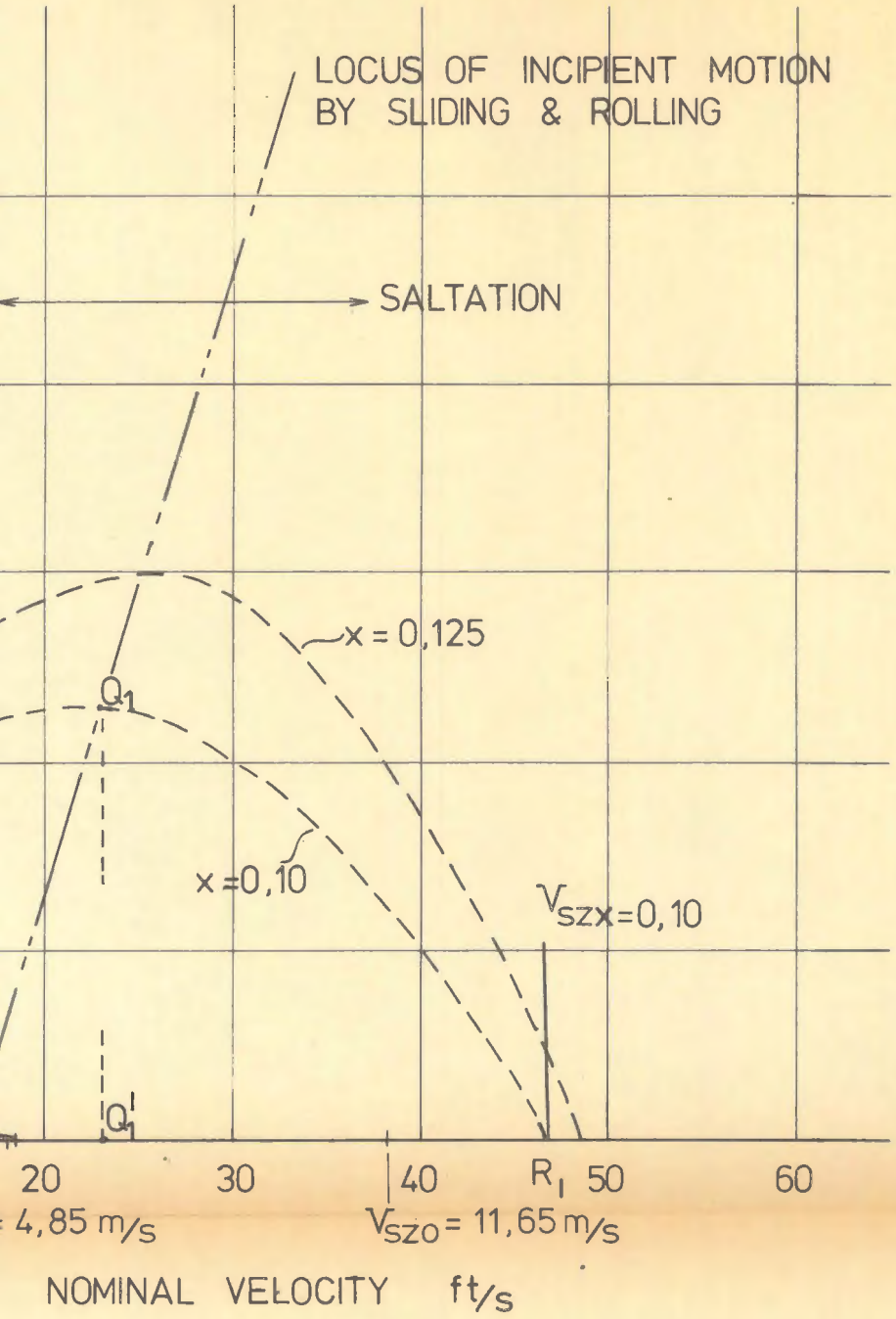

OLATION OF RESULT OF FIGURE 15–A
TO DEVELOPED THEORY.

FIGURE 15 – B

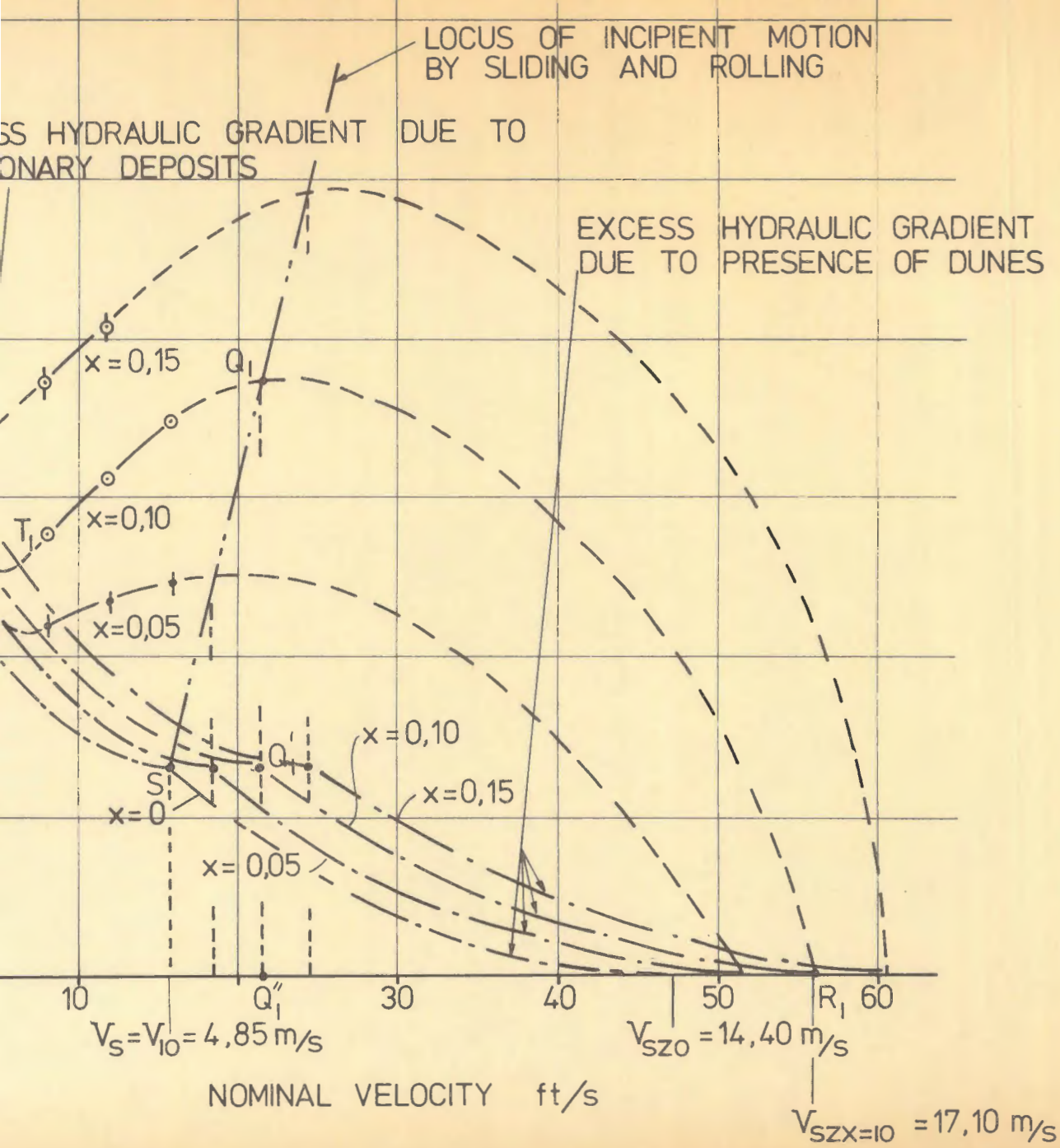

CESS LOSS CURVE FOR
UE TO STATIONARY
IATERIAL DEPOSITS

MATERIAL : SAND
D = 0,700 m
d = 0,0005 m
$\frac{d}{D}$ = 0,00071
f_o = 0,0255
C_d = 1,7

EXTRA POLATION OF RESULTS OF FIGURE 16 - A
CCORDING TO DEVELOPED THEORY

FIGURE 16 - B ; (18)